THE UNIVERSITY OF OKLAHOMA

GRADUATE COLLEGE

MODELLING AND OPTIMIZATION FOR A ROTATING DISC CONTACTOR

A DISSERTATION

SUBMITTED TO THE GRADUATE FACULTY

in partial fulfillment of the requirements for the

degree of

DOCTOR OF PHILOSOPHY

BY

KAMEL HASSANEIN ABOUL-FOTOUH

Norman, Oklahoma

1977

MODELLING AND OPTIMIZATION FOR A

ROTATING DISC CONTACTOR

APPROVED BY

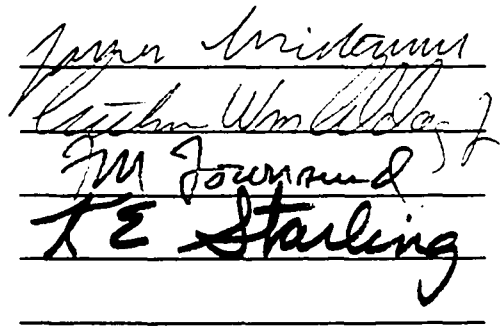

DISSERTATION COMMITTEE

ABSTRACT

The investigation carried out in this project was mainly concerned with modelling and optimization of a rotating disc contactor (RDC) liquid-liquid extraction process. The main goals achieved in this work are:

1. A thorough study of the hydrodynamics of an RDC was carried out, and the physico-hydrodynamic relations were evaluated. A semi-theoretical holdup model was validated experimentally and an axial mixing correlation was recommended.
2. Steady-state models for the process were developed and solved numerically. Steady-state experimental data were used to test alternative mathematical models for the process. The three-section column model with axial mixing was found the most suitable.
3. An operating objective function was developed for steady-state optimization and four gradient optimization techniques were compared numerically for solving the problem. The optimum gradient method proved to be the best for this case.
4. A unique dynamic model with identified order and seven flow conditions was developed and solved for time-invariant and time-varying disturbances. The dynamic

response of the seven flow conditions were compared to experimental data. The model with variable axial mixing in solvent phase only proved to be the best in representing the dynamics of the process.

ACKNOWLEDGEMENTS

I would like to express my appreciation and gratitude to the individuals and organizations which made the completion of this work possible.

Dr. J. H. Christensen, Adjunct Associate Professor, for his guidance and assistance through the last eighteen months, and Dr. J. B. Agnew, Professor at Monash University for his supervision in the early stages of this project.

Professor F. Mark Townsend, Professor K. E. Starling, and Associate Professor A. Aldag for serving on my advisory committee.

Ms. Detia Roe for preparation of this manuscript.

Department of Chemical Engineering, Monash University, Australia for the financial support from November 1968 to May 1971.

School of Chemical Engineering and Materials Science, University of Oklahoma for the financial assistance from September 1975 to December 1976.

I would especially like to express my appreciation to my brother Mohamed for his continuous encouragement and my gratitude and respect to my mother for her love and devotion.

TABLE OF CONTENTS

Chapter Page

LIST OF TABLES

LIST OF ILLUSTRATIONS

MODELLING AND OPTIMIZATION FOR A ROTATING DISC CONTACTOR

CHAPTER I

INTRODUCTION

During the last twenty years process control and optimization for all industries and especially the chemical industry have taken on an increasingly important role.

To have better control is one of the most important demands in modern industry, and this has been brought about by several reasons:

1. New processes have been developed which can operate only if such variables as flow rates, concentrations, temperatures, and pressures are maintained within very close limits.
2. Old industries have found that one way to increase their sales was to improve the quality of their products and to avoid off-specification products.
3. A more fundamental study of the process can lead to better process control, giving higher product quality and lower consumption of materials, labor and energy.

4. To improve working conditions especially as regards safety.
5. The necessity of finding causes for improper performance.
6. The necessity of decreasing the unproductive time required to adjust for upsets.
7. The need to help the engineer make better and faster decisions about the system under his supervision.

During the last ten years on-line computer control has taken on added significance; it is not only enough to be able to control a process (supervisory) but also to be able to control it at optimum conditions (optimal).

Background:

Steady-State Optimization

There are two main approaches to the problem of steady state optimization of a chemical process, namely, on-line search techniques and model-reference optimization.

The former are used if it is not possible to develop a mathematical model for the process because of its complexity or because of unknown physical phenomena. Even if a mathematical model can be prepared, it is often too complex to solve. Therefore, one is forced to resort to a different means of determining the optimum. This can be done by considering the system as a "black box" about which nothing is known except the number of inputs and outputs.

Clearly, this case is rarely, if ever encountered in practice. However, it needs the most general background for the development of theory of system identification. Any theory advanced from this concept, while being completely universal in scope, will suffer from the lack of concern for the physical process involved. The system is viewed as an input-output device with little regard for its internal physical structure.

In model reference steady-state optimization one should postulate a mathematical model for the process performance under steady-state conditions of operation. Mathematical modelling of a process is generally a two-step operation: (1) to define a model structure, (2) to fit, calculate, or adjust the parameters of the model. The identification and estimation of model parameters can be done either from the available information about the process from previous investigations or through known statistical techniques. The first approach is much easier for processes for which the physico-chemical phenomena are well understood, while the second approach is preferable for processes which are not so well characterized.

For the second approach Eykhoff[1] distinguishes two classes of problems, which depend on the initial and desired knowledge of the process:

a. "Identification - the determination of a topology of the process, considering it as a celebrated black box."

b. "Parameter Estimation - the determination of the parameter values of the process, assuming the topology to be known."

The development of a reliable and realistic model for the process is the basis for the development of a Performance Criterion with reference to which the optimum values for the process variables can be obtained.

For commercial processes, maximum return on investment, or profit, is perhaps the most common criterion for optimum engineering design. Since the pilot scale RDC under study is operating on a physical system which is not useful industrially (Amyl Alcohol-Acetic Acid-Water), it is not possible to assign realistic costs for the raw materials or the product and, therefore, to formulate a general profit function.

It would be better then to restrict the objective function to an operating criterion which relates the efficiency of the process (measured by the actual number of transfer units (NTU_M), to the process variables through the steady-state model, and the power required by the rotating shaft. This type of objective function is a measure only of the effectiveness of the process.

To optimize the process performance and to evaluate the optimum levels, an efficient optimization technique must be used. The convergence and efficiency of any optimization technique is of primary importance from the

economic point of view. A preliminary investigation is required to indicate the most useful scheme for a particular application. Among the techniques which have shown considerable success for optimizing a quadratic or non-quadratic constrained objective function are: Optimum Gradient, Conjugate Gradient, Modified Fletcher and Powell, and Variable Metric Methods.[2] Further details about each of the above mentioned steps are detailed later.

Scope of the Project:

In this dissertation the author has tried to answer the following two questions: (1) What benefits will one get from implementing on-line computer control for the process under investigation? and (2) How can a suitable system be implemented?

To answer these questions qualitatively and quantitatively for the extraction process under investigation, one would review the following important stages of operation:

1. Start-up: For the usual start-up of an extraction process, the column is filled with the continuous phase, then the flowrate of this phase is set to the desired value and then the dispersed phase is introduced at the proper flowrate. Within a short period of time the holdup of the dispersed phase attains its steady-state magnitude. A full quantitative description of this period of the start-up would be extremely difficult because of the different displacement velocities

of the different size drops and would lead to very complex results. Therefore, attention should be given at this stage only to actuate the motorized values in an optimum way. This can be done by postulating a suitable control algorithm with an optimum combination of the three PID (Proportional, Integral, Derivative) control parameters.

2. Steady-State is one in which the process is operating under equilibrium conditions for long periods of time. The problem of evaluating the corresponding optimum levels for the process parameters and variables would be evaluated either off-line if the objective function can be evaluated directly from the steady-state model, or on-line as a stochastic search procedure with the past and current values of the input and output variables used to create a surface on which search for optimum is carried out.
3. A Transient State is one in which the system is driven away from the desired steady-state optimum level for a short period of time. The process could be represented by a time-invariant model and a time-optimal control or dynamic optimization procedures can be implemented through the process model to evaluate and renew the controllable variables to achieve minimum deviation error.

4. Unsteady-State is one in which the system operates for relatively longer periods of time under dynamic conditions and the rate of change of the parameters is so high that it would be hard to consider it stationary. A time-varying model is required to represent the process and a suitable control technique is required not only to control the process but also to predict for some time in the future the state of the process.
5. Set-Point Changes: This case could be considered as a special case of case number (3).
6. Process Troubles are states in which the system is forced out of the feasible and controllable range. Without developing a mathematical model for the process, it will be very difficult to detect such troubles, and the only action remaining is to stop the process and leave it to settle down and then repeat case (1) procedure. With a reference model it is possible to avoid these troubles by drawing a margin between the critical region and the feasible one, thereby imposing constraints on the process performance.

Process Models:

As a good process model is necessary for model techniques, attention will be paid to three types of process models: qualitative, static, and dynamic.

1. Qualitative Models

The great majority of control systems are still being designed on the basis of qualitative process models.

Physical insight and experience indicate how to connect the controllers to the control valves. Also, the choice of controller behavior, which usually comes down to the adjustment of P-, I-, and D-action, is realized by trial and error.

2. Static Models

These models have been developed for a variety of processes. They consist of algebraic, ordinary differential, or partial differential equations (linear or nonlinear). They are used generally for static optimization of process operation, resulting in optimum desired values for the controlled variables.

3. Dynamic Models

It is not always appreciated that there are various types of dynamic models, which differ widely from each other. They are: Lumped models of low or high order, models with time delays, and distributed-parameter models. Low-order lumped models consist of a small number of differential equations, e.g., stagewise model for a multistage transfer process. High-order lumped models pertain to so-called multicomponent processes (e.g., polymerization reactors), or multistage processes where the actual stage is the unit for mass and heat balances (mixed-cell models).

Distributed-parameter models arise when the process variables are functions of time and of geometric coordinates, and the dynamic behavior must be described by partial

differential equations. Figure 1 shows the different types of models and the interrelationships between them. We shall find that the steady-state model with end effects adequately describes the steady-state performance of the RDC, and that the dynamic model with variable backmixing in solvent phase only best describes the transient response.

FIGURE 1
CLASSIFICATION OF MATHEMATICAL MODELS
FOR PHYSICO-CHEMICAL PROCESSES.

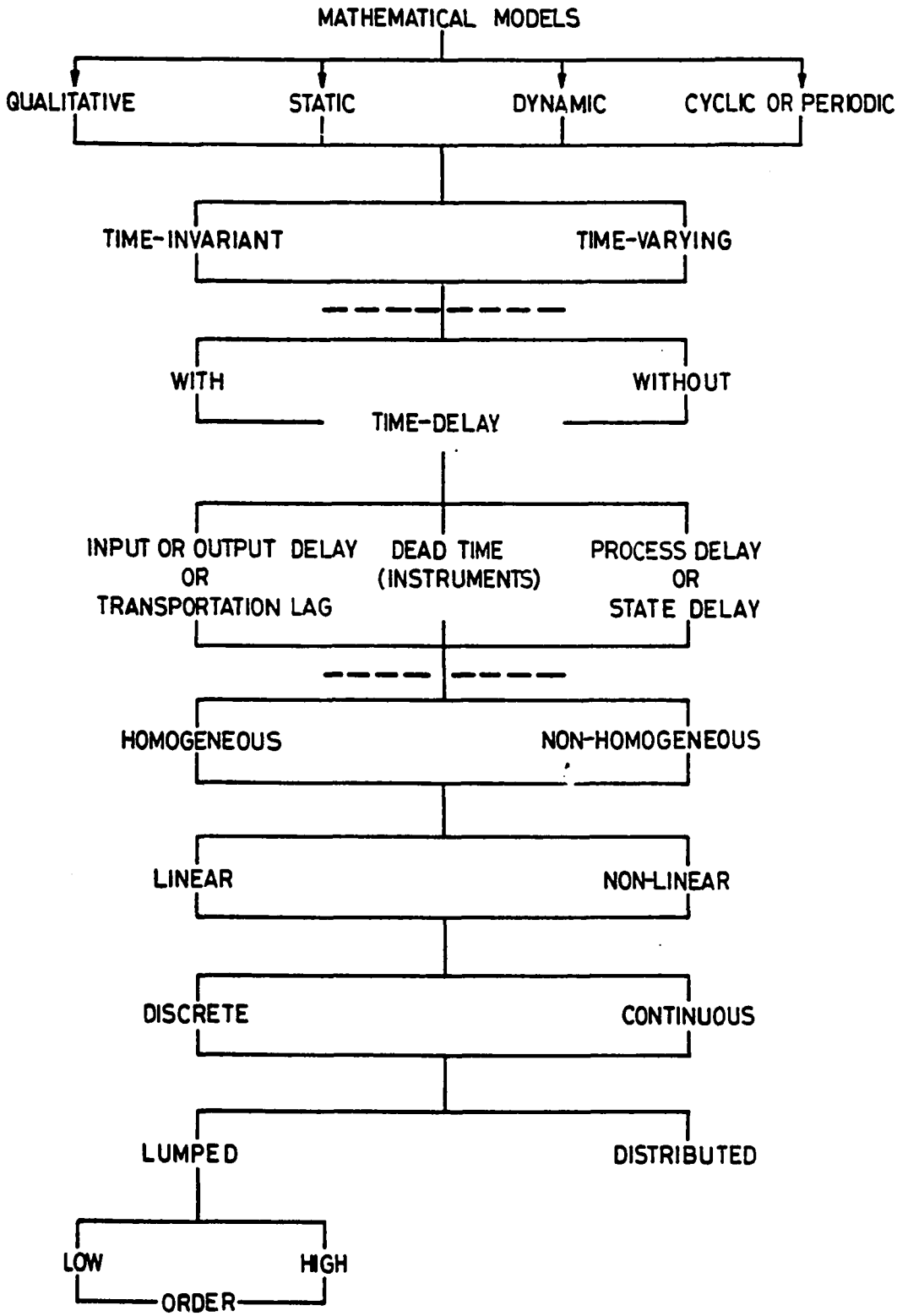

CHAPTER II

HYDRODYNAMIC STUDIES

Introduction

Extensive use is made of the liquid-liquid extraction process in industry; as a result many column designs have been suggested in the literature to perform this liquid separation process efficiently.

Mumford[3] in his review on equipment selection for extraction processes, classified them as:

I. Equipment in which the liquids are mixed, extracted and separated in discrete stages. This class includes the mixer-settler range of equipment and the different plate-type columns.

II. Equipment in which continuous countercurrent flow is established between the immiscible phases to give the equivalent of any desired number of stages.

They may be categorized as follows:

A. Gravity Operated Columns:

1. Non-mechanical dispersion:

a. Spray columns,

b. Baffle-plate columns, and

c. Packed bed columns.

2. Mechanically agitated columns:
    a. Pulsed columns, and
    b. Rotary agitated columns.

B. Centrifugal Columns.

Selection of Equipment

The choice between the various types of extraction columns for any particular application is based largely on experience.

Continuous contact extraction columns are, in general, preferable to mixer-settler units when large throughputs are to be handled since they offer economies in agitation power, equipment cost, floor space, and solvent inventory. They operate with relatively small amounts of holdup of extract and raffinate which is especially important when processing radioactive, flammable or low stability materials.

A prime advantage is their flexibility of operation which enables extraction to be performed with systems likely to form fine dispersions.

Rotating Disc Contactors

The RDC was first proposed by Reman[4,5] in 1951, and consists of a vertical cylindrical shell divided into a number of compartments by a series of stator rings. A rotating disc supported on a central shaft is located in each compartment. The dense phase is introduced into the

top of the column and the light phase into the bottom end. At each end, there is a settling zone to allow for separation and recoalescence of phases.

Mišek[6] studied the conditions under which one of the phases is dispersed, and the second is continuous. He classified the operation of the RDC into two different operating conditions: (a) moderate-intensity, and (b) high-intensity operation. The transition between the two states can be determined only with limited accuracy, because the transitions for individual elementary factors differs to a certain extent.

During intensive operation, the droplets are broken up in a turbulent stream and a transfer of mass from solid droplets with their center at rest results. Practical experience indicates that resistance to mass transfer in the moderate-intensity region is concentrated in a continuous film and in the high intensity region in the dispersed phase.

Tables 1 and 2 give a guide to a decision based on the value of the separation coefficients. When the separation coefficient is less than one ($m << 1$), and the column is under moderate operating conditions, a dispersed feed phase is acceptable. A similar recommendation can be deduced on the basis of the volume of the column and the effect of the longitudinal mixing coefficients. On the other hand, for $m > 1$ and the column operating under moderate conditions, difficulties due to the effect of the longitudinal mixing must be expected.

Mišek concluded that the majority of industrial extraction columns are operating under moderate conditions, and under these circumstances the influence of longitudinal mixing is not dominant. He recommended the following procedure to define the dispersed phase.

1. Using Table 1 as a first approximation for the state of operation for the column.
2. When the dispersed and the continuous phases are known, then the condition

$$\frac{1}{K_d} << \frac{1}{m_c K_c}$$

should be evaluated and K(0) value is determined from Table 2. If K(0) < 1 the feed is the continuous phase.

3. The functional $\chi(K)$ (which describes the ratio of the value of a function in a disperse solvent to the same value obtained when a disperse feed is considered, $\frac{y_{s=d}}{x_{f=d}}$) is illustrated by the following relationships:

$$\chi(m_c) = \frac{1}{m^2}$$

$$\chi(u) = \chi(d)\left(\frac{\rho_s \cdot \mu_s}{\rho_f \cdot \mu_f}\right)^{1/3} \qquad \text{(II-1)}$$

4. If the results from Tables 1 and 2 are in contradiction, trials starting with step two are repeated.

Applications of RDC's

The original use of the RDC by the Shell Companies was for the furfural extraction of petroleum lubricating

oils from which they gained savings of about 60% of the capital cost of equivalent packed towers and had a separating power equivalent to a 14-stage mixer-settler unit.[7]

The RDC has found a wide use in petroleum extraction processes including propane deasphalting,[7] SO_2 extraction of kerosene fractions, sulpholane extraction and naptha sweetening. About one hundred and fifty units were reported to be in commercial use by 1968.[3] More uses have appeared recently for the separation of oxy-compounds from Fisher-Tropsch synthesis and the dephenolization of waste waters from effluents in the coke and gas industries.[9]

Westerterp and Landsman[18,19] have noted the potential of using the RDC as a continuous reactor for homogeneous liquid phases reaction, especially in cases where large heat effects and long holding times are required.

Flow Pattern in an RDC Compartment

Reman[20] studied the hydrodynamics of flow in each compartment, and found that the flow consists, in the first place, of a rotation of the whole mass of liquid superimposed on this motion a slower movement of the liquid from the vicinity of shaft towards the column walls, and from the wall back towards the shaft in the vicinity of the stator rings. The resulting flow in each compartment is toroidal in nature. Two vortices in opposite senses occur; they are geared together to form a complete vortex. The energy transformed from the rotor discs to the liquid creates a fairly uniform turbulence.

Kung et al.[21] in a similar work concluded that the flow consists of two movements: (1) countercurrent flow of phases caused by a density difference, and (2) rotation of the whole liquid mass. Therefore, besides the axial flow there is toroidal flow, the latter causing back-mixing in the column. Diagrammatic sketches for both explanations are shown in Figure 2.

Liquid System Used

In the tertiary system selected, amyl alcohol is used as a carrier, acetic acid as a solute, and distilled water as a solvent. The direction of mass transfer is from amyl alcohol to water.

This system has been chosen on the following basis:

1. The acid content can be accurately determined either on-line by the refractometer for the feed phase, by the conductivity meter for the extract phase, or by the specific gravity meter for the raffinate phase, or manually by titration.
2. The equilibrium relationship is linear below acetic acid concentration in the feed phase of 15%, and depends to a negligible extent on the concentration (below this value), or the temperature.
3. The system shows little tendency to form stable emulsions.
4. The system is not highly corrosive.

Description of the Experimental System

The system used by the author was primarily equipped for on-line experimental optimization studies on the rotating disc contactor. Few necessary modifications and additions were carried out to make the system more reliable and capable of performing various input disturbances to study the dynamics of the process. The following modifications were made:

1. A second feed phase overhead storage tank was installed to be able to switch the inlet feed concentration between two different values.
2. Two solenoid valves (one N/O and one N/C) were fixed on each feed phase tank line with necessary fittings, by-passes and manual valves, to have a flexible access to any feed tank.
3. A filter (-360 mesh) was installed on the main feed line to prevent fine solid particles from blocking the line and a similar one on the solvent line to remove any suspended growth from the water inlet.
4. A pneumatic valve was installed on the main feed line to allow for testing the process for different feed phase flowrate disturbances. A sinusoidal generator was connected to the valve to be able to actuate it in a known signal form (amplitude and duration).
5. An orifice meter (pressure drop = 0-20" meter) with a 75-volt power supply and interface circuit was installed

on the feed line to make more accurate flow measurements than those obtained from the motorized valve. The latter proved inaccurate due to slip in the stem position after a period of use. This makes the calibration curve inaccurate to take by.

6. Also, a hot wire anemometer was installed on the solvent line for the same reason.
7. An electronic tachometer and interface circuits were built by the department electronics workshop to be able to interface the rotating shaft with the computer and include it as another input variable.

A schematic flowchart for the system is shown in Figure 3.

Fundamental Aspects of Mass Transfer in a Continuous Counter-Current Liquid-Liquid Extraction Process

It is essential for many mass transfer studies and modelling to review the characteristics associated with the process, such as holdup, back-mixing, mass transfer coefficients and the interfacial area of contact between phases.

The dispersed phase holdup is expressed as the volume percent occupied by the dispersed phase. Many studies have been carried out on the effect of the different conditions of operation, and the geometry of the column on the holdup distribution and percentage.

Strand et al.[22] determined point values for the holdup along the column axis by drawing samples through probes located at various points on different levels, to

determine the axial and radial values for the holdup. For the feed phase introduced at the bottom end, it has been shown that the value of holdup increases by moving up, probably because it takes time for the phase to break-up by the shear action. Then it decreases towards the top end due to the competing effects of axial diffusion of drops in the contact zone and the drop discharge into the sink or settler provided by the internal settler above the top stator ring.

Vermijs and Kramers[23] measured the holdup for different feed to solvent ratios (G/L), and column throughputs (G + L).

Logsdail, Pratt et al.[24] have related the column geometry, flow conditions, and physical properties of the liquid system to the holdup volume fraction by the following correlation:

$$\bar{V} = K\left(\frac{\gamma}{\mu_c}\right)\left(\frac{\Delta\rho}{\rho}\right)^{0.9}\left(\frac{g}{D_r N^2}\right)^{1.0}\left(\frac{D_s}{D_r}\right)^{2.3}\left(\frac{H}{D_r}\right)^{0.9}\left(\frac{D_r}{D_c}\right)^{2.6} \qquad \text{(II-2)}$$

Kung and Beckmann[21] and Mumford[3] have reached the following conclusions from their experimental work on a similar extraction column:

1. At rotor peripheral speeds less than 300 ft/min, entrapment of the dispersed phase droplets under rotor discs and stator rings occurs. However, this entrapment is not permanent since there is a net movement through the column.

2. The holdup value (average) can be evaluated with reasonable accuracy for a given column geometry and rotor speed by using the following semi-theoretical formula:

$$\frac{V_d}{\varepsilon} + K_1 \frac{V_c}{1 - \varepsilon} = \bar{V}(1 - \varepsilon) \qquad \text{(II-3)}$$

where

$$K_1 = 2.1 \quad \text{at} \quad (D_s - D_r)/D_c < \frac{1}{24}$$

and

$$K_1 = 1.0 \quad \text{at} \quad (D_s - D_r)/D_c > \frac{1}{24}$$

The equivalent values of $\bar{V}$ are estimated from Equation (II-2) for K = 0.0225 for the first case and 0.012 for the second case.

Strand et al.[22] assumed a relation for the characteristic drop velocity ($\bar{V}C_R$), of the same form proposed by Thornton,[17] as follows:

$$\bar{V} = \frac{1}{C_R(1 - \varepsilon)}\left(\frac{V_d}{\varepsilon} + \frac{V_c}{1 - \varepsilon}\right) \qquad \text{(II-4)}$$

where C_R is taken to be the minimum of the following three area ratios given below:

$$\left(\frac{D_s}{D_r}\right)^2, \qquad 1 - \left(\frac{D_r}{D_c}\right)^2, \qquad \text{or}$$

$$\left(\frac{D_s + D_r}{D_c}\right)\sqrt{\left(\frac{D_s + D_r}{D_c}\right)^2 + \left(\frac{H}{D_c}\right)^2}$$

Kung and Beckman have shown that at the flooding point the flowrates and rotating shaft speed reach maximum permissible values. Introducing this condition into Equation (II-3) and by differentiation and setting (dV_d/dZ) and (dV_c/dZ) equal to zero the following two equations are obtained:

$$V_{d_f} = 2\bar{V}\varepsilon_f^2(1 - \varepsilon_f) \qquad \text{(a)}$$

$$V_{c_f} = \bar{V}(1 - \varepsilon_f)^2(1 - 2\varepsilon_f) \qquad \text{(b)} \qquad \text{(II-5)}$$

Equation (II-5) relates the superficial velocity for the dispersed and continuous phases to the holdup fraction at flooding conditions (ε_f).

A relation between ε_f and the superficial velocities ratio at flooding (V_{d_f}/V_{c_f}) is then obtained by eliminating $\bar{V}$ from Equations (a) and (b) in (II-5).

$$\varepsilon_f = \frac{(R^2 + 8R)^{0.5} - 3R}{4(1 - R)} \qquad \text{(II-6)}$$

where

$$R = (V_{d_f}/V_{c_f}).$$

For each new set of conditions of operation, the flooding holdup value can thus be calculated. This value will be a constraint on the process performance. If the actual value of holdup is near the flooding value, a corrective action can be taken to reduce the actual holdup and prevent the system from running in a critical range.

Similar studies on the holdup and flooding conditions for other types of extraction columns have been carried out by other workers, e.g., for packed columns by Watson et al.,[10] for multistage vibrating disc columns by Miyanami et al.,[11] for spray columns by Laddha et al.,[12] and for unbaffled agitated vessels by Weinstein and Treybal.[13]

Delichatsios et al.[14] have shown mathematically and by experimental validation that increased drop size with higher fractional holdup can only be accounted for by allowing for coalescence, while turbulence damping caused by the dispersed phase plays a secondary role. Park and Blair[15] have studied droplet interaction phenomena of liquid-liquid dispersions in a stirred tank, for Methyl Iso-Butyl Ketone (MIBK) in water. They found that drop dispersion and break-up occurred near the impeller and coalescence predominated at other locations, as expected.

Physical Explanation of the Flooding Phenomenon

This phenomenon can be understood well by considering the hydrodynamics of flow in each compartment as follows:

As the liquid mixture comes in contact with the rotating surface, it imparts kinetic energy. The amount of energy imparted to the liquid mixture will depend on the angular speed, the surface roughness, shape, and diameter of the disc, and the physical properties of the liquid mixture. The amount of energy gained by each phase will depend on its physical properties and the quantity present in the mixture.

The centrifugal action will drive the liquid away from the center in the form of a continuous sheet. For low angular speed this sheet will not be strong enough to hold its shape and penetrate a long distance away from the disc edge in the continuous medium filling the compartment. Therefore, it will disperse in the form of large drops for the light phase while the dense phase drops will soon recoalesce with the continuous medium.

A force balance on each drop shows that larger drops will ascend in the axial direction faster than the smaller drops. Therefore, fine drops will have a longer residence time in each compartment while the coarse ones rise up and are subjected to further shear action in the next compartment.

This will make the value of holdup increase proportionally with the shaft speed and the distance away from the dispersed phase inlet to a certain height after which the holdup will decrease by coalescence as it becomes closer to the liquid interface.

By further increase in the shaft speed, a higher dispersion will be achieved and an increase in the residence time for each drop will also increase as a result of further disintegration. This explains the direct increase in holdup with the shaft speed.

A higher shaft speed will make a stronger sheet of liquid which can penetrate further in the continuous phase in the compartment, which will prevent to a certain extent

more drops from ascending in the central part of the column and will be enforced to take the vicinity of the column walls.

A higher speed than the above one might cause a state in which neither the heavy phase can find its way down nor the light phase can find its way up. This is most likely to happen in RDC's with small diameters.

A further increase in the shaft speed will cause another undesirable phenomenon. This is due to the extremely low drop size distribution of the dispersed phase which will make it possible for the droplets to avoid coming in direct contact with the rotating disc surface. Thereby, a great portion of the shear action is applied to the continuous phase which will turn it into a dispersed form also.

When the stage in which both phases are present as fine dispersed emulsion is reached, the rate of entrainment of one phase into another will increase to an extent that the outlet streams will be a mixture of both phases.

This physical explanation is based on observation of the column performance at wide range of operating conditions and gives more insight on the flooding phenomenon in mechanically agitated columns. It can be said now that flooding occurs in two distinct stages:

1. No flow in the axial direction due to density difference, and
2. Emulsion formation.

Mathematical Model for the Holdup Evaluation

A computer program has been written to evaluate the holdup mean value and the equivalent flooding value for the system under study, using Equations (II-2), (II-3) and (II-6), the column geometry, and the physical properties of the liquid system.

Figure 3 shows a flow diagram of the computer program written for this purpose.

The program has been used to solve the above equations for a wide combination of the process variables:

Feed phase mass flowrate (G):	60-180 g/min
Solvent phase mass flowrate (L):	60-180 g/min
Peripheral shaft speed (RN):	0-1800 cm/min

Figures 4 and 5 give the relationship between the column throughput (G + L), and the peripheral shaft speed vs the holdup volume fraction of the dispersed phase.

Holdup Measurements

To check the accuracy of predictions obtained from the semi-theoretical model solved above, many steady-state runs were carried out at various levels of operation. The procedure used for experimental holdup measurement is similar to the one used by Vermijs and Kramers.[23] In this technique the inlet streams and shaft speed were set-up to the desired level manually and kept there until the exit extract concentration shown on the conductivity meter reached a steady-state. Then, the inlet and exit valves

were shut down immediately and the contents of the column were drained and left to settle down in a graduated 4 litre beaker. The volume of the light phase was measured and the holdup volume fraction calculated.

The experimental results showed very close agreement with the semi-theoretical model as shown in Figure 5.

For larger columns, it is possible to measure the variation in holdup along the column axis by inserting probes on different levels and withdrawing samples from them simultaneously by control levers on the side hoses. If the column diameter is large enough, more than one probe could be inserted on the same level and with different taking points-radii.

Longitudinal Dispersion

The second phenomenon to be studied is longitudinal mixing and its effect on the efficiency of mass transfer in liquid-liquid extraction processes.

The longitudinal mixing of phases in extraction columns, which reduces its efficiency, is due to the reverse mixing produced by the entrainment of phases, and the axial mixing or Taylor diffusion[8,28,29,30,31] which causes transverse and longitudinal non-uniformity in the velocity and concentration profiles.

Longitudinal, reverse- or back-mixing, and axial diffusion are characterized by the coefficients E_z, E_r and E_{ax} respectively, which have the units of diffusivity and are related together as follows:

$$E_z = E_r + E_{ax} \qquad \text{(II-7)}$$

Two approaches have been taken to study this phenomenon. The first is based on the diffusion model in which the change in concentration along the column axis is continuous. The characteristics of this approach are the height of transfer unit (HTU), E_z and E_r.

Myauchi[31] has studied the influence of E_z theoretically, by using a simplified model which utilizes mean diffusivities and mean velocities for both the continuous and the dispersed phases. From this theoretical study, it has been shown that the influence of the longitudinal dispersion on the extent of extraction can be expressed as a function of four dimensionless parameters. These parameters include as variables the rates of longitudinal dispersion, the overall mass transfer coefficient, the equilibrium partition ratio, and the rates of fluid flow.

It has been shown theoretically that longitudinal dispersion has the effect of increasing or decreasing the concentration abruptly at the column entrance, Figure 6, and the concentration pattern for each outgoing stream becomes flat as it approaches its outlet.

Miyauchi"s approach led to three different definitions of NTU, depending on how one defines the effective concentration driving force:

a. True value

$$NTU_T = KaZ/G \qquad \text{(II-8a)}$$

b. Plug-flow value NTU_p, obtained from the logarithmic mean driving force,

$$NTU_p = \left\{ \ln \left[(1 - \Delta) \frac{x_{in}}{x_{out}} + \Delta \right] \right\} \Big/ (1 - \Delta) \qquad \text{(II-8b)}$$

c. Measured value, NTU_M, obtained by integration to the calculated concentration profiles

$$NTU_M = \int_{x_{(z=0)}}^{x_{(z=1)}} \frac{dx}{x - my} \qquad \text{(II-8c)}$$

It has been shown that $NTU_T \geq NTU_M \geq NTU_p$.

The second approach for determining the longitudinal dispersion coefficients is to test the process for a known disturbance and to measure the dynamic response.

Rod[32] used a graphical method based on a diffusion model to construct the true operating line for three cases: (1) longitudinal mixing in the continuous phase only, (2) longitudinal mixing in the dispersed phase only, and (3) longitudinal mixing in both phases.

In the last case trial and error is required to determine the concentration jump at the feed entrance and to be able to locate the first point on the operating line.

Danckwerts[33,34] has developed a distributed model representing the process under dynamic conditions. His starting point is the following differential equation, where the longitudinal dispersion coefficient, E , uniquely characterizes the mixing process

$$E_l \frac{\partial^2 x}{\partial z^2} - U_f \frac{\partial x}{\partial z} = \frac{\partial x}{\partial t} \qquad \text{(II.9)}$$

This model assumes a uniform radial concentration in the continuous phase. If the disturbance function is introduced, its concentration becomes established at the inlet cross section almost instantaneously. The dependence of this concentration, x, on time, t, is characterized by the input curve.

The regularity in the variation of the concentration with time in the column being considered is characterized by the output curve.

The type of disturbance used to drive the process to the dynamic state varied from one worker to another and obviously the equations developed to evaluate E_l varied from one another.

(1) Pulse-Input:

Levenspiel and Smith[26] showed that for an infinitely long tube and periodic sampling, the output curve can provide the value of the variance of the dispersion for the tracer concentration (σ^2-tracer):

$$\sigma^2 = \left(\frac{G}{V}\right)^2\left[\frac{\Sigma\theta_i^2 x_i}{\Sigma x_i} - \left(\frac{\Sigma\theta_i^2 x_i}{\Sigma x_i}\right)^2\right] \qquad \text{(II-10)}$$

The longitudinal coefficient of mixing can then be evaluated from the following formula:

$$E_z = \frac{UL}{8}[\sqrt{8\sigma^2 + 1} - 1] \qquad \text{(II-11)}$$

It has been shown by Levenspiel and Smith that at higher Peclet numbers the output curve becomes closer to the normal distribution curve.

Van der Laan[35] has treated the diffusional type of flow for a more general case of a finite pipe length by applying suitable boundary conditions.

(2) Step Input:

Hazlebeck and Geankoplis[36] have calculated the axial mixing coefficients, using Equation (II-11) and making the substitution, Z = x - Ut and the boundary conditions as follows:

$$\begin{aligned} x(Z,0) &= x_o \\ x(0,t) &= x_o/2 \ , \quad \theta \geq 2 \end{aligned} \qquad \text{(II-12)}$$

Equation (II-12) states that half the tracer material is ahead of the point $(q_f t/\varepsilon_d V) = 1.0$, and half behind it. This equation is solved for step input to obtain the following:

$$\frac{x}{x_o} = \frac{1}{2}\left[1 + \text{erf}\left(\frac{x - Ut}{2\sqrt{E_z t}}\right)\right] \qquad \text{(II-13)}$$

Differentiating Equation (II-13) and evaluating it at the reduced time $\bar{\theta} = (q_f t/\varepsilon_d V) = 1$ gives

$$E_z = \left.\frac{UZ}{4\pi\left[\frac{d(x/x_o)}{d(q_f t/\varepsilon_d V)}\right]^2}\right|_{\left(\frac{q_f t}{\varepsilon_d V}\right)=1} \qquad \text{(II-14)}$$

By measuring the slope of the curve of x/x_o vs. $(q_f t/\varepsilon_d V)$ at $\bar{\theta} = 1.0$, E_z can be calculated.

(3) Sine-Wave Input:

Ebach and White[37] and Liles and Geankoplis[38] started with Equation (II-11) and with two boundary conditions imposed at the inlet and the outlet respectively:

$$x(0,t) = x_M + A_o \sin \omega t \qquad \text{(II-15)}$$

$$x(\infty,t) = x_M \quad \text{or} \quad A(z) = 0 \text{ for } z \to \infty \qquad \text{(II-16)}$$

The periodic steady state solution is

$$x(Z,t) = x_M + A(0)e^{-B} \sin(\omega t - \xi) \qquad \text{(II-17)}$$

where

$$B = \frac{z\omega^2 E_z}{U^3} \qquad \text{and} \qquad \xi_{calc} = \frac{\omega z}{U}$$

It has been shown in previous surveys that it is very difficult to evaluate the longitudinal dispersion coefficients for the process investigation through the experimental approach. It would be easier to seek an accurate

empirical formula developed by other workers for such a problem.[104]

Empirical Formulae for the Longitudinal Dispersion Coefficients:

Westerterp and Landsmann[18] have developed the following correlation for the evaluation of the Peclet numbers:

$$P_{e(f \text{ or } s)} = \frac{2n}{1 + 13 \times 10^{-3}\left(\frac{ND_r}{\bar{U}_{f \text{ or } s}}\right)} \qquad \text{(II-18)}$$

where n is the number of compartments, and $(ND_r/\bar{U})$ is a measure of the ratio of the linear stirring velocity and the liquid flow velocity through the column (N = the angular speed of the shaft, rpm).

One of the two RDC's used in their experimental work is similar in dimensions to the one presently under investigation with the only difference being the number of compartments.

Miyauchi et al.[28] carried out experimental work on a two-stage unit under flow and non-flow conditions and obtained the following correlations:

For $nD_r^2/V > 1.2 \times 10^5$:

$$f/nD_r = 4.3 \times 10^{-3}(D_c/H)^{0.5}(D_c/D_s)^{0.25} \qquad \text{(II-19a)}$$

and for $nD_r^2/V < 1.2 \times 10^5$:

$$f/nD_r = 4.5 \times 10^{-2}(D_c/H)^{0.5}(D_c/D_s)^{0.25}(nD_r^2/V)^{-0.2} \qquad \text{(II-19b)}$$

Strand et al.[22] have reached similar formulae for the evaluation of axial mixing coefficients, given as follows:

For the continuous phase:

$$\left(\frac{1-\varepsilon}{V_c H}\right)E_c = 0.5 + 0.09(1-\varepsilon)\,\frac{D_r N}{V_c}\left(\frac{D_r}{D_c}\right)^2\left[\left(\frac{D_s}{D_c}\right)^2 - \left(\frac{D_r}{D_c}\right)^2\right] \qquad \text{(II-20a)}$$

and for the dispersed phase,

$$\frac{\varepsilon E_d}{V_d H} = 0.5 + 0.9\varepsilon\,\frac{D_r N}{V_d}\left(\frac{D_r}{D_c}\right)^2\left[\left(\frac{D_s}{D_c}\right)^2 - \left(\frac{D_r}{D_c}\right)^2\right] \qquad \text{(II-20b)}$$

The above formulae give the average values of the axial mixing coefficients.

If the variation in the axial mixing coefficients along the column axis is required, Gel'perin et al.[40,41] have determined the coefficients of $E_z(h)$ by the pulse method. They found that the dependence of E_z on the important process parameters can be described satisfactorily by the following correlation:

$$E_z(h) = aV_s h + bD_M N h \qquad \text{(II-21)}$$

where a and b are constants characterizing the column.

For RDC the above equation can be reduced to the following form which takes into account the effect of the column-to rotor-diameter ratio:

$$E_z(h) = 0.5\,V_s h + 0.012\,hD_r N(D_c/D_r)^2 \qquad \text{(II-22)}$$

It should be noted that the first term in the above equation accounts for the effect of the height while the second term accounts for the intensity of mixing.

Interfacial Area of Contact and Mass Transfer Coefficients

Two of the most important factors governing mass transfer in liquid-liquid extraction processes are the drop size distribution and the mass transfer coefficients. The pattern of change of these parameters has been studied by various experimental methods (e.g., photography, sedimentation, transmission and dispersion of light) under a wide variety of conditions.[16,17,104]

(1) Interfacial Area of Contact:

Starting from the equality of the capillary pressure and the dynamic pressure of the turbulent pulsating eddies, one could obtain the following equation for the average diameter of a dispersed liquid:[40,105]

$$d = K_1 \frac{\gamma^{0.6}}{\rho_c^{0.2} \phi^{0.4}} \qquad \text{(II-23)}$$

The same formula had been obtained by Hinze[33] from the condition that the ratio of the drop's kinetic energy and surface energy is constant (for maximum stability of the drop diameter, $K_1 = 0.725$). Vermeulen et al.[34] have studied the dispersion of liquids in two geometrically similar mechanically agitated columns. They found that the mean volume surface drop diameter can be

calculated from Equation (II-23) with K_1 = 0.0835. The value of ϕ is related to a unit volume of the liquid being mixed. Miyauchi and Oya[44] studied the fine dispersion which occurs in a pulsed sieve-plate column, using a liquid system MIBK-Water and failed to find the law governing the change in K_1.

Little work has been done on dispersion in continuous flow extraction columns. Strand et al.[22] studied the law governing this phenomenon in RDC's. Attempts by Olney[45] to determine drop diameter in an extraction column from the characteristic drop velocity, can hardly be considered as legitimate, because coalescence and redispersion have not been taken into account. In fact, the literature contains no quantitative data on the effect of mass transfer on the drop diameter and the interface surface.

Finally, it may be noted that the rate of mass transfer is determined, not only by the area of the interface surface, but also by the actual drop size of the dispersion.

(2) Mass Transfer Coefficients:

The problems of mass transfer in extraction columns have attracted the attention of many workers. The complexity of the process is due to the fact that it is usually governed by the diffusion, both in continuous and dispersed phases, and the transfer of the solute in the latter phase is unsteady.

Unfortunately, there are no reliable methods for direct evaluation of mass transfer coefficients in the two phases or for their determination from the values of the overall mass transfer coefficients.

The difference between the mass-transfer mechanisms in the continuous and the dispersed phases, reduces to a marked difference between the methods proposed for their description.

(a) For the Dispersed Phase:

The simplest model of mass-transfer in a drop[41] (assuming it is confirmed) postulates the absence of circulation currents and transfer of solute exclusively by molecular diffusion. Furthermore, it is assumed that the limiting stage of mass-transfer is the diffusion resistance of the dispersed phase.

The solutions given by Calderbank,[46] Handlos,[47] and Thornton[24] for the degree of saturation of a single drop by a substance diffusing into it, enable us to proceed to an expression for K_{d_i} (the coefficient of mass transfer of phase i).

In the work done by Skelland et al.[48,49,105] and Wellek et al.,[50] the equations for K_d for various models are given as follows:

1. For "Hard Globule" Model"

$$K_d = \frac{d}{6\tau} \ln \frac{6}{\pi^2} \sum_{n=1}^{\infty} \left[\frac{1}{N^2} \exp \left(- \frac{N^2 D_d \pi^2 \tau}{(d/2)^2} \right) \right] \qquad \text{(II-24)}$$

2. For "Circulation Currents in the Drop" Model:

$$K_d = - \frac{d}{6\tau} \ln \frac{3}{8} \sum_{n=1}^{\infty} \left[B_n^2 \exp\left(-\lambda_n \frac{16 D_d \tau Pe}{(d/2)^2} \right) \right] \qquad \text{(II-25)}$$

where B_n and λ_n are coefficients of the series.

3. For "Turbulent Mixing" Model:

$$K_d = - \frac{d}{6\tau} \ln 2 \sum_{n=1}^{\infty} \left[B_n \exp\left(-\lambda_n \frac{16 D_d \tau Pe}{2048\ d^2} \right) \right] \qquad \text{(II-26)}$$

At drop saturation less than 0.5 Equation (II-24) reduces to the following:

$$K_d = - \frac{d}{6\tau} \left[1 - \frac{\pi D_d^{1/2} \tau^{1/2}}{(d/2)} \right] \qquad \text{(II-27)}$$

and Equation (II-25) to the following:

$$K_d = - \frac{d}{6\tau} \ln \left[1 - R_e^{1/2} \frac{\pi D_d^{1/2} \tau^{1/2}}{(d/2)} \right] \qquad \text{(II-28)}$$

For conditions of intensive circulation (or fluctuation) in the drop, and by stopping at the first term of the series, Equation (II-26) becomes:

$$K_d = \frac{0.00375\ \bar{V}}{1 + \frac{\mu_d}{\mu_c}} \qquad \text{(II-29)}$$

It has been established[41] that the circulation within a drop is observed, provided that:

$$d_K > 2 \left(\frac{\gamma}{\Delta \rho g} \right)^{0.5} \qquad \text{(II-30)}$$

(b) For the Continuous Phase:

Higbie[51] postulated a theory of penetration. According to this, mass transfer in the continuous phase is effected directly by the transient molecular diffusion towards the interface and away from it to the core of the current in a time $\Delta\tau$.

His equation to determine the coefficient of mass-transfer in the continuous phase during its contact with a drop of diameter (d_K) is given by:

$$k_c = 2\sqrt{\frac{D_c \bar{V}}{\pi d}} \qquad \text{(II-31)}$$

To describe the mass transfer in the continuous phase, Danckwerts[33] proposed a model for the surface renewal, by this means it was found that:

$$k_c = \sqrt{D_c S} \qquad \text{(II-32)}$$

where S is the specific rate of surface renewal.

Levich[52] allowed for the nature of the movement of the continuous phase around a drop and gave the following equation for the mass-transfer coefficient for the continuous phase:

$$k_c = \sqrt{\frac{2}{3}}\left(\frac{D_c V}{d/2}\right)^{0.5} \frac{1}{\sqrt{1 + \mu_d/\mu_c}} \qquad \text{(II-33)}$$

This equation is limited for the conditions $R_e < 1$ (for the drop).

Kafarov[53] concluded that in the presence of developed turbulence the substance is transferred mainly by turbulent diffusion, so that the effect of the individual diffusion properties of the system become negligible. According to Levich, the coefficient of molecular diffusion retains its value under any hydrodynamic conditions.

Conclusions

The holdup model is accurate to predict the holdup fraction of the dispersed phase at any level of operation. The flooding holdup values predicted by this model seemed fairly higher than the actual level at which flooding takes place. Therefore, a safety factor of 15% more was allowed to make sure that the process has not reached the critical region.

If the mechanically agitated column is different in type from the one used in this study (e.g. Oldshue, Treybal, Misek, Scheibel, and Mixer-Settler), and it is desired to replace the axial mixing correlation by a more accurate one, it can be carried out easily by replacing the equivalent set of statements in Subroutine ABMAT given in Chapter 5.

As shown in the above review, the model representing the mass-transfer operation is mainly based on a single drop only. Therefore, it can be used to represent spray columns where the dispersed phase is introduced in a form of a spray. However, they could hardly represent extrac-

tion columns with intense phase mixing, accompanied by repeated fine subdivision and coalescence of the drops and severe checks to the dispersed phase.

Under these circumstances, a theoretical description of mass exchange is made difficult by many factors such as the paucity of data on the laws governing the formation of the interface surface and the absence of methods for direct determination of the coefficient of mass transfer.

Finally, it would be advantageous to by-pass the direct involvement in the experimental evaluation of these coefficients by solving the steady-state mass transfer equations in a dimensionless form and to calculate the NTU's, which includes the overall mass transfer coefficient and the interfacial area of contact.

Details about the steady-state mass-transfer equations, numerical solution, the computer program written for this purpose and graphical representation for the numerical results are presented in the next chapter.

TABLE 1

RECOMMENDED OPERATING CONDITIONS

Operating Conditions	Moderate		Intensive	
Separation Coefficient	$m \ll 1$	$m \gg 1$	$m \ll 1$	$m \gg 1$
Influence of Longitudinal Mixing Negligible	$F \equiv d$	$F \equiv c$	$F \equiv c$	$F \equiv d$
Influence of Longitudinal Mixing Dominant	$F \equiv c$	$(F \equiv d)$	$F \equiv c$	$(F \equiv d)$
Forward Mixing	$F \equiv d$			

TABLE 2

VALUES OF K(0) (Misek)

Operating Conditions		Moderate		Intensive	
		$\frac{1}{K_d} << \frac{1}{m_c K_c}$	$\frac{1}{K_d} >> \frac{1}{m_c K_c}$	$\frac{1}{K_d} << \frac{1}{m_c K_c}$	$\frac{1}{K_d} >> \frac{1}{m_c K_c}$
Influence of Longitudinal Mixing Negligible	$HTU > \frac{1}{R_d}\frac{E_c}{V_c}$	$m\left(\frac{D_s}{D_f}\right)^{2/3}\left(\frac{\rho_f}{\rho_s}\right)^{1/2} \times \left(\frac{\mu_f}{\mu_s}\right)^{5/2}$	$\frac{1}{m}\left(\frac{\rho_f}{\rho_s}\right)^{1/3}\left(\frac{\mu_f}{\mu_s}\right)^{1/3} \frac{1+\frac{\mu_s}{\mu_f}}{1+\frac{\mu_f}{\mu_s}}$	$m\left(\frac{D_s}{D_f}\right)^{2/3}\left(\frac{\rho_s}{\rho_f}\right)^{5/6} \times \left(\frac{\mu_f}{\mu_s}\right)^{1/12}$	$\frac{1}{m}\left(\frac{\rho_f}{\rho_s}\right)^{4/3}\left(\frac{\mu_f}{\mu_s}\right)^{1/3}$
Influence of Longitudinal Mixing Dominant	$HTU < \frac{1}{R_d}\frac{E_c}{V_c}$	$\frac{1}{m^2R^2}\left(\frac{\rho_f}{\rho_s}\frac{\mu_f}{\mu_s}\right)^{1/3}$		$\frac{1}{m^2R^3}\left(\frac{\rho_f}{\rho_s}\right)^{4/3}\left(\frac{\mu_f}{\mu_s}\right)^{1/3}$	

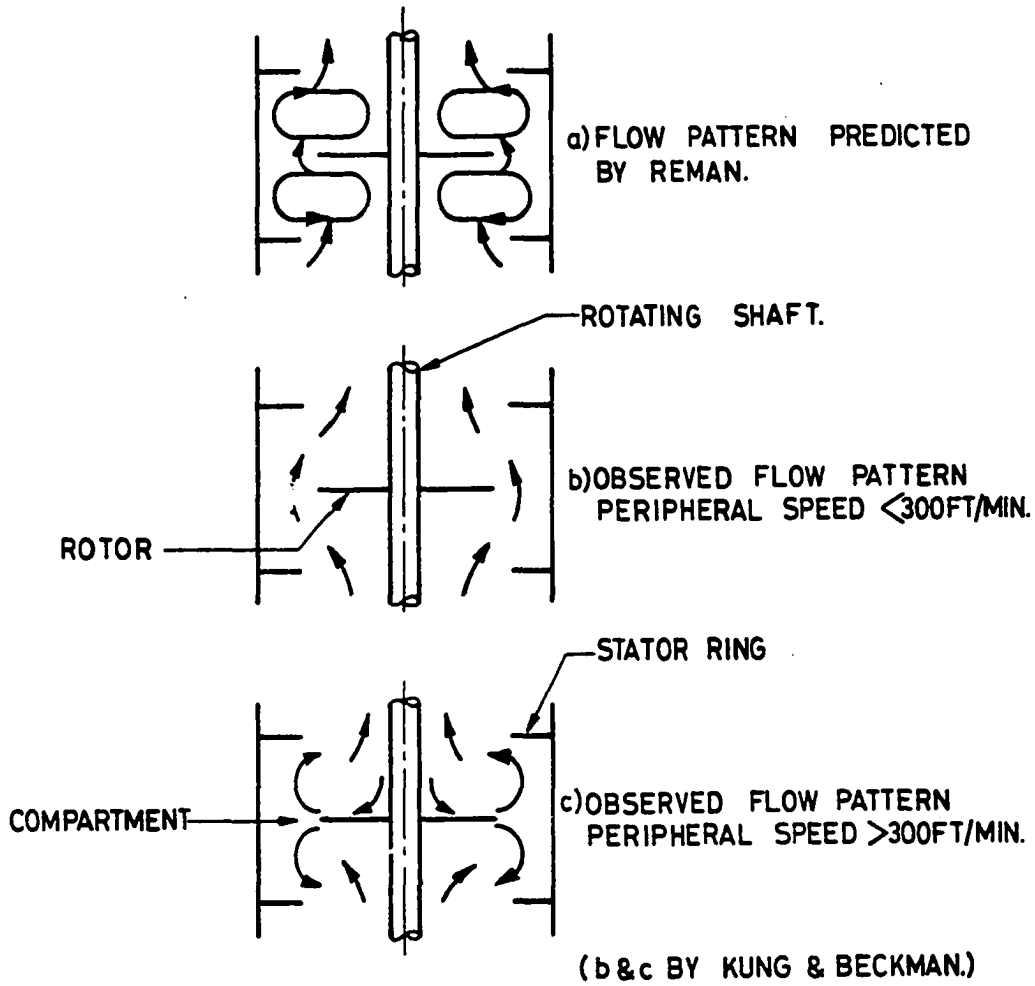

FIGURE 2
DISPERSED PHASE FLOW PATTERNS IN ONE COMPARTMENT OF A RDC.

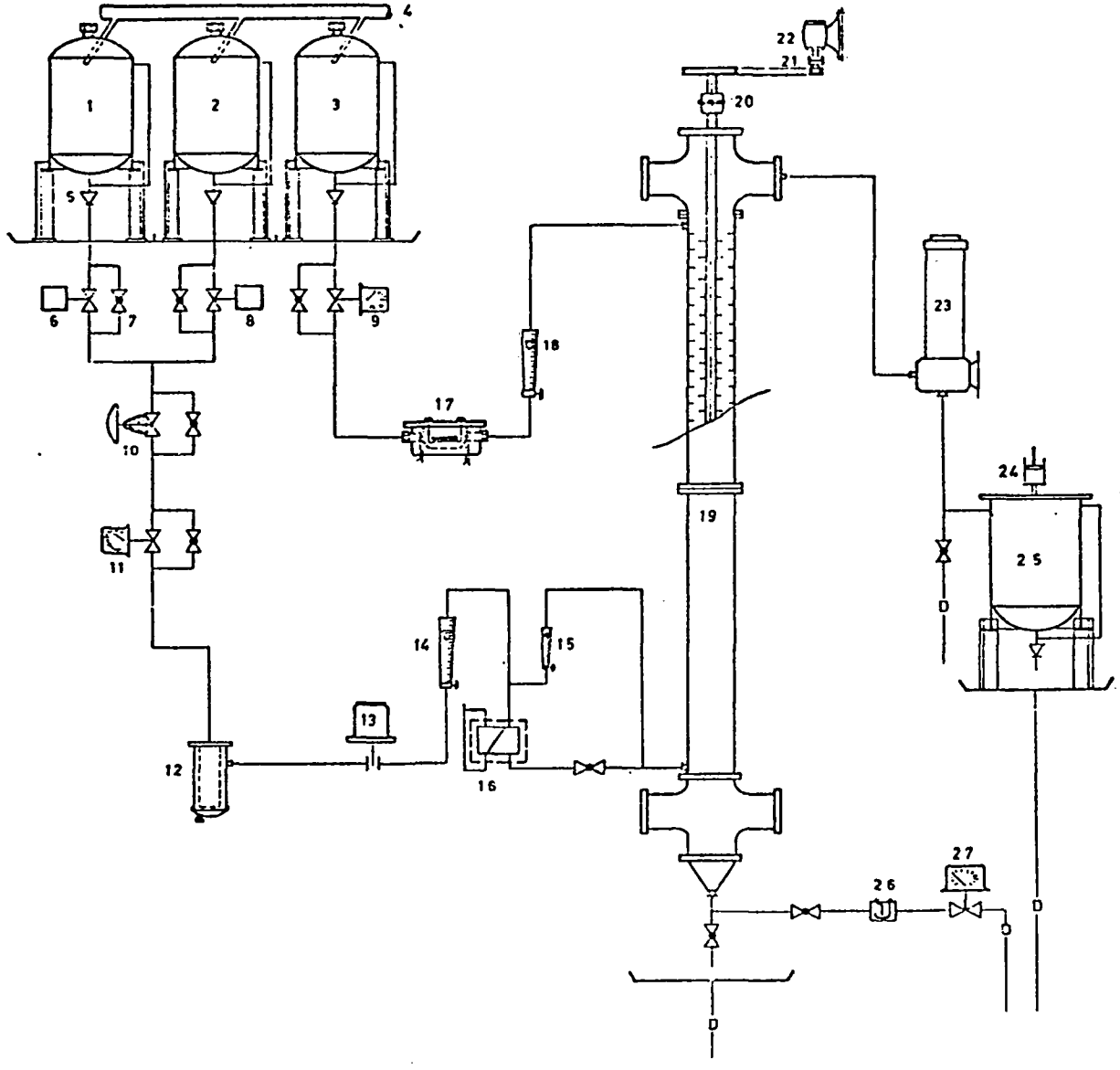

1 FEED PHASE TANK NO.1.
2 FEED PHASE TANK NO.2.
3 SOLVENT PHASE TANK
4 VENTILATION MANIFOLD.
5 CHECK VALVE (Four).
6 SOLENOID VALVE (Normally Open).
7 GLOBE VALVE (Nine).
8 SOLENOID VALVE (Normally Closed).
9 MOTORISED VALVE (On The Solvent Line).
10 PNEUMATIC VALVE.
11 MOTORISED VALVE (On The Feed Line).
12 FILTER (-250 mesh).
13 ORFICE METER.
14 ROTAMETER (For The Feed Phase).
15 ROTAMETER (To Regulate The Amount Of Feed Going Through The Refractometer).
16 REFRACTOMETER.
17 HOT WIRE ANEMOMETER.
18 ROTAMETER (For The Solvent Phase).
19 ROTATING DISK CONTACTOR.
20 COUPLING.
21 GEAR BOX.
22 MOTOR.
23 SPECIFIC GRAVITY METER.
24 PUMP
25 RAFFINATE PHASE TANK.
26 CONDUCTIVITY METER.
27 MOTORISED VALVE (On The Extract Line).

Fig.3: FLOWCHART FOR A LIQUID-LIQUID EXTRACTION PROCESS.

(ON-LINE COMPUTER CONTROL FOR THE PERFORMANCE OF AN RDC)

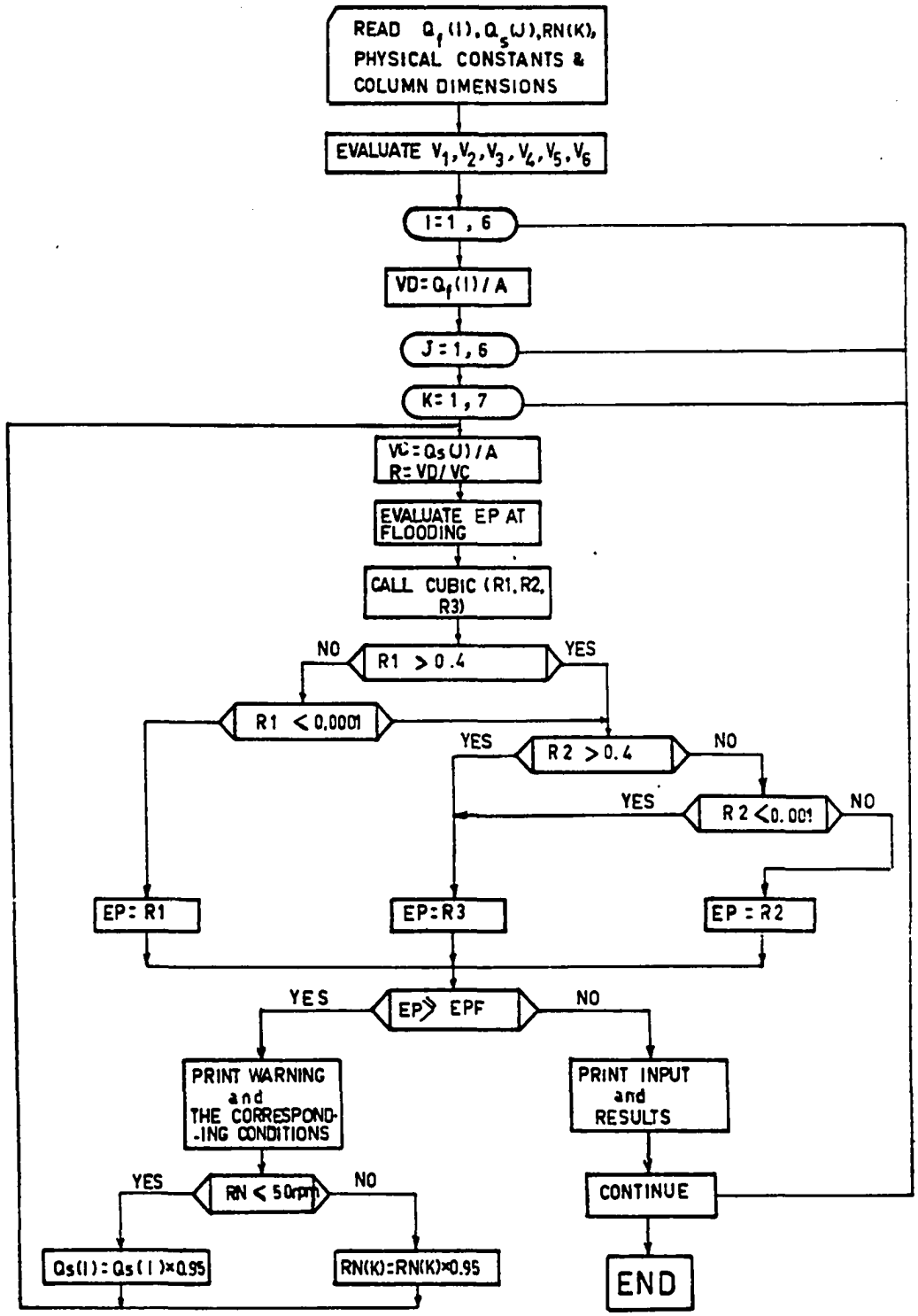

Fig 4. Flowdiagram For The Holdup Program.

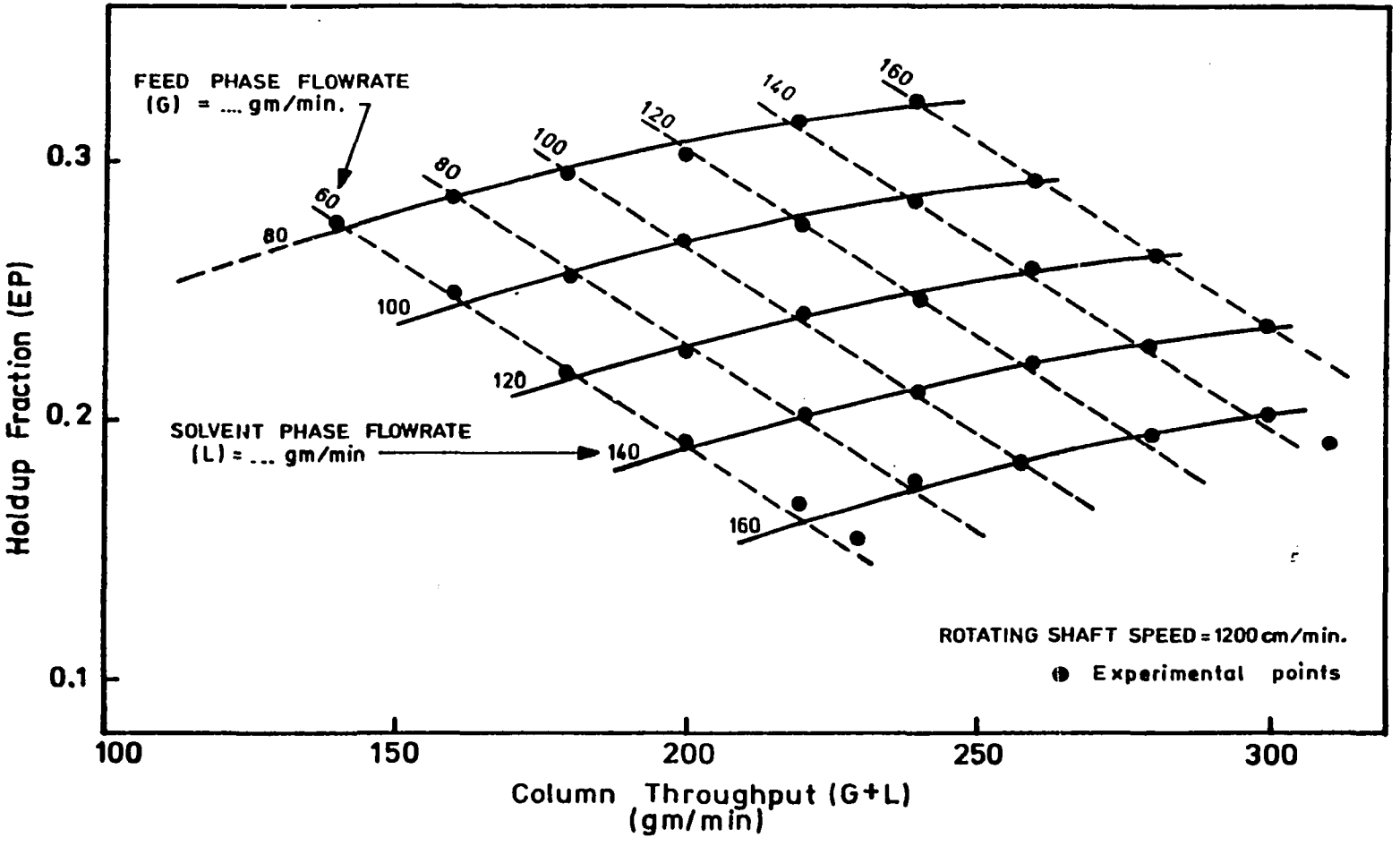

FIG. 5. EFFECT OF THROUGHPUT ON THE HOLDUP VOLUME FRACTION OF THE DISPERSED PHASE

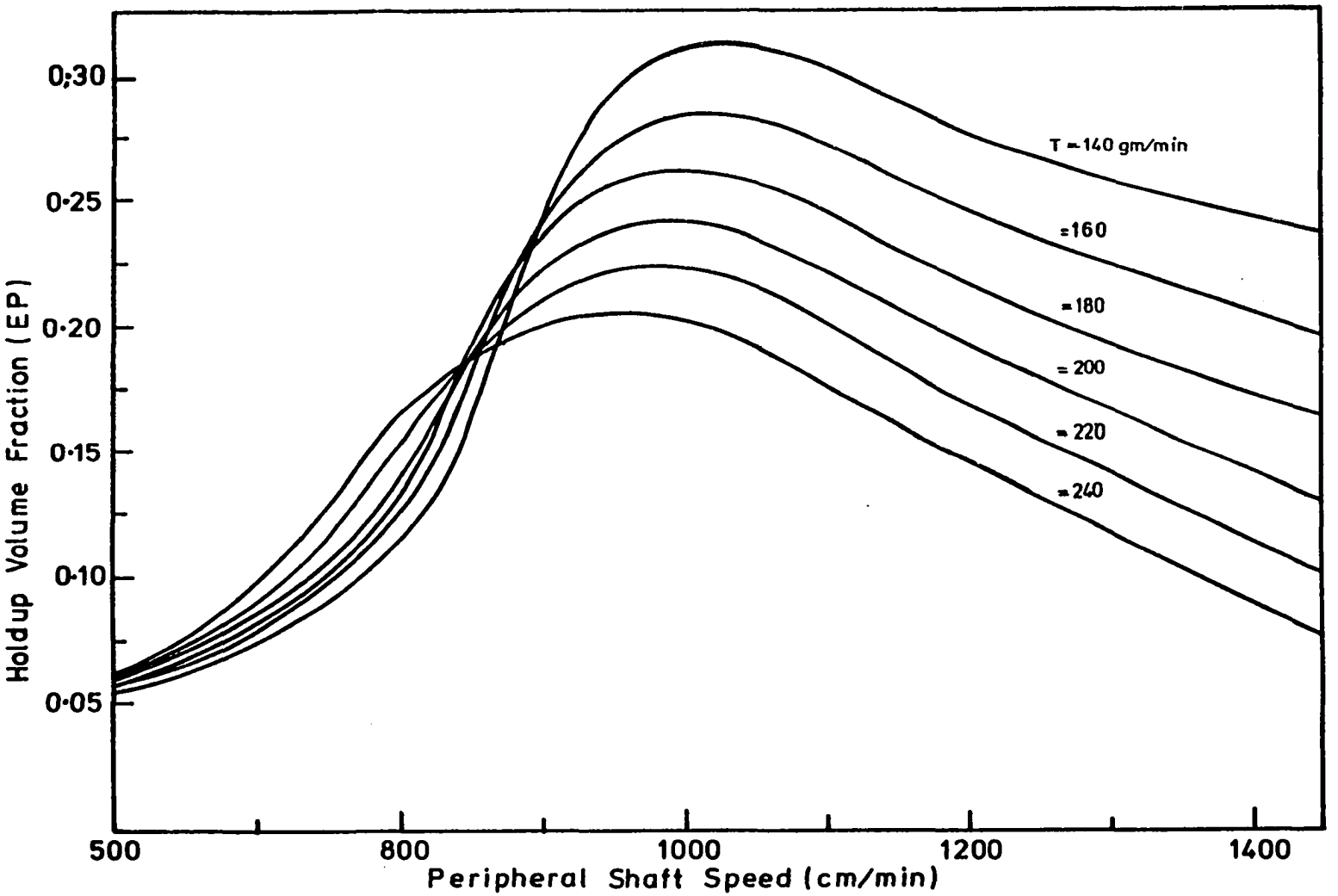

FIG. 6. EFFECT OF SHAFT SPEED ON THE HOLDUP
FOR CONSTANT THROUGH-PUT (T) AND FLOWRATE RATIO (G/L)
(FOR CONVERSION : G= 60 gm/min.)

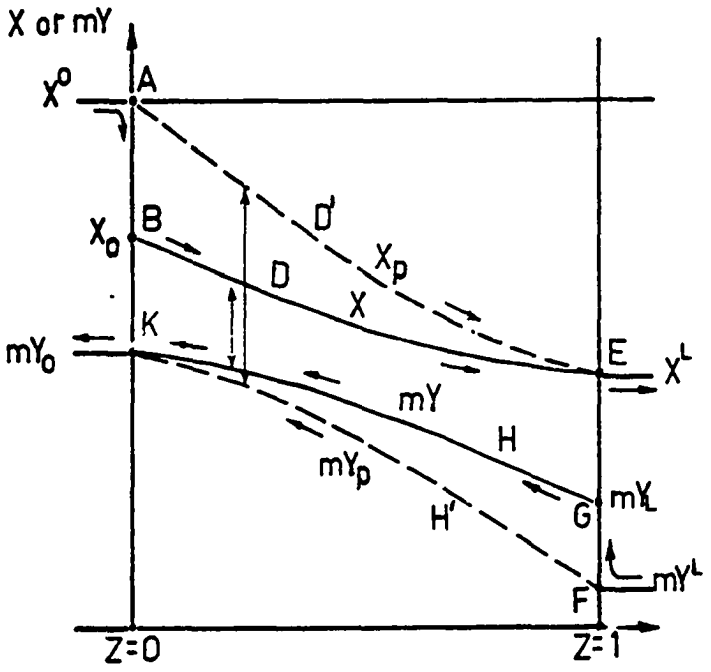

Fig. 7 : Concentration distribution in an extractor;
1.curve ABDE, actual distribution of X,
2.curve FGHK, same for Y,
3.curve AD'E, apparent distribution of X,
4.curve FH'K, same for Y.

(Miyauchi and Vermeulen (1963)).

CHAPTER III

STEADY STATE MODELLING

Introduction

There are two ways of modelling mass-transfer operations in continuous countercurrent liquid-liquid extraction processes:

1. Differentially continuous models, in which a differential element is the unit for material balance. A schematic diagram for this type of presentation is shown in Figure 8. The general mathematical structure of this type of model is a second order ordinary differential equation which could be linear or nonlinear, and homogeneous or non-homogeneous, depending on the conditions of mass-transfer proposed in the assumptions.
2. Stagewise discrete models, in which a discrete actual mixed cell or theoretical stage is used as a unit for material balance. Figure 8 shows a schematic diagram for this type of presentation. Exchange of material between two adjacent stages is due to net flows, (L and G), of the main streams and an additional backflow, of the mixed phases,

which occurs in each direction and is the sum of individual phase backflows s (solvent) and f (feed). Therefore, the total flows between adjacent stages are G + f,s and L + s,f.

For the limiting case of s + f → 0, this system reduces to a "stage model" of perfectly mixed cells in cascade. For another limiting case, with n >> 1, the system reduces to the "differential model" which assumes mean diffusivities and mean velocities for both continuous and dispersed phases (simplified case).

The longitudinal and backmixing coefficients are defined by equations (II-19) to (II-22) given in Chapter II. Backmixing will be taken to mean entrainment of one phase in the main flow of the other in stagewise models, and longitudinal dispersion or eddy diffusion in the differentially continuous one. The effect of backmixing on efficiency for continuous countercurrent extraction processes for different starting assumptions is studied here.

Continuous Model with Axial Dispersion

The model developed by Sleicher[54] is an idealized diffusion model for a three-component physical system. The following assumptions are postulated:

1. The backmixing of each phase may be characterized by a constant axial diffusion coefficient.
2. The boundary conditions assumed for models of this type, which are determined by materials balances

around each phase at each end of the column and have been discussed at some length in the literature[35] are applicable here.

3. The velocity and concentration of each phase are constants across that part of the column which is occupied by the phase.
4. The solvent and solute-free raffinate phases are immiscible (or their solubility does not change with solute concentration and hence the column height).
5. The volume flow rates for the solvent and carrier phases do not change with height.
6. The distribution coefficient is constant and is not a function of concentration.
7. The product of mass transfer coefficient and the interfacial area per unit volume is constant throughout the column.
8. The gradients of solute concentration in each phase are continuous, that is, there are no discontinuities of the type that would occur in a series of discrete well-mixed stages.

Figure 8 shows the notation and the model parameters based on these assumptions. The governing differential equation is:

$$-G \frac{dx}{dh} + AE_x \frac{d^2x}{dh^2} = K_x aA(x - x^*) \qquad \text{(III-1a)}$$

$$-L \frac{dy}{dh} - AE_y \frac{d^2y}{dh^2} = K_x aA(x - x^*) \qquad \text{(III-1b)}$$

The boundary conditions are:

$$-AE_x \frac{dx}{dh} + Gx = Gx_{in} \quad \text{at } h = 0 \qquad \text{(III-2)}$$

$$\frac{dy}{dh} = 0 \quad \text{at } h = 0$$

$$AE_y \frac{dy}{dh} + Ly = Ly_{in} \quad \text{at } h = Z \qquad \text{(III-3)}$$

$$\frac{dx}{dh} = 0 \quad \text{at } h = Z$$

When $E_x = E_y = 0$, the model reduces to that for plug-flow condition. When $E_x = E_y = \infty$, there is perfect mixing in both phases and the column becomes one large stirred tank.

The general solution of Equation (III-1) with the boundary conditions given by Equations (III-2) and (III-3) is developed, for constant backmixing and linear equilibrium relationship, analytically by both Sleicher[55] and Hartland and Mecklenburgh.[56,57]

A computer program (STSTM #1) has been written to calculate the concentration profiles for wide range of operating conditions.

Continuous Model with Longitudinal Dispersion

Miyauchi[27,31] in a similar study to that conducted by Sleicher, made his starting point the equation of continuity developed by Damköhler for single-phase continuous

flow shown below:

$$\frac{\partial x_j}{\partial \tau} = - \text{div}(-D_j \text{ grad } x_j) - \text{div}(\vec{u} x_j) - \phi(x_j) \qquad \text{(III-4)}$$

For a one-dimensional steady-state flow system in which constant diffusivity of the j-th component can be assumed, Damköhler's equation becomes:

$$E_z \frac{d^2 x_j}{dh^2} - U_j \frac{dx_j}{dh} - \phi(x_j) = 0 \qquad \text{(III-5)}$$

Two phase coutercurrent systems can be treated by an extension to this equation. This can be achieved by introducing the volume fraction for each phase, and substituting the mass transfer term for $\phi(x_j)$:

$$\begin{aligned} \varepsilon_x E_x \frac{d^2 x}{dh^2} - F_x \frac{dx}{dh} - K_x a(x - my) &= 0 \\ \varepsilon_y E_y \frac{d^2 y}{dh^2} + F_y \frac{dy}{dh} + K_x a(x - my) &= 0 \end{aligned} \qquad \text{(III-6)}$$

These equations are basically the same as Equation (III-1), and both are based on the assumption that the dispersed phase behaves as another continuous phase. This is a fairly reasonable assumption provided that enough coalescence and redispersion take place in the continuous process.

Rearranging the above equations into dimensionless form, gives

$$\frac{d^2X}{dZ^2} - Pe_x \frac{dX}{dZ} - T_x Pe_x (X - mY) = 0$$

$$\frac{d^2Y}{dZ^2} + Pe_y \frac{dY}{dZ} + T_y Pe_y (X - mY) = 0 \qquad \text{(III-7)}$$

where $X = x/x^o$, $Y = y/x^o$, $Pe_x = U_x H/E_x$, $Pe_y = U_y H/E_y$, $T_x = K_x aH/F_x$, $T_y = K_y aH/F_y$, $U_x = F_x/\varepsilon_x$, $U_y = F_y/\varepsilon_y$, and $Z = h/H$.

Boundary Conditions

At $Z = 0$

$$-\left(\frac{dX}{dZ}\right) = Pe_x(1 - x_o), \qquad -\left(\frac{dY}{dZ}\right) = 0$$

At $Z = 1$ (III-8)

$$-\left(\frac{dX}{dZ}\right) = 0, \qquad -\left(\frac{dY}{dZ}\right) = Pe_y(Y_1 - Y^1)$$

Figure 9 shows a diagramatic presentation for the conditions of flow assumed in this model.

A computer program has been written for the solution of the above model equations (STSTM #2), for the same input variables as those used in the previous model (STSTM #1). Figure 10 shows a flow chart for the program. The symbols used in this chart are those used in the original paper by Miyauchi.[27]

A special case for STSTM #2 is the plug- or piston-flow case which has also been solved (STSTM #3) to be used as a guide for a comparison to be carried out between the different cases.

Characteristics of Sleicher's and Miyauchi's Models (STSTM # 1 and STSTM # 2)

From numerical results obtained for the concentration profiles at wide range of operating conditions, the following characteristics can be deduced:

1. Both models resemble each other and the difference in results were not significant; this is evident from the similarity between the equations solved. The basic difference is in the method of solution. While Sleicher solved the two second order equations separately, Miyauchi augmented them into one fourth order homogeneous differential equation before solving it.
2. The concentration driving force between two-phases is obviously lowered by backmixing in both phases.
3. When longitudinal dispersion is significant, the concentration of the incoming stream increases or decreases abruptly at the point the stream enters the column. On the contrary, the concentration curve for the outgoing streams becomes flat as it approaches the outlet. This is expected from the boundary conditions postulated, Equation (III-8).
4. When extraction is accompanied by longitudinal dispersion, the extent of extraction decreases in comparison with the piston-flow case, especially at high NTU, and low values of Peclet numbers.

Finally, points 1 to 4 given above are well understood in conjunction with Figure 12 given later in this Chapter.

Continuous Model with End Effects

This model has been developed by Wilburn[58] in which the boundary conditions are altered to consider the ends as well as the effective section of the column. Figure 12 shows the schematic for this new representation.

Model Equations

In this representation a separate set of equations has been written for each section of the column. The total height, in dimensionless form, of the column becomes equal to ($\delta + 1.0 + \Delta$), the x-phase is introduced at Z = 0, and leaves at Z = $1.0 + \Delta$, while y-phase is introduced at Z = 1.0, and leaves at Z = $\delta + 1.0$.

The region $\delta \leq Z \leq 0$ is given the number 1, $0 \leq Z \leq 1$ is given the number 2, and $1 \leq Z \leq 1 + \Delta$ is given the number 3.

Region 1:

The x-phase convection term vanishes in Equation (III-6) and can be written as follows:

$$\varepsilon_x E_x \frac{d^2x_{(1)}}{dh^2} - K_x a[x_{(1)} - my_{(1)}] = 0$$

$$\varepsilon_y E_y \frac{d^2y_{(1)}}{dh^2} + F_y \frac{dy_{(1)}}{dh} + K_x a[x_{(1)} - my_{(1)}] = 0 \qquad \text{(III-9)}$$

Region 2:

The two equations represented in this section (the effective height of the column) are similar to those given

by Equation (II-6) and can be written as follows:

$$\varepsilon_x E_x \frac{d^2x_{(2)}}{dh^2} - F_x \frac{dx_{(2)}}{dh} - K_x a[x_{(2)} - my_{(2)}] = 0$$

$$\varepsilon_y E_y \frac{d^2y_{(2)}}{dh^2} + F_y \frac{dy_{(2)}}{dh} + K_x a[x_{(2)} - my_{(2)}] = 0 \qquad \text{(III-10)}$$

Region 3:

The y-phase convection term vanishes in Equation (III-6) which can be written as follows:

$$\varepsilon_x E_x \frac{d^2x_{(3)}}{dh^2} - F_x \frac{dx_{(3)}}{dh} - K_x a[x_{(3)} - my_{(3)}] = 0$$

$$\varepsilon_y E_y \frac{d^2y_{(3)}}{dh^2} + K_x a[x_{(3)} - m_o y_{(3)}] = 0 \qquad \text{(III-11)}$$

The above set of equations (III-9 to 11) for the three sections of the column could be written in a more compact form, using the dimensionless variables (ψ and Γ), as follows:

$$\frac{d^2\psi_j}{dZ^2} - P_j \frac{d\psi_j}{dZ} - TP_j(\psi_j - \Gamma_j) = 0$$

$$\frac{d^2\Gamma_j}{dZ^2} + R_j \frac{d\Gamma_j}{dZ} + TR_j(\psi_j - \Gamma_j) = 0 \qquad \text{(III-12)}$$

for j = 1,2,3, where

$$\psi_j(Z) = \left(\frac{X - mY^1}{1 - mY^1}\right)_j \quad \text{and} \quad \Gamma_j(Z) = \left(\frac{m(Y - Y^1)}{1 - mY^1}\right)_j$$

(Y^1 is the inlet solvent concentration for each section of the column)

$$P_1 \ (\equiv Pe_{x_{(1)}}) = R_3 \ (\equiv Pe_{y_{(3)}}) = 0,$$

$$P_2 = P_3 = P, \quad \text{and} \quad R_1 = R_2 = R$$

Boundary Conditions:

1. At $Z = \delta$

$$\left(\frac{d\Gamma_1}{dZ}\right)_\delta = 0 \text{ and } \left(\frac{d\psi_1}{dZ}\right)_\delta = 0 \qquad \text{(III-13)}$$

2. At $Z = 0$

$$(\psi_1)_0 = (\psi_2)_0; \quad (\Gamma_1)_0 = (\Gamma_2)_0;$$

$$\left(\frac{d\Gamma_1}{dZ}\right)_0 = \left(\frac{d\Gamma_2}{dZ}\right)_0 \qquad \text{(III-14)}$$

$$P[1 - (\psi_2)_0] = \left(\frac{d\psi_1}{dZ}\right)_0 - \left(\frac{d\psi_2}{dZ}\right)_0$$

3. At $Z = 1$

$$(\psi_2)_1 = (\psi_3)_1; \qquad (\Gamma_2)_1 = (\Gamma_3)_1;$$

$$\left(\frac{d\psi_2}{dZ}\right)_1 = \left(\frac{d\psi_3}{dZ}\right)_1 \qquad \text{(III-15)}$$

$$P[0 - (\Gamma_2)_1] = \left(\frac{d\Gamma_2}{dZ}\right)_1 - \left(\frac{d\Gamma_3}{dZ}\right)_1$$

4. $Z = \Delta$

$$\left(\frac{d\psi_3}{dZ}\right)_\Delta = 0 \quad \text{and} \quad \left(\frac{d\Gamma_3}{dZ}\right)_\Delta = 0 \qquad \text{(III-16)}$$

A computer program has been written for the solution of this model equations (STSTM #4). The concentration profiles, for x-phase, for the four developed differentially continuous models are shown in Figure 13.

Input Variables for the Differential Models

In order to evaluate the concentration profile and actual number of transfer units (NTU_M) for a specific column, the following parameters must be evaluated:

1. Peclet numbers for each phase
2. Plug- or piston-flow NTU's, and
3. The extraction factor.

To evaluate the first two, empirical and semi-empirical formulae will be used instead of experimentally determined values. The third will be defined by the equilibrium relationship and mass flow rates of both phases.

1. Peclet's number of each phase has been evaluated for any condition of operation (flow rates and shaft speed), using an empirical formula developed by Westerterp[18] for a column similar in dimensions to the one used in this study. This can be rewritten as follows:

$$Pe_i = \frac{2n}{1 + 0.013\left(\frac{ND_r}{U_i}\right)} \qquad \text{(III-17)}$$

2. Plug- or piston-flow number of transfer units (NTU_p): The logarithmic mean driving force formula given by Treybal[59] is used in this study.

$$NTU_p = \frac{\ln\left\{(1 - \Delta')\frac{X_{in}}{X_{out}} + \Delta'\right\}}{(1 - \Delta')} \qquad \text{(III-18)}$$

Prediction of the Measured Number of Transfer Units (NTU_M)

As shown in Chapter II, there should be three different numerical values of NTU's, depending on the definition of the concentration driving force:

1. True value defined as the ratio of volumetric flow rate across a unit section to the true over-all coefficient of mass-transfer.
2. Measured value defined by the following equation, and which can be evaluated from the concentration profiles for the x- and y-phases:

$$NTU_M = \int_{X|Z=0}^{X|Z=1} \frac{-dX}{X - X^*} \qquad \text{(III-19)}$$

and

$$HTU_M = \frac{1}{NTU_M} \qquad \text{(III-20)}$$

Since Equation (III-19) is calculated in the dimensionless form, Z has been replaced by the value one in Equation (III-20).

3. Plug- or Piston-flow Value defined in terms of the logarithmic-mean driving force, Equation (III-18), calculated from the exterior incoming and outgoing concentrations at both ends of the column.

Equation (III-19) can be evaluated by substituting for x and dx by the equivalent from:

a. Miyauchi's solution (STSTM #2)

$$X - mY = (1 - mY^1) \sum_{j=1}^{4}(1 - a_j)A_j e^{\lambda_j Z}$$

$$dX = (1 - mY^1) \sum_{j=1}^{4} A_j \lambda_j e^{\lambda_j Z} \, dZ \qquad \text{(III-21)}$$

Accordingly, one has:

$$NTU_M = \int_0^1 [\sum_{j=1}^{4} A_j \lambda_j e^{\lambda_j Z} / \sum_{j=1}^{4} (1 - a_j)A_j e^{\lambda_j Z}]dZ \qquad \text{(III-22)}$$

This equation is written for a column with a total height Z = 1 in dimensionless form, considering the total height as an effective section.

b. Backflow Model with Ends Effect Solution (STSTM #4)

The modification given here is developed by the author relying on the principles and conditions developed previously by Miyauchi.

For this model the total height in dimensionless form is the sum of the heights of the three sections (top, effective, and bottom). Therefore, the integration limits for Equation (III-19) will be modified to be from δ to $\delta + 1 + \Delta$ instead of zero to one, and whatever the heights of the two ends in dimensionless form, Z (the middle section) will still be equal to one.

Equation (III-21) can be written for the three sections in compact form as follows:

$$(X - mY)_i = (1 - mY^1)_i \sum_{j=1}^{4}(1 - a_{ij})A_{ij}e^{\lambda_{ij}Z_i}$$

$$(dX)_i = (1 - mY^1)_i \sum_{j=1}^{4} A_{ij}\lambda_{ij}e^{\lambda_{ij}Z_i}\, dZ_i \qquad \text{(III-23)}$$

where i = 1, 2, 3.

Putting $\delta = -0.1$, $Z = 1.0$, and $\Delta = 1.1$ would make the dimensionless height correspond to the column under study.

Equation (III-22) will be written for the three sections of the column with NTU_M being the algebraic sum of the three integrations.

$$NTU_M = \int_{-0.1}^{0.0} [\sum_{j=1}^{4} A_{1j}\lambda_{1j}e^{\lambda_{1j}Z_1} / \sum_{j=1}^{4}(1 - a_{1j})A_{1j}e^{\lambda_{1j}Z_1}]dZ_1$$

$$+ \int_{0.0}^{1.0} [\sum_{j=1}^{4} A_{2j}\lambda_{2j}e^{\lambda_{2j}Z_2} / \sum_{j=1}^{4}(1 - a_{2j})A_{2j}e^{\lambda_{2j}Z_2}]dZ_2$$

$$+ \int_{1.0}^{1.1} [\sum_{j=1}^{4} A_{3j}\lambda_{3j}e^{\lambda_{3j}Z_3} / \sum_{j=1}^{4}(1 - a_{3j})A_{3j}e^{\lambda_{3j}Z_3}]dZ_3 \qquad \text{(III-24)}$$

The computer algorithm developed for the purpose, using STSTM #4 with input variables, Equations (III-17) and (III-18) and measured number of transfer units (NTU_M) calculation, Equation (III-24), shown in Figure 14.

Uses of this algorithm will be pointed out in due course in the chapters to follow on steady-state optimization and dynamic modelling.

Steady-State Experimental Runs

The main purpose of this step is to validate and recommend one of the theoretical models as the most feasible

to represent the process performance under steady-state. The system was operated under steady-state in a procedure similar to the one used for holdup measurements, except, changing from one level of operation to another was made directly by setting up the valves on the desired rates and without purging the column.

Some of the results obtained were used for the comparison purposes. Figure 15 shows five different theoretical methods to calculate the number of transfer units. From this figure one would recommend both steady-state models (with axial mixing and with axial mixing and ends effect) as the best to represent the process performance.

Careful study of the distribution of the experimental points shows a mean square error deviation ($\sqrt{\Sigma e^2/n}$) of (mG/L) for the model with axial mixing (curve 4) equal to 0.437, and for the model with axial mixing and ends effect equal to 0.3655. This would make the use of the last model over the other alternatives advisable.

Finally, these experimental measurements were taken for zero shaft speed which make the degree of entrainment minimum and shows that both models are close in the degree of accuracy. But, it is expected that the model with end effects will be far better for higher shaft speeds as the rate of entrainment will increase. Therefore, the steady-state model with ends effect (STSTM #4) is recommended for later applications.

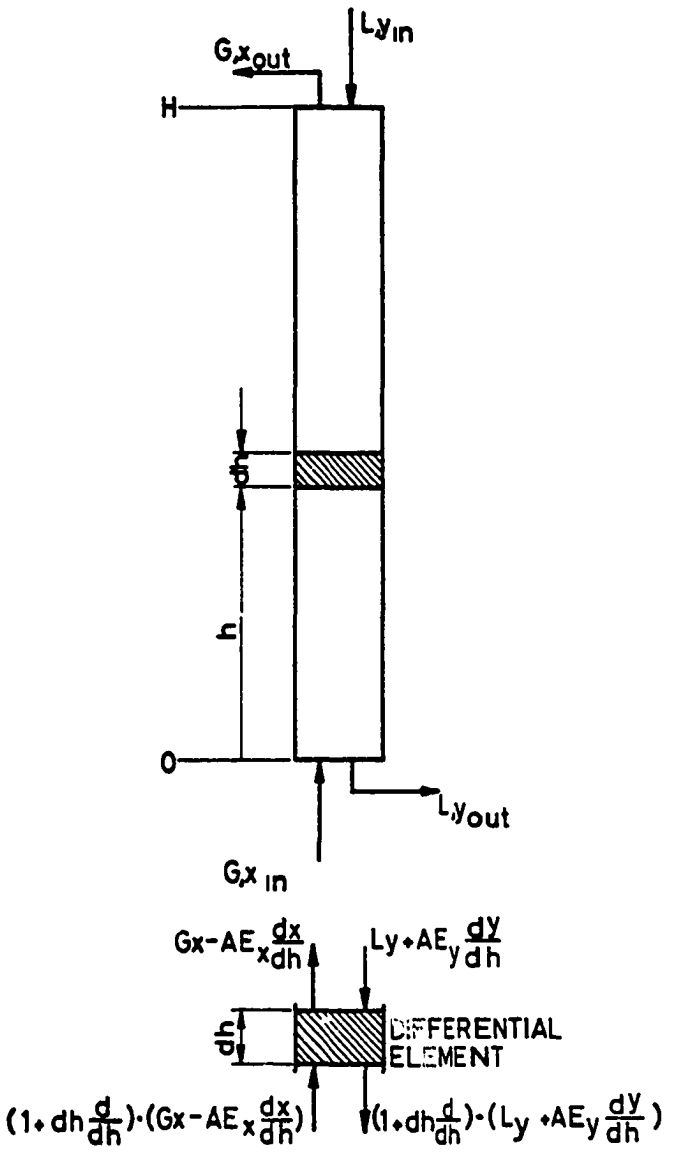

FIG. 8
DIFFERENTIAL BACK MIXING MODEL.

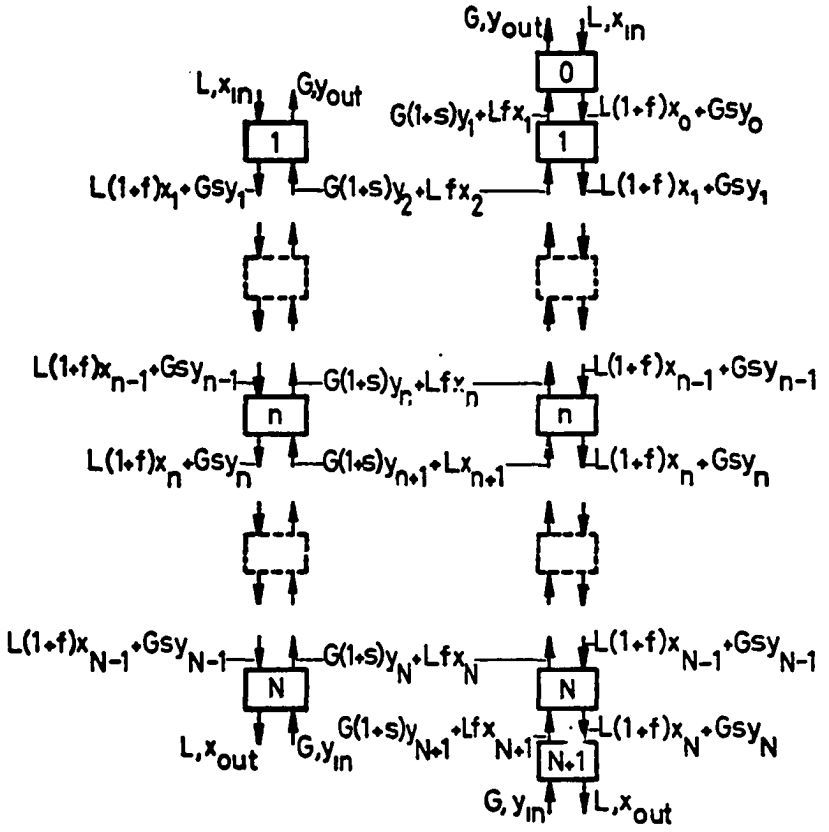

a)ACTUAL FLOWS AND STAGES.

b)WITH FICTITIOUS FLOWS AND STAGES.

FIG. 9
STAGEWISE BACK MIXING MODEL

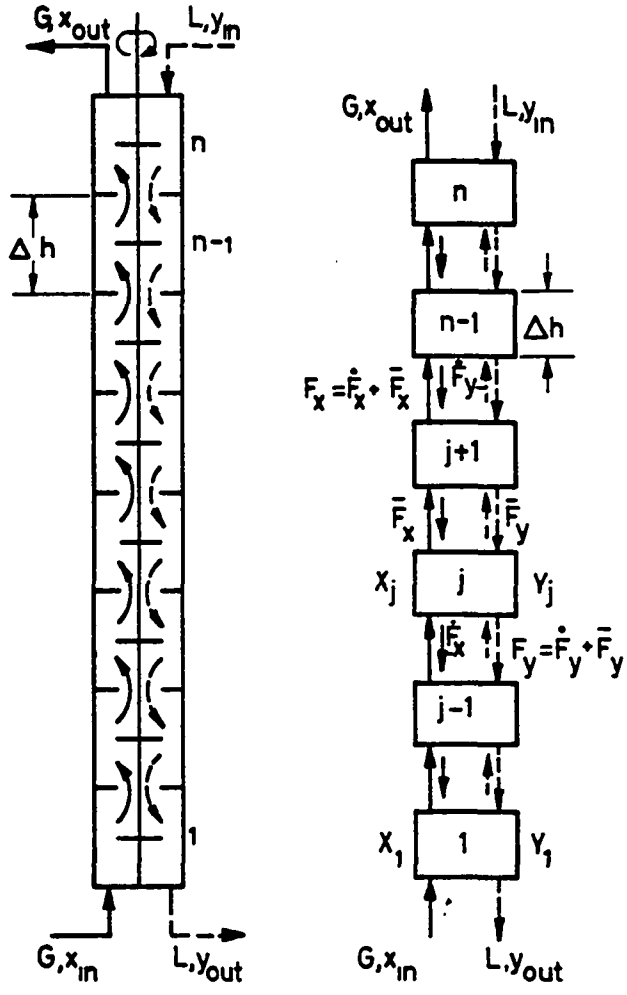

a) MULTICOMPARTMENT R.D.C.

b) IDENTIFICATION OF FLOWS WITH INTERNAL FLOW.

FIG. 10
BACKFLOW MODEL REPRESENTATION FOR A COUNTER CURRENT EXTRACTION PROCESS

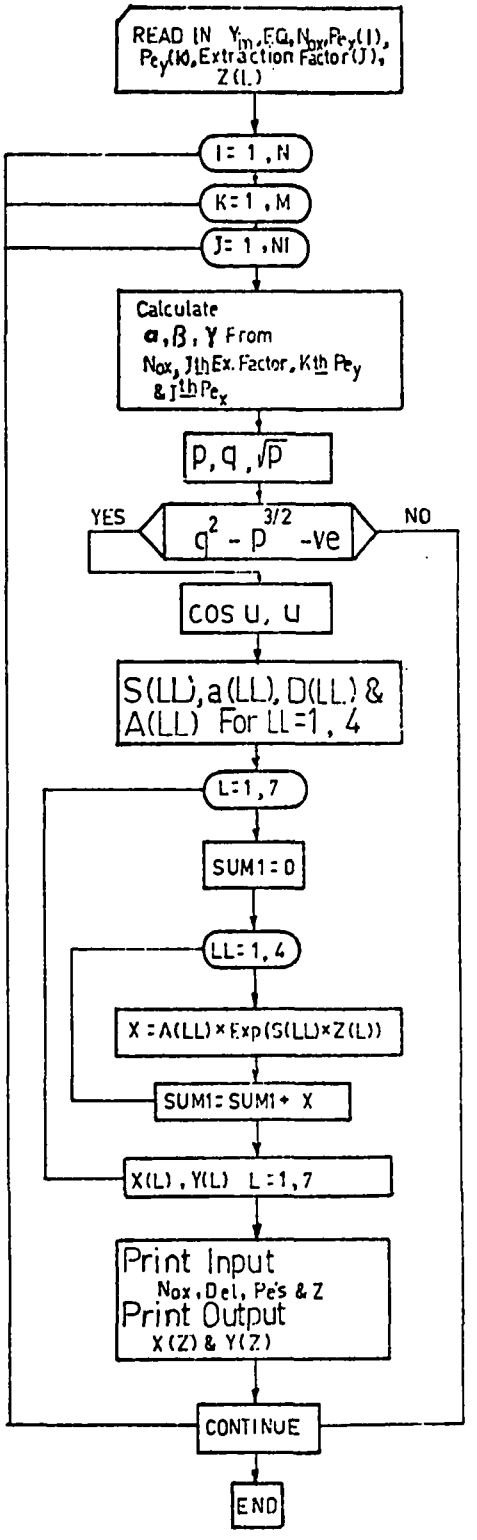

Fig.11. Flowchart For Program-Second.
CONTINUOUSLY-DIFFERENTIAL STEADY-STATE MODEL SOLUTION.

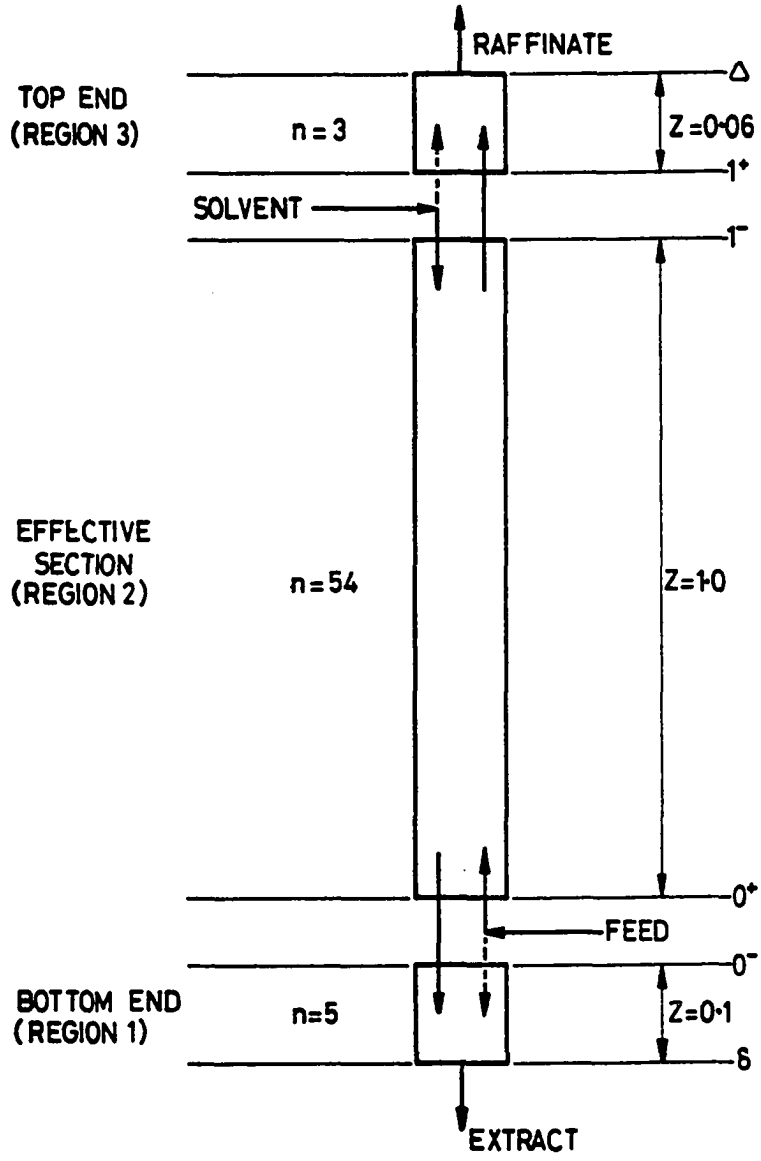

FIG.12
SCHEMATIC OF RDC WITH END EFFECT.

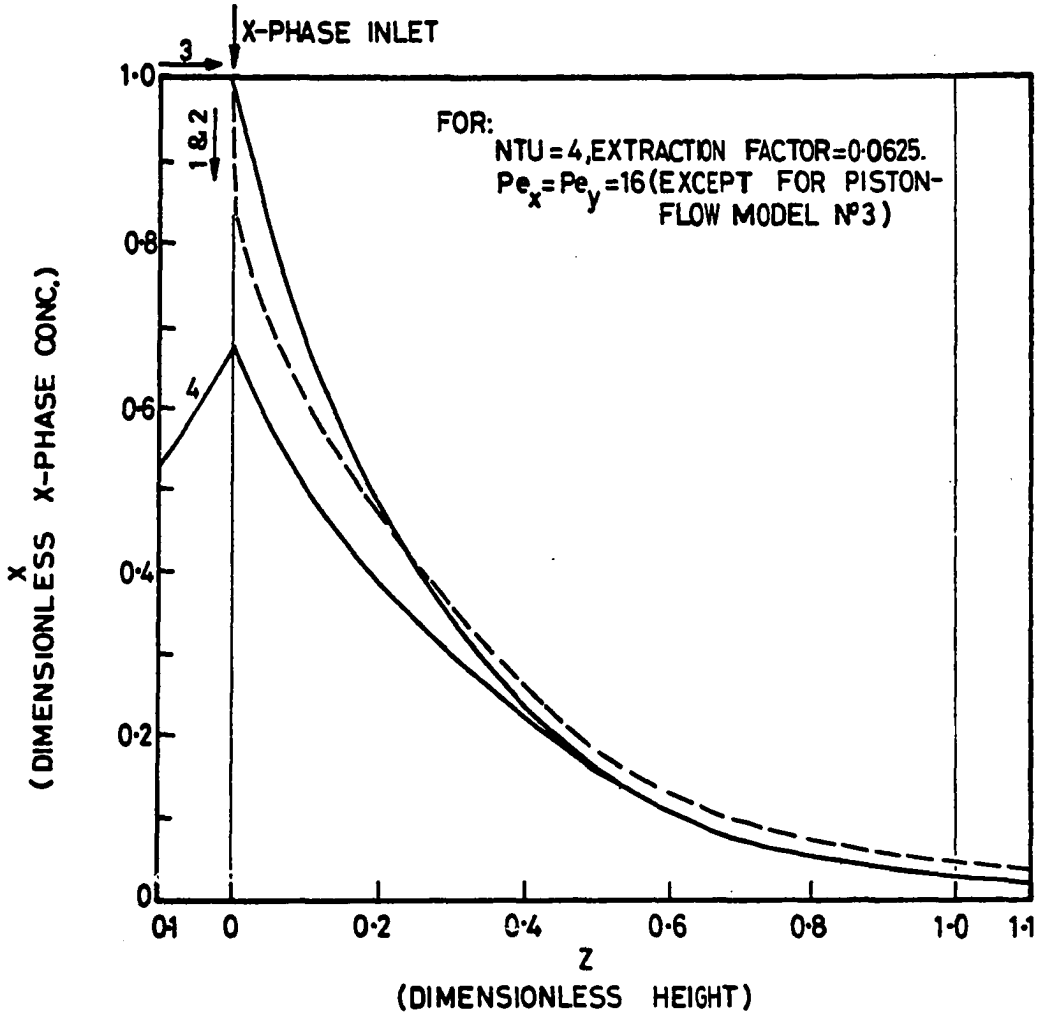

FIG. 13

COMPARISON BETWEEN FOUR STEADY STATE MODELS

1) BACK MIXING MODEL (SLEICHER)
2) BACK FLOW MODEL (MIYAUCHI)
3) PISTON FLOW MODEL
4) BACK FLOW MODEL WITH END EFFECT (WILBURN)

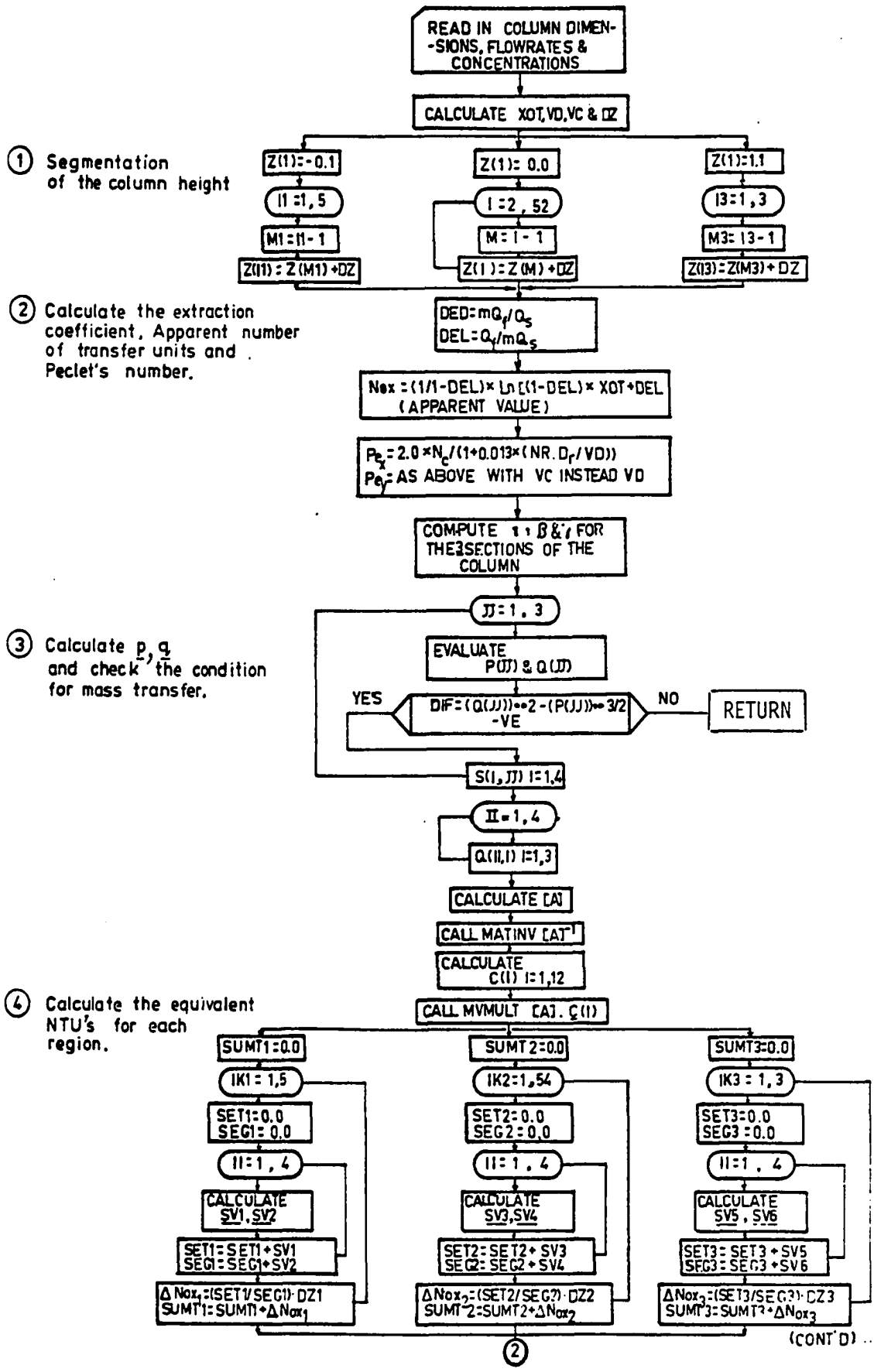
READ IN COLUMN DIMEN-SIONS, FLOWRATES & CONCENTRATIONS
CALCULATE XOT, VD, VC & DZ
① Segmentation of the column height
Z(1):=-0.1
I1 :=1, 5
M1:=I1-1
Z(I1):=Z(M1)+DZ
Z(1):=0.0
I :=2, 52
M:=I-1
Z(I):=Z(M)+DZ
Z(1):=1.1
I3:=1, 3
M3:=I3-1
Z(I3):=Z(M3)+DZ
② Calculate the extraction coefficient, Apparent number of transfer units and Peclet's number.
DED:=mQf/Qs
DEL:=Qx/mQs
Nox :=(1/1-DEL)× Ln[(1-DEL)× XOT+DEL
(APPARENT VALUE)
Pex=2.0×Nc/(1+0.013×(NR.Df/VD))
Pex: AS ABOVE WITH VC INSTEAD VD
COMPUTE τ, β & γ FOR THE 3 SECTIONS OF THE COLUMN
③ Calculate p, q and check the condition for mass transfer.
JJ:=1, 3
EVALUATE P(JJ) & Q(JJ)
YES
DIF=(Q(JJ))**2-(P(JJ))**3/2
-VE
NO
RETURN
S(I, JJ) I=1,4
II=1, 4
Q(II, I) I=1,3
CALCULATE [A]
CALL MATINV [A]⁻¹
CALCULATE C(I) I=1,12
CALL MVMULT [A]. C(I)
④ Calculate the equivalent NTU's for each region.
SUMT1:=0.0
IK1 = 1,5
SET1:=0.0
SEG1:=0.0
II:=1, 4
CALCULATE SV1, SV2
SET1:=SET1+SV1
SEG1:=SEG1+SV2
ΔNox1:=(SET1/SEG1)·DZ1
SUMT1:=SUMT1+ΔNox1
SUMT2:=0.0
IK2=1,54
SET2:=0.0
SEG2:=0.0
II:=1, 4
CALCULATE SV3, SV4
SET2:=SET2+SV3
SEG2:=SEG2+SV4
ΔNox2:=(SET2/SEG2)·DZ2
SUMT2:=SUMT2+ΔNox2
SUMT3:=0.0
IK3 = 1, 3
SET3:=0.0
SEG3:=0.0
II:=1, 4
CALCULATE SV5, SV6
SET3:=SET3+SV5
SEG3:=SEG3+SV6
ΔNox3:=(SET3/SEG3)·DZ3
SUMT3:=SUMT3+ΔNox3
(CONT'D)
②

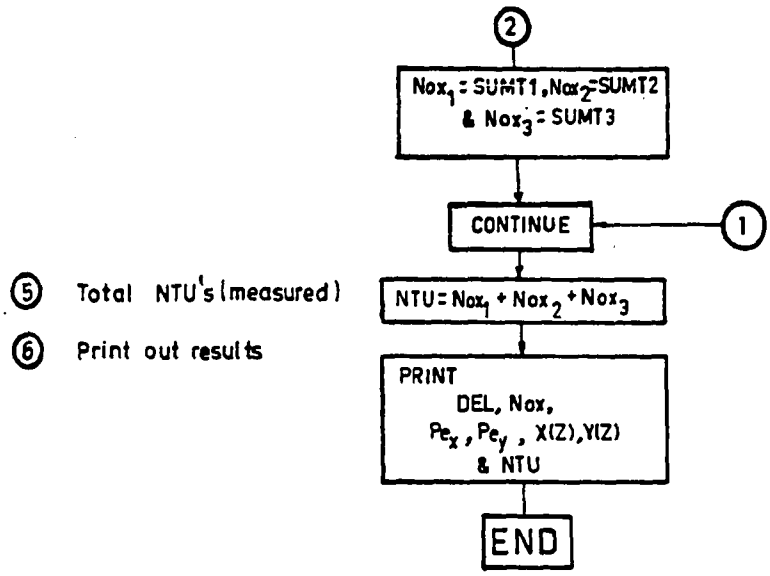

Fig. 14 Differentially-Continuous Model With End Effect.

EVALUATION OF THE ACTUAL 'NTU'

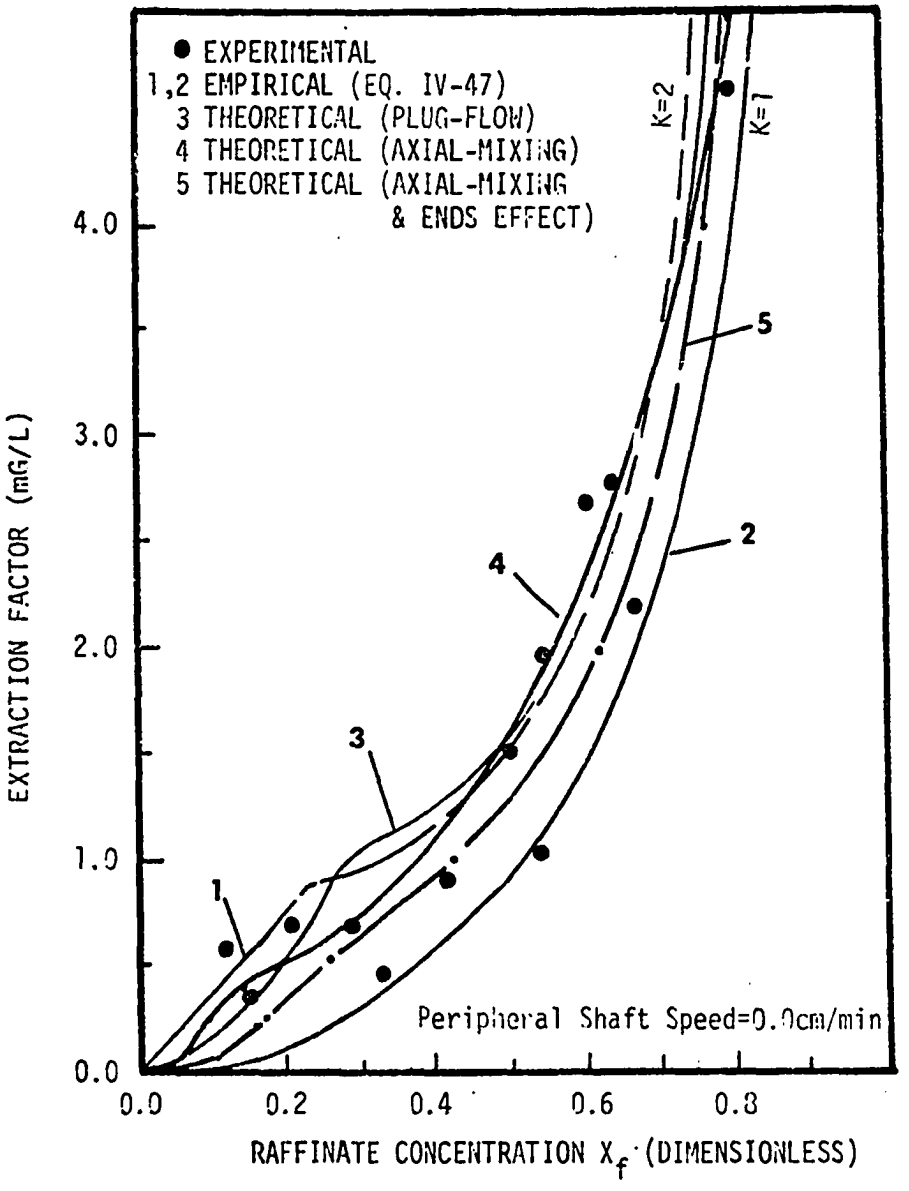

FIGURE 15. RELATION BETWEEN EXPERIMENTAL EMPIRICAL AND THEORETICAL CALCULATION OF THE RAFFINATE EXIT CONCENTRATION FOR DIFFERENT EXTRACTION FACTOR VALUES.

CHAPTER IV

STEADY-STATE OPTIMIZATION

The Objective Function

For commercial purposes, maximum return on investment, or profit, is perhaps the most common criterion for optimum engineering design.

In order to compare different techniques of optimization and to calculate the profit for a particular chemical process, one must formulate the objective function on a realistic basis.

Since the pilot-scale rotating disc contactor under investigation is operating on a physical system which is not used industrially (Amyl Alcohol-Acetic Acid-Water), it is impossible to assign realistic costs and therefore formulate an overall objective function.

Therefore, one is forced to optimize the process performance with respect to an operating objective function, which is only a measure of the effectiveness of the process.

The purpose here is not to discuss the detailed aspects of such an evaluation, but to select a typical form of the cost function which is most likely to satisfy a wide variety of operations, and will keep the complexity of the

problem and its solution within the scope of a particular utility.

The majority of operations demand a product quality within certain tolerances. Deviation from the given specifications may result in loss of product or a product of inferior quality which requires recycling, blending, etc.

The resulting increase in the cost of production can take the form shown graphically by the broken lines in Figure 16, where the quality $\bar{q}$ is measured from a desired reference or set-point $\bar{b}$.

For commercial convenience, this cost-quality relationship is approximated by the solid-line parabola shown on the same figure, and the cost of production resulting from a deviation in product quality is given by $c_2\bar{q}^2$, where c_2 is a constant; the cost of raw materials is considered proportional to the rate of consumption by a factor c_1. Assuming that the product flow rate is constant, the cost equation for the system can be written as follows:

$$f_1(\bar{u},\bar{q}) = c_1\bar{u} + c_2\bar{q}^2 \qquad \text{(IV-1)}$$

This is the basic cost relationship which would be used to optimize the plant performance either for static or dynamic conditions of operation. The difference between them will depend on the definitions of $\bar{u}$ and $\bar{q}$.

For the extraction process shown in Figure 17, the efficiency or effectiveness of the process is measured by the HTU (or HETS) and the column throughput, but for a

mechanically agitated column, the matter would be slightly different and the power should be included as well.

As the hydrodynamics of the process have been studied previously (Chapters II and III), a quantitative mathematical relation has been found to exist between the HTU's and the extraction factor ($\Delta \equiv mG/L$), Peclet numbers, rotating shaft speed, and the column throughput (G + L). The shaft speed, feed phase flowrate, and solvent phase flowrate have been chosen as the manipulated variables while the feed phase inlet concentration is considered constant.

The operating objective function can then be written as follows:

$$f = K_1\left(\frac{L}{NTU}\right)^2 + K_2\left(\frac{N^3D_r^5}{h_c D_r^2}\right)^2 + \frac{K_3}{(G + L)} \qquad \text{(IV-2)}$$

The first term [Eq. (IV-2)] counts for the efficiency of the process (always greater than three times the second term, in absolute value in the feasible operation range); the second term counts for the power input to the rotating shaft; and the third term for the column throughput. The second term of Equation (IV-2) was developed by Reman[7] as a measure of the optimum shaft speed for any given conditions of operation and rotating disc contactor dimensions.

The values of K_i (i = 1, 2, 3) have been specified after a variety of trials to be 0.25, 0.5 x 10^{-2} and 100, respectively. These values weight the three terms of the constrained objective function with respect to each other.

The values assigned to the weighting factors K_i in Equation (IV-2) were such that the operating objective function would include besides the height of transfer unit (HTU), which is a measure of the effectiveness of the mass-transfer process, a second term to represent power which has become a scarce resource, and a third term to count for the throughput of the process. The numerical choice was made such that the effectiveness would be greater or equal to three times the throughput and the latter greater or equal to three times the power input in the most feasible range of operation. The choice was made to make the objective function as close to our experimental system as possible, since the liquid system did not have any industrial value.

For industrial purposes a long term objective function should include raw materials cost, product demand, storage, pumping and equipment depreciation rate. The weighting factors K_i could be easily adjusted to suit any specific case. This will not change the main outlines of the steady-state optimization procedure but will assign different values to the various terms forming the new objective function.

Process Constraints:

1. The extent of extraction (denoted by XOT in subroutine STSMOD) should be equal to or greater than a specified limit to ensure minimum recovery, recycling, and solute waste

$$XOT = \frac{x_{in}}{x_{out}} \geq 2.0$$

or in dimensionless form

$$XOT = \frac{1}{x_{out}} \geq 2.0 \qquad \text{(IV-3)}$$

2. The holdup value for any given conditions of operation should be less than the equivalent flooding holdup value by a certain reasonable safety margin,

$$CR2 = \frac{\varepsilon_f - \varepsilon}{\varepsilon_f} \geq 0.15 \qquad \text{(IV-4)}$$

3. The necessary condition for mass-transfer in a two-phase contact should be ensured. This has been carried out by applying Miyauchi's necessary condition for mass-transfer. It can be written as follows:

$$CR3 = q^2 - p^3 = \frac{1}{27}(\alpha^3\gamma - \alpha^2\beta^2/4 + 9\alpha\beta\gamma/2 - \beta^2 + 27\gamma^2/4) < 0 \qquad \text{(IV-5)}$$

The equivalent meaning of these parameters are given in Appendix A.

4. To evaluate the apparent number of transfer units (NTU_p) using the mean logarithmic driving force, which can be rewritten as follows:

$$NTU_p = \frac{1}{(1 - \Delta)} \ln\left\{\frac{x_{in}}{x_{out}} (1 - \Delta) + \Delta\right\} \qquad \text{(IV-6)}$$

For a new set of conditions of operation determined by the optimization search technique, it might happen that the value of the argument of the logarithm becomes less than or equal to zero. To avoid this difficulty a constraint is imposed on the argument to ensure that it always has a positive value.

$$CR4 = \frac{x_{in}}{x_{out}} (1 - \Delta) + \Delta > 0 \qquad \text{(IV-7)}$$

Process Bounds:

1. The inlet mass flow rates, G and L, must be within the possible valve ranges.

$$\text{Valve 1:} \quad K_{1_{min}} \leq G \leq K_{1_{max}} \qquad \text{(IV-8)}$$

$$\text{Valve 2:} \quad K_{2_{min}} \leq L \leq K_{2_{max}}$$

2. The rotating shaft speed limits must be considered:

$$R_{min} \leq R \leq R_{max} \qquad \text{(IV-9)}$$

Subroutine BOUNDS has been written to include these limits on the process variables.

The CRST Technique

As can be seen from the above discussion, both the objective function and the constraints are nonlinear functions. Spang[60] has reviewed three methods to deal with such systems:

1. Direct Search: in which the actual value of the function is replaced by a very large value whenever the constraints are violated. This pseudo-value must be proportional to the amount the inequality is violated so that the search routine will force the test points towards the region where the inequality can be satisfied.

Thus a typical sequence of equation would be written as follows:

$$\bar{C} = f(\bar{u}_i, \bar{x}_n, \bar{y}_q, t) \begin{cases} T_i(\bar{u}_i, t) = 0, \; i = 1, \cdots, p \leqslant m \\ T_i(\bar{u}_i, t) \geqslant 0, \; i = p+1, \cdots, m \end{cases} \qquad \text{(IV-10)}$$

and

$$\bar{C}_N = 1 \times 10^{20}\left[\sum_{\alpha} |T_\alpha(u_i, t)|\right] + f(\bar{u}_i, \bar{x}_n, \bar{y}_q, t) \qquad \text{(IV-11)}$$

where $\bar{C}_N$ is the value of the function used in the search and the sum, α, consists of these T_i which are not satisfied. $\bar{C}_N$ is now an unconstrained function whose minimization is within or on the boundary of the region defined by the constraints.

2. Lagrangian Method: in which the inequality constraints are converted to equality constraints by introducing a non-negative "slack" variable Π_i. Thus

$$T_i(\bar{u}_i, t) - \Pi_i = 0, \quad (i = p+1, \cdots, m), \; \Pi_i \geqslant 0 \qquad \text{(IV-12)}$$

The lagrangian function could be defined in the usual manner as follows:

$$\Phi(\bar{u}_i,\bar{x}_n,\bar{y}_q,\Pi_i,t) = f(\bar{u}_i,\bar{x}_n,\bar{y}_q,t) - \sum_{i=1}^{p} \lambda_i T_i(\bar{u}_i,t)$$

$$- \sum_{i=p+1}^{m} \lambda_i[T_i(\bar{u}_i,t) - \Pi_i] \qquad \text{(IV-13)}$$

where λ_i is a non-negative variable independent of $\bar{u}_i$. It has been shown that a necessary and sufficient condition for $\bar{u}_i^*$ to be a solution of the minimization problem is that $f(\bar{u}_i^*,\bar{x}_n,\bar{y}_q,t)$ be concave and the constraint set be convex in the vicinity of $\bar{u}_i^*$, and that $\bar{u}_i^*$, λ_i^*, and Π_i satisfy the following set of equations:

$$\frac{\partial \Phi}{\partial \bar{u}_i^*} = \frac{\partial f(\bar{u}_i^*,\bar{x}_n,\bar{y}_q,t)}{\partial \bar{u}_i^*} - \sum_{i=1}^{m} \lambda_i^* \frac{\partial T_i(\bar{u}_i^*,t)}{\partial \bar{u}_i^*} \qquad \text{(IV-14)}$$

$$\frac{\partial \Phi}{\partial \lambda_i^*} = -T_i(\bar{u}_i^*,t) = 0, \quad i = 1,\cdots,p \leqslant m \qquad \text{(IV-15)}$$

$$\frac{\partial \Phi}{\partial \lambda_i^*} = -T_i(\bar{u}_i^*,t) + \Pi_i = 0, \quad i = p+1,\cdots,m \qquad \text{(IV-16)}$$

$$\Pi_i \geqslant 0, \quad i = p+1,\cdots,m$$

$$\lambda_i^* \geqslant 0, \quad i = 1,\cdots,p \qquad \text{(IV-17)}$$

$$\lambda_i^* \Pi_i = 0, \; i = p+1,\cdots,n$$

From Equations (IV-16) and (IV-17), it follows that Π_i is completly determined by $\bar{u}_i^*$ and λ_i^*. It can be also shown that:

$$\Phi(\bar{u}_i^*,\lambda_i,\Pi_i) \leqslant \Phi(\bar{u}_i^*,\lambda_i^*,\Pi_i) \leqslant \Phi(\bar{u}_i,\lambda_i^*,\Pi_i)$$

For large problems, according to Carrol, the Lagrange multiplier technique may be quite unwieldy.[61]

3. Created Response Surface Technique:

The CRST as developed by Carrol[61] and mathematically proved by Fiacco and McCormick[62,63] is based mainly on solving a sequence of unconstrained problems whose solutions approach the solution of the constrained function, i.e. $\Phi \rightarrow f$ when $R \rightarrow 0$, where R is the penalty factor weighting the constraints T_i to the constrained function f.

Equation (IV-2) would be written as follows to include all the equality and inequality constraints:

$$\Phi(\bar{u}_i,\bar{x}_n,\bar{y}_q,t) = f(\bar{u}_i,\bar{x}_n,\bar{y}_q,t) + R_j \sum_{i=1}^{m} \frac{W_i}{T_i} \quad \text{(IV-18)}$$

$W_i > 0$ weight the individual penalties amongst themselves, while R_j (always ≥ 0) weights the sum of the constraints in relation to the constrained function to be optimized.

The minimization of $\Phi(\bar{u}_i,\bar{x}_n,\bar{y}_q,R,t)$ for $R_j > 0$ yields a point that is dual-feasible, as well as a point that is primal-feasible. It follows that the process explicitly generates the associated "Lagrange Multipliers," and hence, the dual solution vector.

The optimum of the function is evaluated for different values of R (decreasing in value) and for each level the equivalent optimum level of the manipulated variables ($\bar{u}_i$) is used as a starting point for the next level of the criterion function, with less value of R, evaluation. The procedure continues until $R_j \rightarrow 0$ and therefore, Φ optimum approaches f optimum without violating any of the constraints.

The choice of R_j-values can be arbitrary or included as an unknown parameter to be identified by the optimization technique. The first approach is used in the present study, while the second would be preferable for large problems which are extremely nonlinear and partially unknown.

This technique seems more simple, logical and practical to use. Therefore, the optimization of the operating objective function for the RDC operating under steady-state conditions has been solved using the CRST.

Unconstrained (Dual Problem) and Constrained Objective Functions

The constrained objective function has been written to include three important parameters, considering the importance of each parameter separately on the process performance. It has been given the name OBJ in Subroutine PROC, and can be written as follows:

$$f = 0.25(HTU)^2 + 0.005\ P_{con}^2 + 100(1/T) \qquad \text{(IV-19)}$$

where

P_{con} = the power consumption by the rotating shaft, and

T = the column throughput expressed in terms of the sum of the superficial velocities ($V_d + V_c$) instead of the sum of the mass flow rates (L + G).

In the CRST a modified path is formed which, while optimizing the unconstrained function as quickly as possible, it steers automatically clear of the constraints and thus

prevents their violation. Near the very optimum, however, solutions are allowed on or very close to, critical constraints surfaces.

Following the CRST procedure and incorporating the above mentioned four constraints with the constrained objective function, to form the Dual unconstrained function, Equations (IV-19) can be modified thus:

$$\Phi = f - R_1\left(\frac{W_1}{XOT - 2} + \frac{W_2}{0.85\varepsilon_f - \varepsilon} + \frac{1}{CP3} + \frac{1}{CR4}\right) \qquad \text{(IV-20)}$$

The Objective Function Evaluation

A computer program has been written for the purpose of evaluating the objective functions (both constrained and dual unconstrained) for a wide range of combinations for the process variables. The variables taken into consideration are the feed and solvent mass flowrates and the peripheral shaft speed. The inlet feed phase concentration has not been considered because the concentration is expressed in dimensionless form which gives the outlet raffinate concentration as a fraction of the inlet (which is unity).

The contours of the constrained function have been plotted for various combinations of the process variables and the equivalent important parameters. Figure 18 shows the variation of the function as a function of the solvent and feed flowrates, while the shaft speed is kept constant and equal to zero. It has been found that the topology of the function plotted for any other value of the shaft speed

is similar in shape while it varies in the absolute values.

Figure 19 shows the contours of the constrained function for a wide combination range for the extraction factor (mG/L), and the sum of the superficial velocities ($V_d + V_c$) which is a measure of the column throughput.

Figure 20 shows the contours for the constrained function for different values of the extraction factor and peripheral shaft speed.

Figure 21 shows a similar plot for the constrained function for different values of the sum of the superficial velocities and peripheral shaft speeds.

Figures 18 to 21 show that the objective function is nonlinear with respect to the three process variables considered (feed mass flowrate, solvent mass flowrate, and peripheral shaft speed). The characteristics, dependency, topology, and minimum region for different combinations of the process variables and parameters are shown graphically.

From Figure 18 one can see the function as a set of multi-level surfaces for different shaft speeds. For constant shaft speed and fixed solvent rate, the value of the constrained objective function changes slowly. The absolute minimum for the constrained objective function, for any constant shaft speed value, is on the upper limit of the feed rate, corresponding to the minimum solvent rate. This is valid theoretically but not possible practically. Flooding might possibly prevent the process from reaching this operation level.

From Figure 19 the contours of the objective function are symmetrical around $V_d + V_c \approx 13.5$. The direction of curvature is reversed at extraction factor $\Delta \approx 0.5$. For each value of extraction factor, there are two equivalent values of column throughput ($V_d + V_c$) which have the same value of objective function. The radius of curvature decreases rapidly as the extraction factor increases. The absolute minimum for the objective function lies on the line of symmetry for the column throughput, and for the maximum possible extraction factor.

Figure 20 shows the contours of the objective function to be considerably irregular and nonlinear due to the change in the value of the shaft speed. This is because of the complexity of flow changes accompanying any variation in the shaft level used (e.g., degree of dispersion, hydrodynamics of flow, and Peclet number values).

In Figure 21 the objective function contours form an eccentric elliptical set of curves with an increasing radius up to 800 cm/min shaft speed. Over this speed the degree of nonlinearity and irregularity increases noticeably.

From the above results, it appears that the approximate combination of process variables which tend to give a feasible minimum for the objective function would be:

i. A column throughput ($V_d + V_c \approx 13.5$.
ii. A maximum possible extraction factor (mG/L), and
iii. A shaft speed which is combined with the above two

parameters would give a minimum power inlet, optimum Peclet numbers, and maximum feasible holdup value for the dispersed phase.

Solution of Quadratic Optimization Problems

One would like to find that value of the independent variables, $\underline{x}^* = |x_1^*, x_2^*, \cdots, x_n^*|$ such that $f(x^*)$ is a minimum subject to the restrictions that,

$$g_i(x_1^*, \cdots, x_n^*) = 0, \quad i = 1, \cdots, p < n$$
$$g_i(x_1^*, \cdots, x_n^*) \geq 0, \quad i = p+1, \cdots, m \qquad \text{(IV-21)}$$
$$m \leq n$$

For an unconstrained function with continuous derivatives, a minimum occurs at that point where the first partial derivatives of the function with respect to the independent variables are zero and its matrix of second derivatives is positive definite.

A minimization procedure for a digital computer provides an algorithm by which the function is tested at a set of points. These points then provide information about the function and the location of its minimum. The way the test points are chosen divide these procedures into two very general classes: sequential and non-sequential. In a sequential procedure the test points are determined by a fixed set of operations. The values of the independent variables are completely determined by the previous measurements while in a non-sequential procedure the points are picked up essentially at random.

If the objective function is quadratic and has the form,

$$F_q = F_o + c^T\underline{x} + \frac{1}{2} x^T Q x \qquad \text{(IV-22)}$$

where

x is an n-dimensional vector,

c is an n-dimensional vector of constants, and

Q is an n x n symmetric positive definite matrix.

If the objective function is nonquadratic, expanding the function about the minimum point $\underline{x} = \underline{x}^*$ gives:

$$F_n = F_o + \frac{1}{2} (x - x^*)^T Q(x - x^*) + R \qquad \text{(IV-23)}$$

The remainder R estimates the error between F_n and its quadratic approximation. Since R becomes negligible when x is sufficiently close to x*, the general function is approximated by a quadratic in a neighbourhood of the minimum; hence algorithms converging rapidly for quadratics are of interest.

Since it is possible to convert constrained functions to the equivalent unconstrained functions, one would limit his analysis to unconstrained functions only.

Now let us say that x minimizes F(x*) is determined by constructing a sequence $\{x_i\}$ that converges to x* as i becomes greater or equal to n (where n is the number of variables). A procedure for constructing the x_i is said to be quadratically convergent[60] if x* is determined after n-gradient evaluations. The four procedures considered herein all exhibit this property.

Certain conventions and properties[67] associated with the problem of minimizing Equation (IV-23) will be used frequently. The gradient of F evaluated at the point x_i is defined as

$$g_i = \left| \frac{\partial F(x_i)}{\partial x} \right|^T = Qx_i + c \qquad \text{(IV-24)}$$

For Equation (IV-23), a necessary and sufficient condition for x* to minimize F is that

$$g(x^*) = 0. \qquad \text{(IV-25)}$$

So it follows immediately from Equation (IV-24) that

$$x^* = - Q^{-1}c \qquad \text{(IV-26)}$$

It is also well known that if one has the point x_i and the gradient at the point g_i, then the minimum x* is found from the following relation:

$$x_i^* = x_i - Q^{-1}g_i \qquad \text{(IV-27)}$$

From Equations (IV-26) and (IV-27), it is clear that if Q^{-1} is known, one can obtain the minimizing points. In most problems of practical interest the objective function F is not quadratic, so that equation (IV-22), similarly Equation (IV-23), is at best an approximation of the objective function surface in the vicinity of the minimum. Even then, it is not likely that the approximating Q is known, or if it is, the difficulties involved in finding Q^{-1} are significant enough to warrant seeking alternative methods for finding x*.

For a general function F, the derivative $(\partial^2 F/\partial x^2)$ provides a linear relationship between infinitesimal changes in x and the resulting changes in the gradient g given by

$$dg = \frac{\partial^2 F}{\partial x^2}\, dx \qquad \text{(IV-28)}$$

For a quadratic function, this linear relationship is true for all changes in x and g with Q replacing $(\partial^2 F/\partial x^2)$. Thus the gradient difference vector γ is defined as:

$$\gamma_i \approx g_{i+1} - g_i \qquad \text{(IV-29)}$$

and can be written, analogous to Equation (IV-28) as

$$\gamma_i = Q(x_{i+1} - x_i) \approx Q(\Delta x_i) \qquad \text{(IV-30)}$$

The gradient difference vector plays an important role in subsequent discussions.

In all of the procedures that are discussed, the search for optimum proceeds iteratively according to

$$x_{i+1} = x_i + K_i p_i \qquad \text{(IV-31)}$$

where K_i is always chosen so that x_{i+1} minimizes F in the direction p_i starting from x_i. The x_1 and p_1 are chosen arbitrarily. The manner in which the direction vector p_i is selected is defined by the particular procedure. The p_i are restricted to satisfy

$$p_i^T g_i < 0 \qquad \text{(IV-32)}$$

to ensure that the objective function is reduced through

the choice of K_i. The minimizing choice of K_i results in the satisfaction of the condition,

$$p_i^T g_{i+1} = 0 \qquad \text{(IV-33)}$$

for all i. The procedure for determining the desired K_i is an important part of the actual minimization procedure. For this discussion, it shall be assumed that the minimization can be accomplished so that Equation (IV-33) is always valid.

The problem of determining the x* that minimizes (IV-23) is seen from Equations (IV-24) and (IV-25) to be equivalent to solving the linear equations,

$$Qx = -c \qquad \text{(IV-34)}$$

It has been shown by Hestenes and Stiefel[64] that this can be accomplished by constructing a set of n mutually conjugate or, equivalently, Q-orthogonal vectors. To be precise, vectors $p_1, p_2, \cdots, p_n$ are said to be mutually conjugate if for all i and j,

$$p_i^T Q p_j = 0, \quad i \neq j \qquad \text{(IV-35)}$$

This is clearly a generalization of the concept of orthogonal vectors.

The determination of n mutually conjugate vectors allows the solution of Equation (IV-34) to be constructed immediately. To see this, one must first note that the set of n-mutually conjugate vectors p_i in an n-dimensional space are linearly independent. Then, the p_i span the space

and any vector (but particularly x*) can be written as a linear combination of the p_i.

$$x^* = \sum_{i=1}^{n} a_i p_i$$

so that

$$Qx^* = \sum_{i=1}^{n} a_i Q p_i = -c$$

then

$$p_j' Q x^* = \sum_{i=1}^{n} a_i p_j Q p_i = a_j p_j' Q p_j$$

from the mutual conjugacy of the p_i. The coefficients a_j are given by

$$a_j = \frac{-p_j' c}{p_j' Q p_j} \qquad \text{(IV-36)}$$

and x* is

$$x^* = - \sum_{i=1}^{n} \frac{p_i' c}{p_i' Q p_i} p_i \qquad \text{(IV-37)}$$

The inverse Q^{-1} can be constructed from the p_i by noting that Equation (IV-37) can be rewritten as

$$x^* = - \sum_{i=1}^{n} \frac{p_i' p_i}{p_i' Q p_i} c$$

so that

$$Q^{-1} = \sum_{i=1}^{n} \frac{p_i' p_i}{p_i' Q p_i} \qquad \text{(IV-38)}$$

It is now seen that the determination of n-mutually conjugate vectors provides the solution of a system of linear equations or, equivalently, provides the minimum of a quadratic function. Thus, if this set can be constructed as the n-directions in the iterative procedure Equation (IV-31), it follows that the procedure is quadratically convergent. This is a characteristic of all the procedures discussed below.

Davidon's Variable Metric Method

The variable metric method (VAM) of minimization as developed by Davidon and discussed by others is simply another gradient method.[65,66,67,68]

In the process of locating each minimum, a matrix which characterizes the behavior of the function about the minimum is determined. For a region in which the function depends quadratically on the variables, no more than n iterations are required, where n is the number of variables.

Outlines of Method:

1. The metric matrix and the gradient are used to establish a search direction.
2. Successively larger steps are taken in this direction until the relative minimum is encompassed.
3. A linear search is performed to locate the minimum within the interval. The improvement in the criterion function is compared with a step perpendicular to this direction at the relative minimum.

4. The metric matrix is updated based on information about the function obtained in this direction.

In the neighborhood of any point the second derivatives of F(x) specify a linear mapping of changes in position, dx, onto changes in gradient dg. For example in the case of the i-th variable

$$d\left(\frac{\partial F}{\partial x_i}\right) = \sum_{j=1}^{n} \frac{\partial^2 F}{\partial x_i \partial x_j} dx_j \qquad \text{(IV-39)}$$

where

$$\sum_{i=1}^{n} \frac{\partial^2 F}{\partial x_i \partial x_j} = H_{ij}$$

(H_{ij} is the Hessain Matrix and H_{ij}^{-1} is the variance matrix.)

If these matrix parameters are constant and explicitly known, then the value of the gradient at any point would suffice to determine the minimum. In this case the desired step Δx_j would be given by

$$\Delta x_j = H_{ij}^{-1} \Delta\left(\frac{\partial F}{\partial x_i}\right) \qquad \text{(IV-40)}$$

Since the matrix H is neither constant nor known, this method employs an iterative technique to improve the estimates of H_{ij} based on the changes in the gradients and the parameters. To start the method, H_{ij} is set equal to unity, making the first-step in the direction of steepest descent. After every n-1 iterations the metric matrix is set back equal to unity. In the linear search part of the program, cubical interpolation is used to locate the minimum.

The method is designed for problems where an analytical expression is available for the derivatives. However, a modification of this method have been published which used difference approximations instead.[75]

Optimum Gradient Method

The method of optimum gradient used is due to Beckey[69] and the main steps of the algorithm are:

1. Determine the direction of the gradient at the starting point x_0.
2. Perform a linear search in the negative gradient direction to locate the minimum point x_1.
3. Repeat steps (1) and (2) until minimum is located.

Discrete approximations for the partial derivatives are used in the calculation of the gradient and are obtained by perturbing each parameter by $\approx 0.01\%$. The method can be expressed by a generalized equation

$$x_{i+1} = x_i - \lambda_i G_i \qquad \text{(IV-44)}$$

This equation represents a simple iterative procedure in which new optimal settings can be obtained for the vector x at the i-th iteration. Thus the gradient method for the step-by-step approach to an optimum point may be divided into two parts:

1. finding the direction G in which the function will decrease, and
2. finding the step size λ which will bring the function nearest to its minimum.

The method is called "Optimum Gradient," as an optimum point is located in each linear search and an optimum step size is calculated, based on a modified Newton-Raphson method. The step is taken in the negative gradient direction and the criterion function is evaluated at this point, half-way between this point, and the original point. On this basis the step size is doubled or halved until the approximate minimum is located.

In order to determine the minimum more accurately, quadratic interpolation is used over the last three values of the criterion function. The step size for future iterations is determined from the results of previous iterations. The iteration loop is terminated when the gradients and parameter changes become very small.

Conjugate Gradient Method

The method of conjugate gradients used in this study was developed by Fletcher and Reeves.[70] The heart of this algorithm is in the way the matrix H_{ij} is updated.

Outline of Method:

1. At the starting point x_0, evaluate the gradient vector g_0 and set the search direction $d = -g_0$.
2. Perform a linear search in the direction d_i on the line through x_i to locate the relative minimum x_{i+1}.
3. Evaluate the gradient g_{i+1} at x_{i+1} and calculate $\beta_i = g_{i+1}^2/g_i^2$.
4. Calculate the new direction $d_{i+1} = -g_{i+1} + \beta_i d_i$.

5. The method is terminated if $g_i = 0$ or if an n + 1 iterations starting from a steepest descent search, produces no reduction in the value of the function, otherwise a new iteration is started.

After every n + 1 iterations, a step is taken in the negative gradient direction to prevent oscillations and slow convergence.

The linear search used in this program is similar to the one used in the variable metric method and Fletcher and Powell method.

Fletcher-Powell Modification of Davidon's Method

The method is a modification of Davidon's method.[67,71]

Outline of Method:

1. Given the parameter vector x_i and the gradient vector g_i, the direction d_i is calculated.

$$d_i = -H_{ii}g_i$$

where H_{ii} is the metric matrix which is taken initially equal to unity.

2. Find σ_i so that the criterion function $F(x_i + \sigma_i d_i)$ is a minimum along $x_i + \sigma_i d_i$.
3. Set $x_{i+1} = x_i + \sigma_i d_i$ and calculate $g_{i+1} \equiv g(x_{i+1})$ and $Y_i = g_{i+1} - g_i$.
4. Form H_{i+1} by

$$H_{i+1} = H_i + \sigma_i \frac{d_i' d_i}{d_i' Y_i} - \frac{H_i Y_i Y_i H_i}{Y_i' H_i Y_i} \qquad \text{(IV-42)}$$

5. Terminate the search when the direction d_i and the parameter σ_i become less than some specified minimum prescribed value.

This method, like Davidon's, has a quadratic convergence property, and will require n iterations to converge for a minimum.

If convergence in general is not reached in n iterations or if the directions derivatives are positive, the metric matrix is set equal to unity and the search starts again.

These techniques will be compared for solving the minimization problem of an operating objective function for a liquid-liquid extraction process. Appendix B shows computer flow diagrams for the four optimization techniques.

The Steady-State Optimization Program

The computer program for steady-state optimization of the RDC has been written in such a form as to facilitate changes in logic, options, sequences, and input-output format. The subroutines are used as a part of one main program, while all the variables and constants are flowing in and out of each subroutine through a common statement.

Figure 22 shows the general outlines of the program which is called "STSOP", as a abreviation for steady-state optimization, with the interrelationships between the different subroutines.

The main parts of the program are:

1. Main Program: Its function is to read in necessary data

about the process such as:

a. Column configurations,

b. Physical system properties,

c. Size of the problem,

d. Upper and lower bound vectors,

e. An initial starting feasible point for the process variables vector,

f. Penalty vector values, and

g. Another feasible trial point, to assure that the first evaluated optimum is absolute.

The variables considered are the feed phase mass flowrate, the solvent phase mass flowrate, and the peripheral shaft speed. The fourth variable (feed phase inlet concentration) has been proved to be of no value in this program due to the dimensionless representation of the process model, which considers the inlet concentration equal to unity and the outlet concentration as a ratio.

To neutralize the effect of any variable, if it is desirable to keep it constant, the upper and lower bounds as well as the first guess values are made equal.

The second purpose of this program "MAIN" is to call in the optimization subprogram which can be any of the following four.

1. Variable Metric Method "VAMM": In this case an auxiliary subroutine is required. Subroutine INPUT is called in to provide the optimization subprogram with the following necessary information:

D - an estimate of the expected minimum of the function

PMIN - an estimate of the allow minimum changes in any of the process variables,

EP - a small parameter (ε), twice the accuracy required in evaluating the optimum of the function, and

IPRNT - an index to control the amount of information printed out.

2. Optimum Gradient Method "OPTGRD": In this subprogram most of the information required is evaluated or given within the program. The only subroutines called in are the objective function (PROC), and the bounds on the process variables (BOUNDS).
3. Modified Fletcher-Powell Method (FLTPOM): In this subprogram matrix presentation is eliminated and equivalent vectors are generated to save a considerable amount of storage.
4. Conjugate-Gradient Method (CONJGR): A similar procedure to method (3) is incorporated. For the last two methods an index "IER" has been set to indicate how far the optimization search has gone and the reason for any failure in reaching the optimum.

IER - error parameter

= 0 means convergence is obtained

= 1 means no convergence in a limited number of iterations

= 2 means linear search indicates that no minimum exists, and

= -1 means error in gradient calculations.

Optimization Subprogram:

The subprogram is written in a standard form to perform a sequence of calculations; the outcome is the feasible minimum of an objective function written for the case under investigation, and the equivalent optimum levels for the process variables vector.

Subroutines called in by the subprogram are:

1. DERF - to calculate the derivative or gradient vector values of the process variables vector at any stage of the search. This has been performed numerically by increasing each variable by an incremental value while the other variables are kept constant and the corresponding change in the objective function value is calculated. This can be expressed mathematically as follows:

   a. For the constrained function (OBJ):

$$g_i(x) = \nabla_x f = \frac{f(x_i + \Delta x_i) - f(x_i)}{\Delta x_i} \qquad \text{(IV-43)}$$

   and

   b. For the Dual Unconstrained function,

$$g_i'(x) = \nabla_x \phi = \nabla_x f - R_j \frac{\nabla_x T_i(x)}{[g_i(x)]^2} \qquad \text{(IV-44)}$$

where

R_j is the penalty factor which weights the constraints to the constrained function (f ≡ OBJ).

$T_i(s)$ are the constraints

2. BOUNDS - to impose the lower and upper limits on the process variables vector. These limits are expressed as lower and upper limit vectors, XL(M) and XU(M), where n is the number of variables.

The starting point for the search must be within the feasible range. If at any stage in computation the predicted or new evaluated value(s) of the process variable(s) violated these limits, one of the following actions will be taken:

1. the variable value is replaced by the nearest bound, or
2. an index is transferred to the optimization subprogram showing the violation, and consequently a cut-down or scaling-up in the step size is taken. The new evaluated value is again checked and further corrective action is taken.

3. PROC - to evaluate the three terms of the objective function: NTU, power consumption, column throughput; the constrained objective function (OBJ), and the dual unconstrained function (PHI). A factor is set equal to unity in the beginning of the subroutine, and at any occasion when one of the constraints is violated, the value of this factor will increase proportionally to

the degree of violation. The value of PHI will be equal to the calculated value multiplied by the value of the factor (equal to unity when there is no violation). This will make the optimization search interpolate between the last feasible value and the value of the variables causing this violation and determine a new feasible point. Therefore, the search will continue only in the feasible region.

Subroutines called by PROC:

1. Steady-State Model Subroutines (STSMOD): from which the value of the HTU is calculated, the extent of extraction constraint (XOT), and the necessary condition for mass transfer between two phases constraint (DIFNG) (equivalent meaning for the last two is given in Chapter I of this section).

   A difficulty can arise in this subroutine when the logarithmic mean driving force equation (c.f.2) is used to evaluate the apparent number of transfer units, rewritten as follows:

$$NTU_p = \frac{\ln\left|\frac{x_i - y_{2/m}}{x_2 - y_{2/m}}(1 - \Delta') + \Delta'\right|}{(1 - \Delta')} \qquad \text{(IV-45)}$$

where

$$\Delta' = \frac{G}{mL} \left(\equiv \frac{\text{feed mass flowrate}}{\text{Equilibrium constant x solvent mass flowrate}}\right)$$

For the process under investigation a pure solvent is used ($y_2 = 0$). Therefore,

$$XOT = \frac{x_1 - y_{2/m}}{x_2 - y_{2/m}} = \frac{x_1}{x_2}$$

Equation (IV-45) is simplified to

$$NTU_p = \frac{\ln|(1 - XOT)\Delta' + \Delta'|}{|1 - \Delta'|} \qquad \text{(IV-46)}$$

On many occasions the argument of the logarithm becomes less than, or equal to, zero because of unrealistic values postulated by the search technique.

To overcome this difficulty an empirical formula developed by Reman,[5] and tested versus the mean logarithmic driving force equation experimentally, has been used:

$$NTU_p = K[\Delta']^{0.5} \qquad \text{(IV-47)}$$

Figure 15 (Chapter III) shows that Equation (IV-47) is in close agreement with Equation (IV-46) when the proportionality constant (K) is equal to 2.

Equation (IV-47) was added to the Steady-State Model Subroutine to be a stand-by for any negative or zero argument for the logarithm in Equation (IV-46).

2. Holdup Subroutine (HOLDUP) - from which the power consumption term in the objective function is calculated as well as the holdup volume fraction (EP), the flooding equivalent holdup (EPF), and Peclet numbers (Pe_x and Pe_y).

Auxiliary Subroutines Used:

1. CUBIC - to solve an algebraic cubic equation for the holdup subroutine.
2. MATINV - to evaluate the inverse of a (12 x 12) matrix generated in the STSMOD Subroutine.
3. MVMULT - to evaluate the product of a matrix with a vector.
4. INPROD - to evaluate the inner product of a vector with another vector.
5. TIME Function - to calculate at any stage in the computations the time in seconds taken to execute any part of the program.

Numerical Results

For the objective function developed earlier, the four optimization techniques, Optimum Gradient, Variable Metric, Conjugate-Gradient, and Modified Fletcher-Powell have been tested. It has been found numerically that each technique has taken a separate trajectory path towards the optimum.

For an extraction process (specifically an RDC) the expected optimum conditions of operation would be a minimum solvent rate use (or maximum G/L), a minimum solute waste in the outlet raffinate phase (minimum x_F), maximum throughput ($V_d + V_c$), and minimum power input per unit volume of extract. This would be the optimum operating condition if no constraints, limits or bounds are violating the process performance.

For the process under study the evaluated optimum, with respect to the postulated constrained function, from the four optimization techniques used, is summarized in Table 3.

Discussion

It is impossible to find one optimization technique to handle all engineering problems. Also, in the solution of real engineering problems, each method must be "tuned up" by trial and error to obtain the best results in the minimum period of computer time and storage required.

Some of the parameters which have to be considered for modification and imporvement are:

1. The method for evaluating the gradient of a vector. In the present methods the finite difference variable (Δx_j) must be fine-tuned.

2. The step size to be taken to initiate the linear search.

3. The optimum value of the weighting factor (R) to give the best results without violating any of the constraints.

Following the previous argument, a comparison between the four optimization techniques is carried out. Table 4 shows the various important factors on which the somparison has been based.

From this table the following conclusions can be drawn:

1. For any RDC there is an optimum shaft speed, and for any specific shaft speed there is an optimum combination of

the feed and solvent flowrates. The shaft speed, as a variable, does not change considerably in the moderate conditions of operation (with the operating condition far from flooding conditions). Under intensive conditions of operating (shaft speed over 800 cm/min), it changes considerably to counteract a violation in the flooding constraint.

2. Once the search technique has driven the system away from the feasible range and consequently violated any of the imposed constraints, a corrective action must be taken to return the system to another feasible region. If it fails to do so, it will be rather difficult to correct it, unless a new iteration is started from the last feasible point.

3. The possibility of a local optimum existing anywhere else on the surface has been checked by starting the search from the other extreme side of the conditions of operation. This has shown that there is one, and only one, optimum for a rotating disc contactor operating under steady-state conditions.

4. From the previous comparison of search methods, it can be said that the optimum gradient, followed by the variable metric is the most suitable for dealing with the problem under study.

5. The four methods of optimization have been tested for a postulated performance criterion. Changing the form of this criterion to include economic factors may invalidate this comparison.

TABLE 3

COMPARISON BETWEEN THE OPTIMUM LEVEL OF OPERATION
ESTIMATED BY FOUR OPTIMIZATION TECHNIQUES

Process Variables	Estimated Optimum Values Obtained by			
	Optimum Gradient	Variable Metric	Conjugate Gradient	Modified Fletcher-Powell
Feed Phase Man Flowrate (g/min)	180.	179.9995	143.278	178.8716
Solvent Phase Man Flowrate	94.52	95.2738	75.3374	94.6338
Rotating Shaft Speed (cm/min)	468.3	470.9	437.8	468.5
Raffinate Concentration (dimensions for inter feed concentration equal to unity and pure solvent)	0.49939	0.49628	0.498369	0.496459
Constrained Objective Function Valve (F)	157.743	159.296	162.173	159.062
Unconstrained Objective Function Value (ϕ)	158.149	159.3676	162.3292	159.1369

TABLE 4

COMPARISON BETWEEN FOUR SEARCH TECHNIQUES OF OPTIMIZATION

Item	Search Technique / Property	Optimum Gradient	Variable Metric	Conjugate-Gradient	Fletcher-Powell
(1)	Simplicity of formulamulation and implementation (in order)	1	3	4	2
(2)	Core Storage Usage (Bytes)	36,332	43,020	37,764	36,968
(3)	Compilation Time	1.94 secs	3.23 secs	1.98 secs	1.98 secs
(4)	Convergence Sensitivity	Very Good	Very Good	Fair	Good
(5)	CPU Time	64.20 sec	46.672 secs	149.157 sec	127.59 sec
(6)	Number of Function Evaluations	88	21	72	61
(7)	No. of Iterations	26	14	21	19
(8)	Total CPU Time used for 7 starting points	455 secs	373.317 secs	536.75 secs	498.35 secs

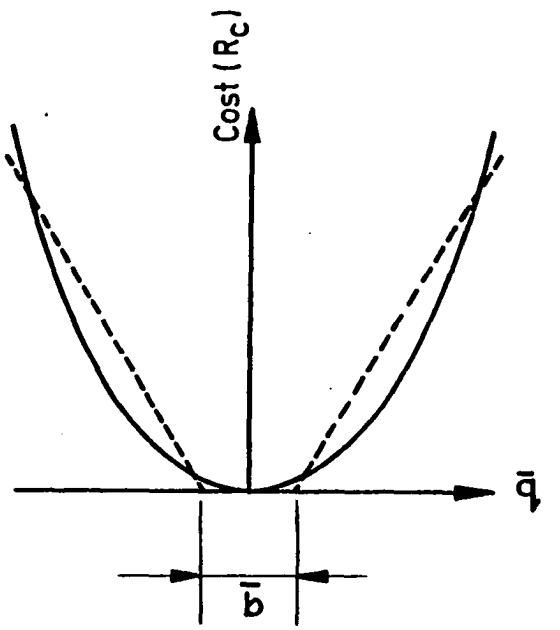

FIG. 16 PRODUCTION COST Vs. DEVIATION $\bar{q}$ IN PRODUCT QUALITY

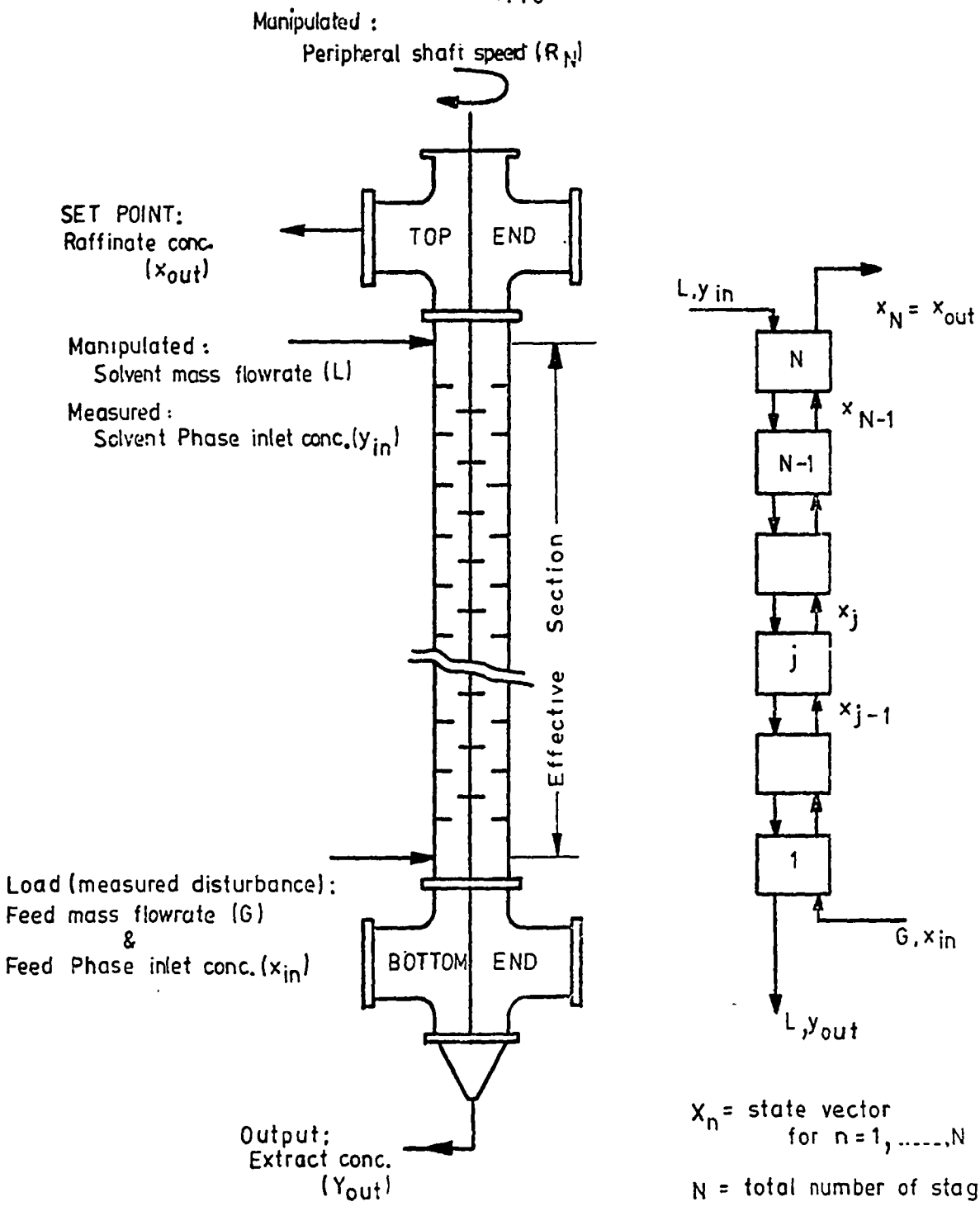

X_n = state vector
for n = 1, ..., N

N = total number of stages

y_m = output vector : m = 1, 2
$y_1 = y_{out}$ & $y_2 = x_{out}$

(a) CLASSIFICATION OF VARIABLES FOR A MECHANICALLY AGITATED LIQUID—LIQUID EXTRACTION PROCESS.

(b) STAGEWISE REPRESENTATION SHOWING THE STATE — AND OUTPUT — VECTORS.

FIG. 17 GENERALIZED CONFIGURATION OF A CONTINUOUS EXTRACTION PROCESS

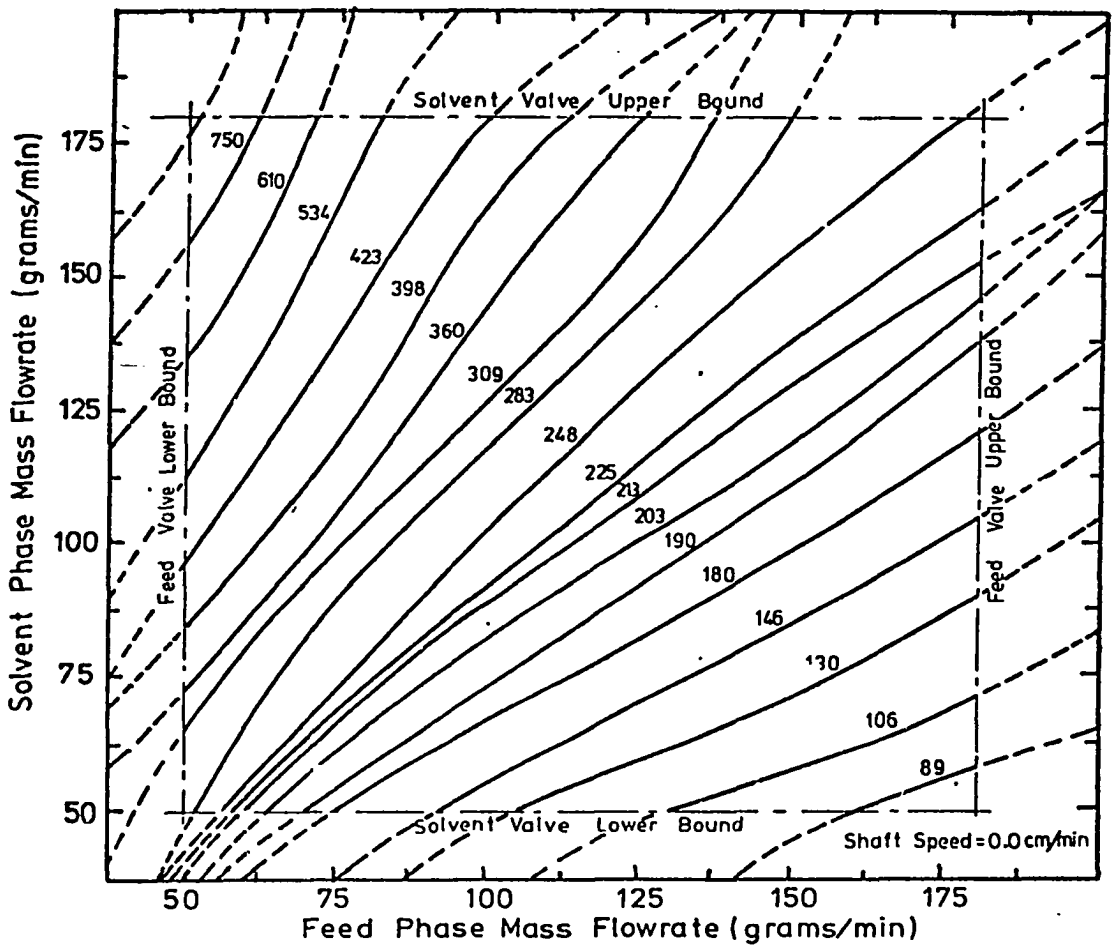

FIG. 18. THE CONSTRAINED FUNCTION CONTOURS FOR DIFFERENT COMBINATIONS OF FEED & SOLVENT PHASE FLOWRATE VALUES.

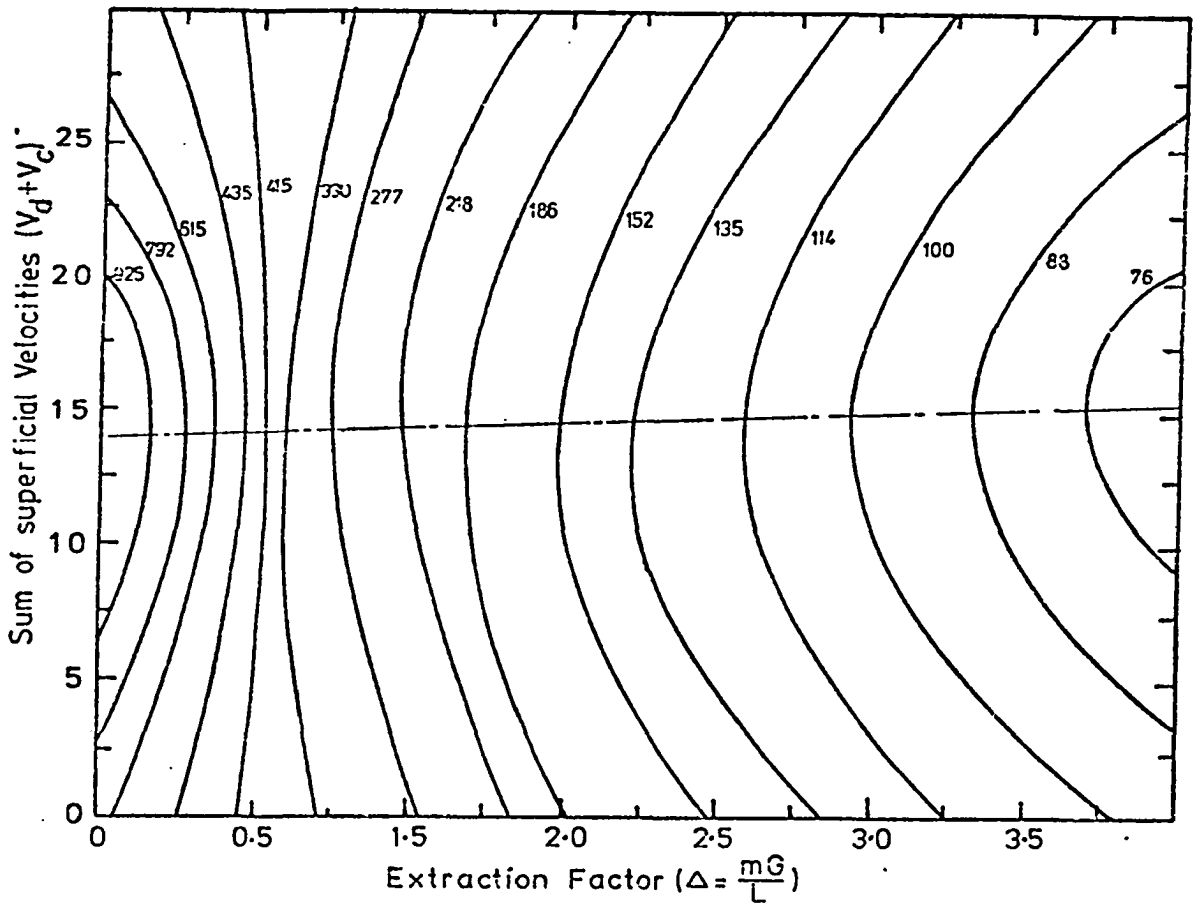

FIG. 19. THE CONSTRAINED FUNCTION CONTOURS FOR DIFFERENT VALUES OF EXTRACTION FACTOR & COLUMN THROUGHPUT.

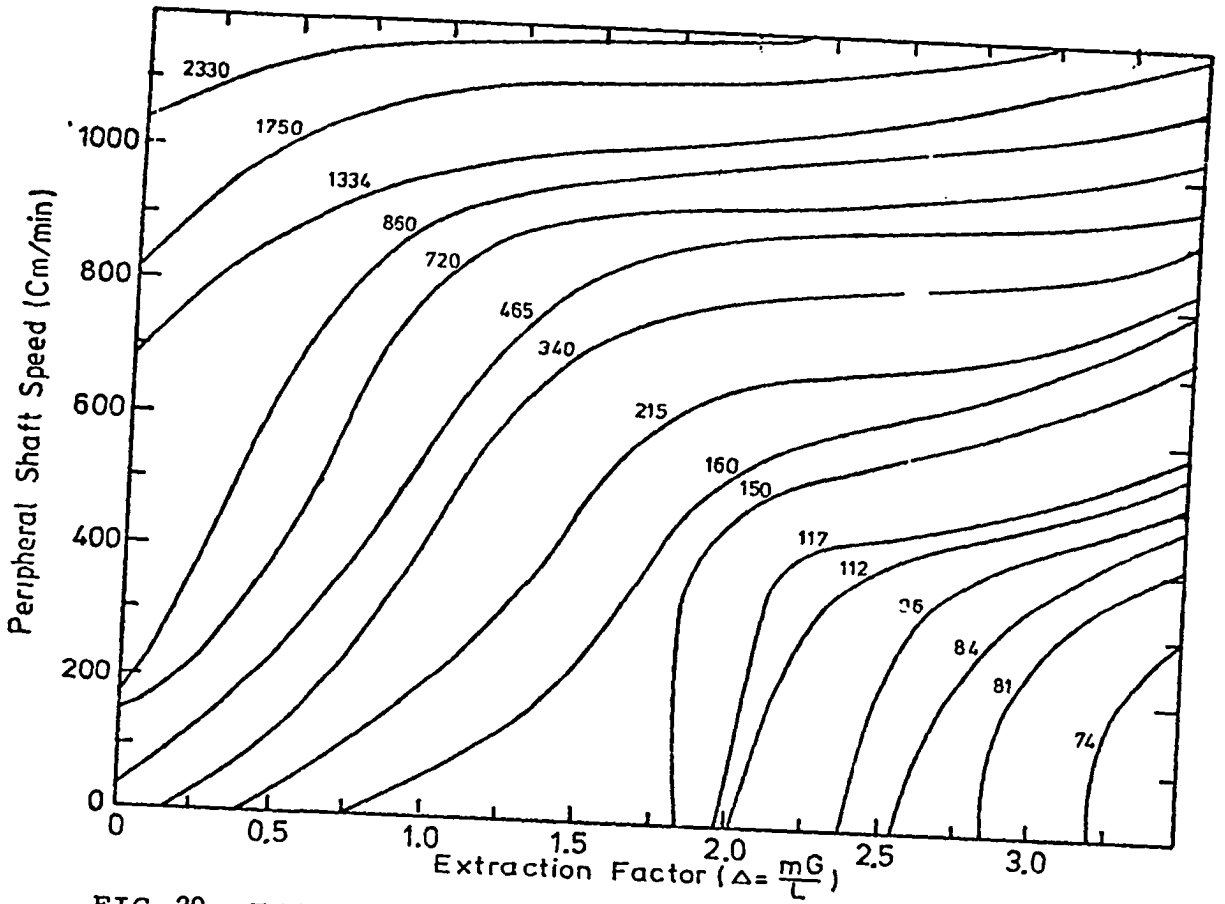

FIG. 20 THE CONSTRAINED FUNCTION CONTOURS FOR DIFFERENT VALUES OF EXTRACTION FACTOR & SHAFT SPEED.

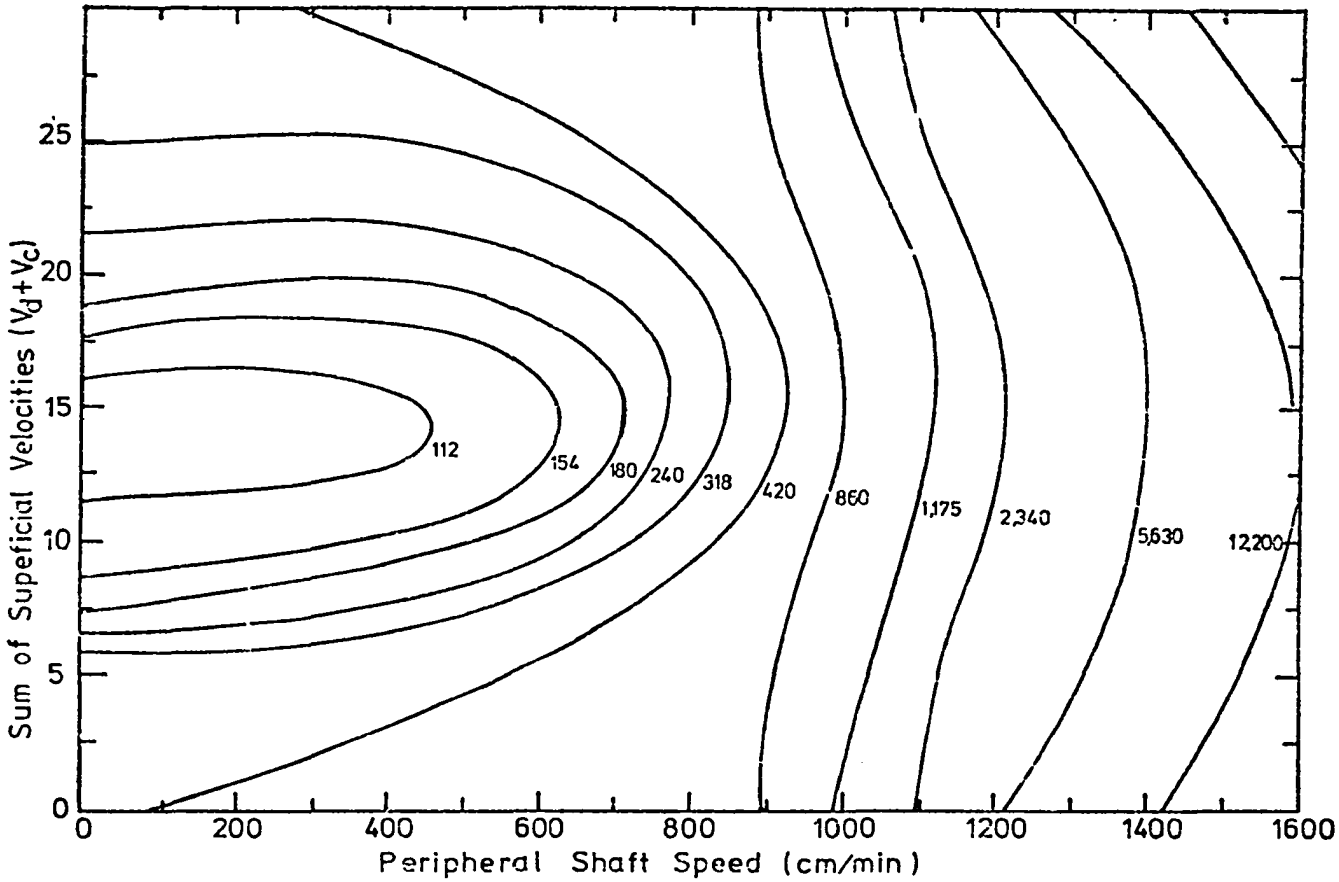

FIG. 21 THE CONSTRAINED FUNCTION CONTOURS FOR VARIABLE COLUMN THROUGHPUTS & SHAFT SPEEDS.

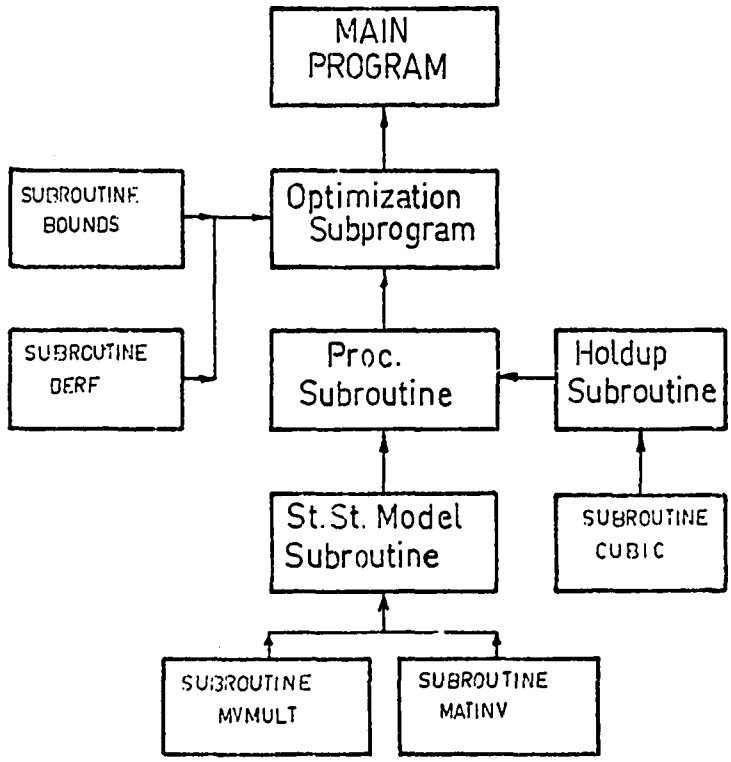

FIG. 22 GENERAL OUTLINES FOR MODEL REFERENCE STEADY-STATE OPTIMIZATION PROGRAMS.

CHAPTER V

DYNAMIC MODELLING

As has been mentioned briefly in the introduction of this thesis, a dynamic model of the process is necessary for dynamic optimal control, time-optimal control for the start-up period, and recovery of the process if it has already gone through the critical region.

Each mathematical model developed for a specific purpose must fulfill certain requirements:

1. For dynamic optimal control, it must yield a solution rapidly, and be sufficiently accurate.
2. For time optimal control for the start-up period a highly accurate model is required over the entire period while the time required for obtaining the solution is not a critical factor.
3. For trouble shooting, cases one and two should include necessary constraints to avoid the critical and unstable region.

Previous Work on Extraction Dynamics

Table 5 shows a summary of the previous investigations carried out by a number of authors on the dynamics

of liquid-liquid extraction processes. Further details about each of these investigations can be found in the critical review published by Pollock and Johnson.[76]

The following work is the most relevant to this study. Mixed cell model with constant back-mixing coefficients, developed by Pollock and Johnson.[77] In this model, the following assumptions were postulated.

1. Within the narrow range of concentrations used experimentally, the feed phase flowrate, the solvent phase flowrate, the equilibrium distribution coefficient, and the product of mass transfer coefficient and interfacial area per unit volume are constant.
2. The gradient of solute concentration in each phase is composed of finite steps associated with the area between two successive stator rings.
3. The mean velocity and concentration of each phase are constant across that part of the column cross-section occupied by the phase. Thus the concentration gradients exist only in the direction of flow.
4. The composition of the back-mixed stream from a given stage is the same as that of the main stream leaving the stage.
5. Variation in holdup, efficiency, and back-mixing coefficients over the transient period are negligible.
6. The coefficients of back-mixing between stages do not vary from one stage to another.

The model being considered can be represented diagrammatically as shown in Figure 23.

For the conditions outlined above, the following mass balance for the solute can be written as follows:

For the first stage:

$$ax_0 + arx_2 - (1 + r)ax_1 + (1 + e)y_2 + (1 + e)y_1 = \frac{\varepsilon_1}{L}\frac{dx_1}{dt} + \frac{(1 - \varepsilon_1)}{L}\frac{dy_1}{dt} \qquad (V\text{-}1)$$

For any intermediate stage (k):

$$(1 + r)ax_{k-1} + rax_{k+1} + (1 + e)y_{k+1} + ey_{k-1} - (1 + 2r)ax_k - (1 + 2e)y_k = \frac{\varepsilon_k}{L}\frac{dx_k}{dt} + \frac{(1 - \varepsilon_k)}{L}\frac{dy_k}{dt} \qquad (V\text{-}2)$$

and, for the last stage (n):

$$(1 + r)ax_{n-1} + ey_{n-1} + y_{n+1} - (1 + r)ax_n - (1 + e)y_n = \frac{\varepsilon_n}{L}\frac{dx_n}{dt} + \frac{(1 - \varepsilon_n)}{L}\frac{dy_n}{dt} \qquad (V\text{-}3)$$

In the case of equilibrium being attained in each stage, the steady-state mass balances for the solute in the outgoing streams are:

For the first stage:

$$(1 + r)ax_1 + (1 + e)y_1 = (1 + r)ax_1^* + (1 + e)y_1^* \qquad (V\text{-}4)$$

For the intermediate stages:

$$(1 + 2r)ax_k + (1 + 2e)y_k = (1 + 2r)ax_k^* + (1 + 2e)y_k^* \qquad (V\text{-}5)$$

and, for the last stage:

$$(1 + r)\, ax_n + (1 + e)y_n = (1 + r)ax_n^* + (1 + e)y_n^* \qquad (V\text{-}6)$$

The stage efficiencies can be defined as:

$$\eta_1 = \frac{x_0' - x_1}{x_0' - x_1^*}, \qquad \eta_k = \frac{x_{k-1}' - x_k}{x_{k-1}' - x_k^*}$$

$$\text{and} \qquad \eta_n = \frac{x_{n-1}' - x_n}{x_{n-1}' - x_n^*} \qquad (V\text{-}7)$$

where

$$x_0' = \frac{x_0 + rx_2}{1 + r} \quad \text{and} \quad x_{k-1}' = \frac{(1 + r)x_{k-1} + rx_{k+1}}{1 + 2r}$$

Further, the steady-state mass balance for the solute over the k-th stage corresponding to Equation (V-5) is

$$(1 + r)ax_{k-1} + rax_k + (1 + ey_{k+1} + ey_{k-1}$$

$$= (1 + 2r)ax_k + (1 + 2e)y_k \qquad (V\text{-}8)$$

and, for the entire system of stages it is

$$a(x_0 - x_n) = y_1 - y_{n+1} \qquad (V\text{-}9)$$

Finally, the general equilibrium relationship is

$$y^* = D_i x + q_i, \quad i = 1, \cdots, n \qquad (V\text{-}10)$$

Pollock and Johnson ended by putting Equations (V-1) to (V-3), after a few replacements and arrangements, in vector-matrix form as follows:

$$[A]\cdot\dot{\underline{x}} = [C]\underline{x} + \underline{G} \qquad \text{(V-11)}$$

The above equation represents the unforced dynamic model for the process and can be rewritten in more compact form as follows:

$$[A]\cdot\dot{\underline{x}} = \underline{B} \qquad \text{(V-12)}$$

where

$$\underline{B} = [C]\underline{x} + \underline{G} \qquad \text{(V-13)}$$

In these relations [A] is the tridiagonal matrix

$$[A] = \begin{bmatrix} a_{11} & a_{12} & 0 & & \cdots & & 0 \\ a_{21} & a_{22} & a_{23} & 0 & \cdots & & 0 \\ \vdots & \cdots & & & \cdots & & \\ 0 & 0 & a_{k,k-1} & a_{k,k} & a_{k,k+1} & & 0 \\ \vdots & \cdots & & & \cdots & & \\ \vdots & & & & & & \\ \cdots & 0 & a_{n-1,n-2} & a_{n-1,n-1} & a_{n-1,n} & & \\ 0 & \cdots\cdots & 0 & a_{n,n-1} & a_{n,n} & & \end{bmatrix} \qquad \text{(V-14)}$$

[C] represents the codiagonal matrix:

$$[C] = \begin{bmatrix} c_{11} & c_{12} & c_{13} & & & & & \\ c_{21} & c_{22} & c_{23} & c_{24} & & & & \\ & & & \vdots & & & & \\ & & & c_{k,k-2} & c_{k,k-1} & c_{k,k} & c_{k,k+1} & c_{k,k+2} \\ & & & & \vdots & & & \\ & & & & c_{n-1,n-3} & c_{n-1,n-2} & c_{n-1,n-1} & c_{n-1,n} \\ & & & & & c_{n,n-2} & c_{n,n-1} & c_{n,n} \end{bmatrix} \qquad \text{(V-15)}$$

The column vector G is given by the expression:

$$G^T = [g_1, g_2, \cdots, g_k, \cdots, g_{n-1}, g_n] \qquad \text{(V-16)}$$

where "T" denotes transpose.

Parameters a_i, b_i, c_i, and d_i are now defined by the following equations:

$$\begin{aligned}
a_i &= \frac{\eta_{i-1}}{\eta_i}, && \text{for } i = 1,\cdots,n \\
b_i &= \frac{a}{1+e} + \frac{D_i}{1+r} && \text{for } i = <_n^1 \\
b_k &= \frac{a}{1+2e} + \frac{D_k}{1+2e} && \text{for } k = 2,\cdots,(n-1) \\
c_i &= \frac{1+r}{1+e} && \text{for } i = <_n^1 \\
c_k &= \frac{1+2r}{1+2e} && \text{for } k = 2,\cdots,(n-2) \\
d_i &= \frac{D_i}{\eta_i} && \text{for } i = 1,\cdots,n
\end{aligned} \qquad \text{(V-17)}$$

The elements of the matrix [A] are represented for $i = 1,\cdots,n$ by the following expressions:

$$a_{i,i-1} = \frac{(1-\varepsilon_i)}{L}(1+r)a_i b_i$$

$$a_{i,i} = \frac{1}{L}[\varepsilon_i + (1-\varepsilon_i)(d_i - \alpha a_i e_i)]$$

$$a_{i,i+1} = \frac{(1-\varepsilon_i)}{L} r a_i b_i$$

Similarly, the elements of [C] are represented by

$$c_{11} = (1+e)(1+r)a_2 b_2 - (1+e)(d_1 - \alpha a_1 c_1) - (1+r)a$$

$$c_{12} = ar + (1 + e)(d_2 - \alpha a_2 c_2) - (1 + e)ra_1 b_1$$

$$c_{12} = (1 + e)ra_2 b_2, \quad \text{and} \quad c_{13} = (1 + e)ra_2 b_2$$

For $i = 2, \cdots, (n-1)$

$$c_{i,i-2} = e(1 + r)a_{i-1} b_{i-1}$$

$$c_{i,i-1} = (1 + r)\alpha + e(d_{i-1} - \alpha a_{i-1} c_{i-1}) - (1 + 2e)(1 + r)a_i b_i$$

$$c_{i,i} = (1 + e)(1 + r)a_{i+1} b_{i+1} + era_{i-1} b_{i-1} - (1 + 2r)\alpha - (1 + 2e)(d_i - \alpha a_i c_i)$$

$$c_{i,i+1} = r\alpha + (1 + e)(d_{i+1} - \alpha a_{i+1} c_{i+1}) - (1 + 2e)ra_i b_i$$

$$c_{i,i+2} = (1 + e)ra_{i+1} b_{i+1}$$

and

$$c_{n,n-2} = c_{i,i-2}$$

$$c_{n,n-1} = (1 + r)\alpha + e(d_{n-1} - \alpha a_{n-1} c_{n-1}) - (1 + e)(1 + r)a_n b_n$$

$$c_{n,n} = era_{n-1} b_{n-1} - (1 + r)\alpha - (1 + e)(d_n - \alpha a_n c_n)$$

Finally, the elements of the column vector $\underline{G}$ are represented by:

$$g_1 = q_2 - q_1 + [\alpha - (1 + e)a_1 b_1]x_o$$

$$g_2 = (1 + e)q_3 + eq_1 - (1 + 2e)q_2 + eq_1 - (1 + 2e)q_2 + ea_1 b_1 x_o$$

$$g_i = (1 + e)q_{i+1} + eq_{i-1} - (1 + 2e)q_i, \text{ for } i = 3, \cdots, (n-1)$$

and

$$g_n = eq_n - (1 + e)q_{n-1} + y_{n+1}$$

For a forced dynamic system Equation (V-12) can be rewritten as follows:

$$\dot{\underline{x}} = [A]^{-1}[C]\underline{x} + [A]^{-1}\underline{G} + [B^*]\underline{u} \qquad \text{(V-18)}$$

where [B*] is the control matrix, letting the asterisk differentiate between the one given in the forced dynamic system equation and the matrix [B] in Equation (V-12).

$$[B^*] = \begin{bmatrix} a_{1,0} & & 0 \\ \vdots & & \\ 0 & & a_{n,n+1} \end{bmatrix}$$

and $\underline{u}$ is the control vector.

The above model developed by Pollock and Johnson is a mixed cell model with constant back-mixing coefficients. The basic equations have previously been postulated by other workers. The only difference here is the vector matrix notation used.

Undoubtedly it is more accurate to present the process dynamics, especially in the start-up period, by the mixed cell model. But the difficulty in using this type of model lies in the high order of the vector-matrix equation produced. The RDC under investigation has 50 compartments. However, the height differences between the inlets of both phases and the first stator ring at both ends could be considered as another two compartments. This means that the dimensions of the matrices will be (52 x 52) and the vectors (52) which will make a numerical solution of the problem off-line very difficult and on-line impossible. This limitation, in addition to the complexity of the model structure

will make the vector-matrix manipulations time-consuming. Therefore, if one can represent the process dynamics by a stage-wise model, with the order equivalent to the number of theoretical stages (N.E.T.S.), then there is no point in adding such complications for little difference in accuracy.

The main advantage of the Pollack-Johnson model lies in its importance in possible theoretical investigations to be carried out on the effect of variable back-mixing coefficients, variable holdup volume fraction, and handling systems with nonlinear equilibrium relationship.

Biery[82] has mentioned that the influence of exponential terms with small time constants which occur in the solution of the dynamic equations is to produce a time-delay at the beginning of the response period. This dead-period is the time required for the physical displacement of phases after introducing a disturbance. The exponential terms with large time constants determine the overall time for the system to reach steady-state. When the finite set of equations is used to represent the dynamic behavior of the column (pulsed), the lag period is fore-shortened because only a small number of exponential terms are produced. Thus, in a stagewise model, a very poor representation of the lag portion of the response curve is produced when the number of equilibrium stages in the column is small.

The importance of the above findings is found in its support for conclusions to be drawn at the end of this chapter.

Chernyshev[95] has tried to solve a distributed, plug-flow dynamic model equation analytically, starting with a hyperbolic partial differential equation. He has obtained semi-quantitative solutions in terms of wave superposition and dispersion which, however, cannot precisely represent a mechanically agitated column with a special flow dynamics inside each compartment, created by the rotating discs, and between adjacent ones.

Lumped-Parameter Model for Seven Flow Concepts

As the literature survey shows, all theoretical and numerical work in the field of extraction dynamics has been built on one of the following three basic assumptions:

a. two-phase differential contact with plug-flow conditions.
b. two-phase stagewise contact with constant back-mixing conditions.
c. two-phase finite contact (mixed-cell) with constant back-mixing conditions.

However, in computer control, the possible range of variation in process variables is expected to be very large and is only bounded by the minimum and maximum limits for the input variables. Therefore, the consideration of one concept of flow to present the process dynamics over a wide range of operation in the transient period would not be entirely accurate, and it would be more advantageous to incorporate as many as possible of the flow concepts in one

algorithm. In the remainder of this chapter, a stagewise dynamic model will be developed and solved numerically for seven different concepts of flow.

1. Plug-flow condition
2. Constant back-mixing coefficients
   a. In both phases
   b. In solvent phase only
   c. In feed phase only
3. Variable back-mixing coefficients

   for three similar cases as in (2).

Solutions will be carried out for both time-invariant and time-varying feed rates and shaft speeds.

Considering the height equivalent to a theoretical stage is the basis for transient material balance. The column is divided into a whole number of stages nearest to the number of equilibrium stages for the given conditions of operation. Figure 24 shows a schematic representation for this type of model, and it is assumed that the two phases are uniformly mixed and in equilibrium in each stage.

The model order has been characterized for the given conditions of operation by solving the steady-state differential model and calculating the HTU (or NTU). Subroutine NORD developed in Chapter III had been written for this purpose.

Model A: Plug-Flow Stagewise Model

For this type of model the following assumptions were postulated:

1. The mass flowrate for both phases were constant. This was a good approximation since the flowrates were expressed on a solute free basis, and the feed and solvent phases had limited mutual solubility.
2. The mass flowrates (G and L) were functions only of column height and not of time or solute concentration.
3. Linear equilibrium relationship was taken.
4. $(K_x a)$ was assumed to be a function of column height, shaft speed, and degree of column sub-division but not a function of concentration or time.
5. The holdup volume fraction along the column axis was considered to be constant.

For the conditions outlined above, the dynamic material balance for the n-th equilibrium stage can be written as follows:

$$\frac{V}{N}\left[\varepsilon \frac{dx_n}{dt} + (1 - \varepsilon) \frac{dy_n}{dt}\right] = G(x_{n-1} - x_n) + L(y_{n+1} - y_n)$$

$$\text{for } n = 1,\cdots,N \qquad \text{(V-19)}$$

Making use of the equilibrium relation,

$$y = mx \qquad \text{(V-20)}$$

for the given physical system, the following equation results:

$$\frac{V}{N}\left[\varepsilon \frac{dx_n}{dt} + m(1 - \varepsilon) \frac{dx_n}{dt}\right] = mLx_{n+1} - (G + mL)x_n + Gx_{n-1} \qquad \text{(V-21)}$$

By rearranging Equation (V-21) to give the rate of change in feed phase concentration with respect to time as a function of the other parameters of the equation, it follows that

$$\frac{dx_n}{dt} = \frac{mL}{\frac{V}{N}[\varepsilon + m(1 - \varepsilon)]} x_{n+1} - \frac{(G + mL)}{\frac{V}{N}[\varepsilon + m(1 - \varepsilon)]} x_n + \frac{G}{\frac{V}{N}[\varepsilon + m(1 - \varepsilon)]} x_{n-1} \qquad \text{(V-22)}$$

for $n = 1,\cdots,N$.

It is important here to realize that the feed phase concentration at each stage is a function of time, namely $x_n = x_n(t)$, where x_n is the state vector of the order (N).

Assuming that the system will have an initial equilibrium point $[x_n(0) = x_{n_o}]$, one can write the set of equations (V-22) in vector-matrix form as follows:

$$\dot{\underline{x}}(t) = [A]\underline{x}(t) + [B]\underline{u}(t) \qquad \text{(V-23)}$$

where

$\underline{x}(t)$ is the state vector $(x_1, x_2,\cdots,x_N)^T$

$\underline{u}(t)$ is the control vector $[u_1(t),\cdots,u_m(t)]^T$

Superscript T denotes transpose,

[A] is the coefficient matrix, (N x N)

and

[B] is the control matrix (N x m)

For time invariant models, the two matrices [A] and [B] are considered constant over all the transient period,

giving

$$E_c = \frac{V}{N}[\varepsilon + m(1 - \varepsilon)]$$

$$A = \frac{G}{E}, \quad B = \frac{(G + mL)}{E_c}, \quad \text{and} \quad C = \frac{L}{E_c} \tag{V-24}$$

The coefficient matrix will have the following tridiagonal form:

$$[A] = \begin{bmatrix} -B & C & 0 & \cdots & 0 \\ A & -B & C & \cdots & 0 \\ 0 & A & -B & C \cdots & 0 \\ \vdots & & & \cdots & \vdots \\ 0 & 0 & 0 & 0 \cdots A & -B \end{bmatrix}$$

an N x N matrix, and the control matrix can be written as follows:

$$[B] = \begin{bmatrix} A & 0 \\ \vdots & \vdots \\ 0 & C \end{bmatrix}$$

an N x 2 matrix.

The two elements of the control vector, u(t), are defined as: (1) $u_1(t) = y_{N+1}(t)$, the inlet solvent concentration, and (2) $u_2(t) = x_0(t)$, the inlet feed phase concentration.

Models B, C, and D:

Stagewise Models with Constant Backmixing Coefficients.

Model B: Constant Backmixing in Both Phases.

Model C: Constant Backmixing in Feed Phase Only.

Model D: Constant Backmixing in Solvent Phase Only.

The effect of constant backmixing coefficients on the dynamic response of a time-invariant model is considered.

For this set of models, the following assumptions were adopted:

1. The composition of the back-mixed stream from a given stage is the same as that of the main stream leaving the stage.
2. The coefficient of backmixing, of each phase, between stages do not vary from stage to stage.

Assumptions (3), (4), and (5) are the same as those given for Model A.

For the conditions outlined above, the mass balance equations for the solute are similar to those given by Pollock and Johnson,[86] Equation (V-8).

Following the same procedure as in Model A, the following set of equations can be developed:

$$\frac{dx_n}{dt} = \frac{meL + G(1 + r)}{\frac{V}{N}[m(1 - \varepsilon) + \varepsilon]} x_{n-1} - \frac{mL(1 + 2e) + G(1 + 2r)}{\frac{V}{N}[m(1 - \varepsilon) + \varepsilon]} x_n + \frac{mL(1 + e) + rG}{\frac{V}{N}[m(1 - \varepsilon) + \varepsilon]} x_{n+1} \qquad \text{(V-25)}$$

for $n = 1, \cdots, N$.

The above set of equations can be presented in vector-matrix form following the same procedure used in

Model A, with the exception that the terms A, B and C will be equivalent to the three terms on the right hand side of Equation (V-25) respectively.

The backmixing coefficients r and e are similar to those obtained by Stainthorp and Sudall,[109] and can be written as follows:

1. For the dispersed phase

$$r = 0.09\varepsilon\left(\frac{D_r N_r}{V_d}\right)\left(\frac{D_r}{D_c}\right)^2\left[\left(\frac{D_s}{D_c}\right)^2 - \left(\frac{D_r}{D_c}\right)^2\right] \qquad \text{(V-26)}$$

2. An equivalent equation for the continuous phase can be written with $(1 - \varepsilon)$ instead of ε, and V_c instead of V_d in Equation (V-26). The equivalent meaning for these symbols are given in the nomenclature.

Models E, F, and G:

Stagewise Models with Variable Backmixing Coefficients

A similar procedure to that given for the last set of models has been used, except that the coefficients of backmixing are taken as a function of the variable column height, h (i.e. r_n and e_n - f(h)).

The variable backmixing coefficients r_n and e_n are similar to those developed by Gel'perin.[41,104]

The equation which has been used is:

$$e_n(h) = h\left[(0.5 \times 10^{-3})u_e + 0.012\, D_r N_r\left(\frac{D_s}{D_c}\right)^2\right] \qquad \text{(V-27)}$$

where

$$v_e = \frac{V_c}{(1 - \varepsilon)} .$$

A similar expression for $r_n(h)$ can be written with v_r instead of v_e, where $v_r = V_d/\varepsilon$.

Equation (V-25) can be modified to take into account the variation in backmixing coefficients by replacing e and r by e_n and r_n.

Notice here that the terms of the matrices [A] and [B] will be different due to the difference in the values of e_n and r_n, from one stage to another.

A subroutine ABMAT has been written to evaluate the coefficient and control matrices for the seven imporved dynamic models. Figure 25 shows a computer flow diagram for the subroutine.

The computer program algorithm developed for time-invariant models can be modified to consider the change in the parameters of the matrices [A] and [B] due to change in one of the inlet streams or the shaft speed. This is achieved by calculating the coefficient and control matrices at each discrete interval of time to count for any change in the parameters of the two matrices during the transient period. In this algorithm any change in the order of the model due to change in the operating conditions can be taken into account by solving the steady-state model equations for the new level of operation. This can be simply carried out by calling in subroutine NORD.

Initial State Vector

The procedure chosen to evaluate the initial state vector depends on the requirements from the model solution. The dynamic model has two main tasks: (1) controlling the process during the start-up period, and (2) controlling the process during the transient period either by returning it to the old steady-state level of operation or for a set-point change.

Pollock and Johnson[86] have discussed the dynamics of the process during the start-up period. The usual procedure, for an extraction process, is to fill the column with the continuous phase at first and then to set up the flowrate of this phase to the desired value. The dispersed phase is then introduced with an initial feed concentration x_0. Within a short period the holdup of the dispersed phase practically attains its steady-state value. A full quantitative description of this period would be extremely difficult because of the different displacement velocities of the different drop sizes and would lead to very complex results. It is possible to assume that the holdup successively builds-up to its steady-state value in consecutive stages.

The most suitable way of evaluating the initial state vector for this stage of operation is to equate the rate of change in concentration vector to zero ($\dot{\underline{x}} = 0$) and to solve the resulting homogeneous set of equations (discussed in steady-state model comparison given later).

Assuming the state of the process during the transient period will be controlled to approach a new equilibrium state, $\underline{x}_e$, different from x_o, one can make the following change in the state vector

$$\begin{aligned} Z(t) &= x(t) - x_e \\ m(t) &= u(t) - u_e \end{aligned} \tag{V-28}$$

where $u_e(t)$ represents the inputs which yield the equilibrium $x_e(t)$.

The state equation can be represented in the form of the state changes instead of the absolute values of the state vector.

The dynamic equation becomes now

$$\begin{aligned} \dot{\underline{Z}}(t) &= [A]\underline{Z}(t) + [B]\underline{m}(t) \\ \underline{Z}(0) &= \underline{Z}_o = \underline{x}(0) - \underline{x}_e \end{aligned} \tag{V-29}$$

In this form the dynamic balances are equivalent to the generalized form with the final equilibrium being taken as the origin. For example:

$$x^T(0)\Big|_{u^T=[u_1,u_2]} = [x_1(0),x_2(0),\cdots,x_N(0)]$$

The initial condition vector.

$$\underline{x}_e^T\Big|_{\underline{u}_e^T=[u_{e_1},u_{e_2}]} = [x_{e_1}(0),x_{e_2}(0),\cdots,x_{e_N}(0)]$$

The final condition vector.

If normalization is carried out to make the final condition the origin,

$$Z(0)\Big|_{\underline{u}=[\underline{u}^T-\underline{u}_e^T]} = \begin{bmatrix} x_1(0) - x_{e_1}(0) \\ x_2(0) - x_{e_2}(0) \\ \vdots \\ x_N(0) - x_{e_N}(0) \end{bmatrix}$$

would be the normalized initial condition vector.

Method of Solution

Several methods for solving the state-space equation are given in the literature.[103] The following method of solution has been chosen for its simplicity.

The forced dynamic system equations can be written in vector-matrix form as follows:

$$\dot{\underline{x}}(t) = [A]\ \underline{x}(t) + [B]\ \underline{u}(t) \qquad \text{(V-30)}$$

The solution for the above equation in continuous form can be written as follows:

$$\underline{x}(t) = [G(t)]\ \underline{x}(0) + \int_0^t [G(t-\tau)][B]\ \underline{u}(\tau)\ d\tau \qquad \text{(V-31)}$$

where

$$G(t) \triangleq e^{[A]t} \triangleq [I] + t[A] + \frac{t^2([A][A])}{2!} + \ldots$$

is called the impulse response matrix for the system.

The first term on the right-hand side of Equation (V-31) represents the homogeneous solution of Equation (V-30)

while the second term (the convolution integral) represents the forced solution.

It is assumed that $\underline{u}(t)$ is piecewise constant, as is the case when sampled-data control is used. Then for each sampling period T,

$$\underline{u}(t) = \underline{u}(KT) \ , \qquad KT \leqslant t \leqslant (K + 1)T \tag{V-32}$$

Then, Equation (V-31) becomes

$$\underline{x}(K + 1) = [\phi]\ \underline{x}(K) + [\Delta]\ \underline{u}(K)$$

where $[\phi] = [G(T)]$

$$[\Delta] = \int_0^T [G(T - \tau)][B]\ d\tau$$

Figure 26 shows a flow diagram for computing system response for a given system with known [A] and [B], as well as the initial state vector.

The program written for this purpose has a self-checking procedure to minimize the truncated error for the evaluation of $e^{[A]t}$ by series expansion.

Keeping in mind the purpose of developing and solving this model as well as the dynamics of the RDC studied, the author has preferred to accommodate the seven concepts of flow in one algorithm to present the process dynamics over a wide range of operation. This complex unique algorithm will make it possible to compare the process output to seven model outputs for the same input. Then, the model with minimum deviation of error will be chosen for optimal control strategy design.

The dynamic model algorithm is considered to be a new form structure and method of solution for control computer purposes, which made the author call it by his first name: "PROGRAM KAMEL".

Figure 27 shows the main outlines of the program which included the following steps:

1. Subroutine NORD: Solving the steady-state equations to calculate the number of theoretical stages for the corresponding condition of operation. Details are given in Chapter III.
2. Subroutine ABMAT: Evaluating the coefficient and control matrices for the seven sets of dynamic equations.
3. Subroutine XOVEC: Calculating the initial steady-state vector by solving N-linear equations in N unknowns (x_0).
4. Subroutine INPUT: To read-in the input vector values either a testing function or a real input data measured from the system.
5. Main Program: The functions of this part are:
   a. To read-in necessary data for the process.
   b. To call-in the values of [A], [B], and $\underline{x}(0)$ from the corresponding subroutines.
   3. To call-in many standard subroutines to carry out specific calculations:
      (1) SETUNI: Set the matrices [ϕ] and [Δ] equal to unity
      (2) MVMULT: Matrix-Vector multiplication.

(3) MMULT: Matrix-Matrix multiplication.

(4) SMULT: Scalar-Matrix multiplication

(5) COPYM: Copy a matrix in another matrix space.

(6) MADD: Matrix-Matrix addition

(7) CPYVEC: Copy a vector in another vector space.

(8) MSUBT: Matrix-Matrix subtraction.

(9) MATMPB: Matrix-Matrix multiplication and storing the product in another matrix space.

(10) Standard Printing Subroutines:

PRINTV: Print a vector

PRINTM: Print a matrix.

d. Calculating the matrices $[\phi]$ and $[\Delta]$ from the following series:

$$[\phi] = [\phi'] + \frac{1}{m!}([A]\,\Delta t)^m$$
$$[\Delta] = [\Delta'] + \frac{1}{(m+1)!}([A]\,\Delta t)^m \qquad \text{(V-33)}$$

e. Checking the value of the matrix $[\phi']$ and the matrix $[\Delta']$ at m iteration. If the value of any of the matrices at (m + 1) iteration is very small compared to that at iteration m, proceed; otherwise increase the number of terms by one and check again.

Finally, calculate $[\Delta]$ according to the following equation:

$$[\Delta] = [\Delta'][B]\,\Delta t \qquad \text{(V-34)}$$

f. Calculating the dynamic response at any period of time from the following equation:

$$x[(K + 1)\Delta t] = [\phi]\, x(K,\Delta t) + [\Delta]\, u(K,\Delta t) \qquad (V\text{-}35)$$

This brief outline is the same for both time-invariant and time-varying models. The latter has the matrices $[\phi]$ and $[\Delta]$ varying with time, making it necessary to evaluate the values of the matrices $[A(t)]$ and $[B(t)]$ at each time interval.

g. The time interval (Δt) for discrete systems, which is used here and equivalent to the sampling period in sampled-data systems, is a very important parameter to be chosen. It must be chosen carefully so that:

(1) the variations in the model parameters are too small to be considered constant during the time-interval,

(2) the value of Δt should not be too small to make data-logging in real-time operation an impossible task, and

(3) for a process with time-dealy to be taken as an integer number of the sampling intervals without much error in calculation.

Lapidus[102] in his work on optimization and control of a gravity type extraction column has proposed a one minute time-interval to be a good guess for this type of processes.

Numerical Results

Time-Invariant Conditions:

The previously developed set of dynamic models have been tested for the same input disturbance, which is a step change in the inlet feed phase concentration equal to -2% by weight.

The numerical computations are conducted for the following conditions of operation:

Feed Phase Mass Flowrate = 68 gm/min

Solvent Phase Mass Flowrate = 80 gm/min

Peripheral Shaft Speed = 625 cm/min

Initial Feed Phase Inles Concentration = 10 wt.%

Inlet Solvent Concentration = 0.0 wt.%

The Number of Equilibrium Stages = 3

The Equilibrium Constant = 0.875

The characteristics of this model for different flow conditions can be expressed in terms of the coefficient matrix [A], the input matrix [B], the transfer matrix [ϕ], the control matrix [Δ], the input vector ($\underline{u}$), and the initial state variables vector ($\underline{x}_0$). The corresponding values for these matrices and vectors as obtained from the numerical solution of the equivalent equations for the seven flow conditions of the time-invariant model are given in Table along with the state-vector values after 30 minutes of applying a step change in the feed phase concentration, and the time-delay for each stage response.

Time-Varying Model:

A similar set of seven concepts of flow has been used in the time-varying model and tested for a ramp change in the feed phase flowrate [= 0.05 x time(mins) x feed phase mass flowrate (gm/min)]. The program was initiated with similar values for the time-invariant model, but due to changes in the mass flowrate of one of the phases the above mentioned matrices and vectors values vary with time.

Comparison of Dynamic Models

For the set of seven time-invariant versions of the model, Figure 28 shows a comparison between the time-response curves of the outlet raffinate concentration for a step change in the inlet feed concentration (- 2.0 wt.%). Also the same set of seven concepts of flow in the time-varying model were tested for a ramp change in the feed phase flowrate. The time-response curve of the last stage for the seven conditions of flow are plotted on the same graph for comparison purposes, Figure 29.

The following conclusions can be drawn from this comparison:

1. The dynamic model with variable back-mixing coefficients in both phases followed by the one with variable back-mixing in solvent phase only and then the one with constant back-mixing coefficients in both phases have the lowest exit raffinate concentration for the same input conditions.

2. The shape of the time-response curve for any time-invariant model disturbed by a step change in the inlet feed phase concentration is either exponential, exponential with pure time-delay, or oscillatory.
   a. Exponential: For a process model with a small number of equilibrium stages, the first stage response is almost exponential.
   b. Exponential with Process-Delay: For any equilibrium stage except the first, the value of the process-delay increases as the number of stages increases.

      For case (a), it has been shown that the last equilibrium stage has the maximum value of time-delay.
   c. Oscillatory: For a process with a large number of equilibrium stages, the first stage shows an oscillatory nature of response in the first period of time. This oscillation is damped down in the stages after the first stage, then an exponential with time-delay response curve results for higher stages number.

      This oscillation is caused mainly by the small time constants in the coefficient matrix and due to this an overlap of the response curves for two successive stages may result. This is not consistent with the practical expectation from a time-invariant process with linear characteristics.
3. The process time-delay appearing in the dynamic response curves is very difficult to predict its value although

a physical explanation for its existence is possible.

The only way to evaluate it quantitatively is to solve the dynamic equations numerically for the given conditions of operation.

4. Effect of backmixing on the dynamic response of a rotating disc contactor:

   a. For constant backmixing coefficients along the column axis, the dynamic response has been evaluated quantitatively by solving the model equations for various values of the backmixing coefficients.

      The calculated values of backmixing coefficients for the solvent and feed phases ($E_{s_{calc}}$ and $E_{f_{calc}}$) have been obtained from the following equation:

$$E_{i_{calc}} = KE_i$$

      where K is a constant with the value 2, 4, or 6, and the E_i's have been obtained from Equation (II-20), Chapter II.

      Typical numerical values obtained for the given conditions of operation by using this equation are:

$$E_s = 1.1 \text{ gm/cm} \quad \text{and} \quad E_f = 0.075 \text{ gm/cm}$$

      where subscripts s and f stand for solvent and feed respectively.

Figures 30-a, b, c, and d show the dynamic responses of a five stage extraction unit for a step change (= -2%) in the inlet feed concentration, and different values for the backmixing coefficients.

From these figures, one would find that a limited change in the backmixing coefficient would not make a noticeable change in the system dynamics.

The second point to be noticed is the very small effect of the feed phase backmixing coefficient (E_f) on the system response, even when $E_{f_{calc}}$ is six times its estimated value.

This could be explained as follows: Backmixing results in an abrupt change of concentration in each phase at its entrance level. Therefore, the solvent phase concentration will increase at the top section (where it enters) while the feed phase has a small solute content. Thus, the concentration driving force will be small.

At the bottom end where the feed phase enters, the feed phase solute content will increase, therefore, an increase in the mass-transfer rate will result.

This explanation affirms the following two points:

1. A great part of mass transfer occurs in the first section of the column, measured from the feed phase inlet point.
2. The backmixing phenomenon causes an undesireable deficiency in mass-transfer operation in both the steady- and transient-states.

b. For variable backmixing throughout the column, little has been done to study the rate of change in backmixing along the column axis in the transient period, firstly

because of the difficulties in computations involved, and secondly, the lack of experimental techniques to measure continuously the coefficients of backmixing.

5. Effect of Shaft Speed

The time varying algorithm was used further to study the effect of the shaft speed on the dynamic response of the process. The model was tested for step changes, of various degrees, in the shaft speed.

From the dynamic response curves obtained, it has been found that the effect of small changes in the shaft speed (±50 rpm) have negligible effect on the quality of the output. This is the case if the process is operating far from the flooding region. For larger step sizes, the effect was still small, but there is a possibility of change in the NTU's for the column. Therefore, the apparent small effect of a large change in the shaft speed on the raffinate concentration obtained from the model is possibly misleading. It is recommended to call frequently the steady-state model subroutine (NORD) to check for any significant change in the dynamic model order for any large change in the shaft speed.

This possible change in the order of the time-varying model due to large change in feed-phase flowrate or shaft speed would make model-following optimal control far more difficult.

6. Stagewise Steady-State Model

The main idea in solving this stagewise model is using the state space dynamic model structure and reducing it to consider the initial steady-state condition before introducing any disturbances. The rate of change in concentration with respect to time is equal to zero, this can be explained mathematically as follows:

Rewrite the dynamic model vector-matrix equation,

$$\dot{\underline{x}}(t) = [A]\ \underline{x}(t) + [B]\ \underline{u}(t) \qquad \text{(V-35)}$$

Equating $\dot{\underline{x}}(t)$ to zero results in

$$0 = [A]\ \underline{x}(t) + [B]\ \underline{u}(t)$$

Rearranging, we obtain,

$$x(t) = -[A]^{-1}[B]\ \underline{u}(t) \qquad \text{(V-36)}$$

Solving Equation (V-35) for $\underline{x}(t)$ as in Equation (V-36) involves inverting matrix [A], matrix by matrix multiplication and matrix by vector multiplication.

A flow chart for the computer program main calculation steps is shown in Figure 31.

Comparison of Steady-State Stagewise and Differential Models

Miyauchi and Vermeulen[27,31] have related the differential model to the stagewise model, for a mass-transfer liquid-liquid extraction process by converting the differentials to the equivalent finite difference equations, which are shown as follows:

$$\frac{dx}{dz} = \frac{(x_{n+1} - x_{n-1})N}{2}$$

$$\frac{dy}{dz} = \frac{(y_{n+1} - y_{n-1})N}{2} \qquad \text{(V-37)}$$

$$\frac{d^2x}{dz^2} = N^2(x_{n+1} - 2x_n + x_{n-1})$$

and

$$\frac{d^2y}{dz^2} = N^2(y_{n+1} - 2y_n + y_{n-1})$$

Substitution of these equivalents in the differential equation (Chapter III) and comparison of the resulting finite-difference equation with that given for the stagewise model, shows the following:

$$\frac{f}{N} + \frac{1}{2N} = \frac{1}{Pe_x} \quad \text{and} \quad \frac{s}{N} + \frac{1}{2N} = \frac{1}{Pe_y} \qquad \text{(V-38)}$$

Equation (V-37) gave approximate relationships, the accuracy of which increases as the total number of stages (N) increases. When N goes to infinity, the relationships become more exact and the two models will be exactly similar. If f and s go to infinity, f/N and s/N remain finite, then;

$$\frac{f}{N} = \frac{1}{Pe_x} \quad \text{and} \quad \frac{s}{N} = \frac{1}{Pe_y} \qquad \text{(V-39)}$$

Numerical Comparison

Wilburn's differential model with end effects was solved co-currently in the steady-state stagewise model with seven concepts of flow. The raffinate concentration for

these models, for the same conditions of operation, are summarized in Table 7.

From this table, one can realize that the stagewise models with constant or variable axial mixing coefficients in the solvent phase only are the closest to the differential model.

Experimental Validation of the Dynamic Model

A schematic diagram of the process and the various manual and automatic instruments mounted on it is given in Figure 3, Chapter II. The continuous sensors and actuators were calibrated off-line and the smoothed curves were used for on-line measurements. Also, an up-dating on-line procedure was used to check on the validity of the calibration curves and modify them if necessary.

The instruments can be categorized into two main groups: (a) concentration probes, e.g., conductivity, refractometer, specific gravity, and (b) actuators or flow measuring devices, e.g., motorized valves, hot-wire anemometer, shaft-speed tachometer and orifice meter.

Interface

This is comprised of

(i) an analogue-to-digital converter (ADC)

(ii) a digital-to-analogue converter (DAC)

(iii) an analogue selection unit (ASU)

(iv) output relays

(v) status lights and alarms

Computer

A Ferranti "Sirius" computer with a storage capacity of 7K words each of 10 decimal digits and a memory cycle time of 0.24 msec was employed. It has two tape readers and a "flexowriter" for printing out as peripherals.

Software

Programs necessary for on-line supervisory control, data logging and first-level control can be classified as

1. First-level programs which include commands to read the digital clock, to select and read analogue inputs, to control the position of motorized valves through interface relays, to read an auto/manual digital handset for timing the start-up or interrupting on-line operation by the operator, to zero index all variables before start-up and to initialize valves and rotating shaft.
2. Second-level programs which include first level-control algorithms for initializing the process, valve actuation and control, interface level control, and an executive routine to define priorities of scanning and processing different parts of the heirarchy.
3. Third-level programs for data logging, acquisition and smoothing.

Procedure

Due to the large storage requirements for the dynamic model algorithm it was impossible to carry out the validation on-line. Therefore, a set of runs in which the system

was operating in the dynamic (transient) range is used to validate the model off-line.

The procedure adopted to obtain this type of dynamic response data is simply operating the process on-line with a supervisory control program to take the necessary data for the dynamic response comparison.

Results

The time-varying algorithm with seven different flow conditions was used for the comparison purposes because of its capability of handling disturbances in flowrates as well as in concentrations.

The experimental feed and solvent phase inlet flowrates and concentrations were fed in with the dynamic model program and used as input to the algorithm. The experimental raffinate outlet concentration was compared with the exit feed concentration as calculated from the seven flow conditions. It was found that, due to the small size of the column and low level of operation, the number of transfer units (i.e., the order of the dynamic model) is very small. This low dynamic model order turned out to be a too sensitive estimate to rely on in comparing the model with the process.

The steady-state plug-flow number of transfer units (NTU_p) calculated for the given level of operation is 1.247. The steady-state axial mixing flow number of transfer units (NTU_M) required to achieve the same level of extraction

capability, calculated by integration of the concentration profiles as described in Chapter III, is equal to 2.065. Two procedures were taken to compare the dynamic model responses with the experimental measurements:

1. By solving the dynamic model for two theoretical stages and linear interpolation for the dynamic response, between exit of stages one and two, to give the equivalent dynamic response for 1.247 stages. Table 8 (Case 1) shows a comparison between the measured and calculated dynamic response. Also, Table 9 (Case 1) shows a comparison between the root mean square error for the seven flow conditions.
2. By solving the dynamic model for two theoretical stages and comparing the exit raffinate concentration for each condition of flow with the measured. Similar tabulated results are shown in Tables 8 and 9 (Case 2).

The first set of results shows that plug-flow condition (No. 1) comes first, followed by variable axial mixing in feed phase only (No. 6), and thirdly the constant axial mixing in feed phase only condition (No. 3).

The second set of results shows that, although the root mean square error (RMS) is relatively higher than that for the previous case, the variable axial mixing in both phases and in solvent phase only are the most representative of the process.

The last finding confirms the implicit validation which was carried out between the steady-state model with

constant axial mixing and ends effect (STSM #4), and the seven flow condition stagewise model as solved for an initial unforced state.

This sudden swing from one flow regime to another, due to difference in estimated order, should become less severe as the order of the model becomes higher. For full-scale industrial columns the number of transfer units becomes larger (in the order of 10-30 stages), and a fraction of a stage would not show that large a difference on the dynamic response predictions. Therefore, this problem is particular to very small scale columns operated at low level.

Finally, one should not put a 100% confidence in continuous instruments measurements due to many problems associated with them such as drift, sensor fouling-up or interaction. As a result, one would expect the process dynamics to be represented by different flow conditions for different levels of operation and disturbance magnitude. Hence, the dynamic model with seven flow conditions algorithm will be a useful reference structure to guide and control the process in the transient period over a wide range of disturbances.

Conclusions

1. The dynamic model algorithm with seven possible flow regimes would prove flexible to accommodate a wide range of operation for the column. The version with

minimum error deviation with the process is used directly for model-reference control and/or dynamic optimization. This would save computer storage and running time necessary for on-line up-dating of the model parameters by nonlinear regression techniques.

2. The use of state-space formulation and solution would make the algorithm very reliable for optimal control and dynamic stability studies.
3. From the steady-state stagewise vs. differential models comparison, it became evident that the dynamic model with either constant or variable axial mixing in the solvent phase only would be the most likely close flow condition version of the model to represent the actual performance of the process in the transient stage.
4. Experimental studies further confirm that the dynamic model with variable axial mixing in solvent phase only most closely represents the process dynamics.

TABLE 5

SUMMARY OF LITERATURE ON THE DYNAMIC BEHAVIOR OF EXTRACTION PROCESSES

1. Stagewise Contact

a. Theoretical

1947 Marshall and Pigford
1950 Lapidus and Amundson
1961 Gray
1961 Wilde
1962 Wilde
1963 Biery and Royland
1966 Hartland and Mechlenburgh
1967 Kafarov, Vygon, and Gordeev
1968 Lees
1969 Pollock and Johnston
1970 Souhrada, Landau, and Prochazka

b. Numerical

		Type of Column
1960	Diliddo	Pulsed
1961	Biery and Royland	Pulsed
1962	Watjen	Pulsed
1963	Chiu	Scheibel
1964	Foster	Pulsed
1965	Pollock	Scheibel

c. Experimental

1959	Staffin	Pulsed
1961	Biery	Pulsed
1962	Watjen	Pulsed
1963	Chiu	Scheibel
1965	Pollock	Scheibel
1965	Evans	Pulsed
1967	Burns and Hanson	Mixer-Settler
1969	Pollock and Johnston	Mechanically Agitated
1970	Pollock and Johnston	Mechanically Agitated

d. Control

1960	Diliddo	Pulsed
1965	Evans	Pulsed

2. Differential Contact

a. Theoretical

1947 Marshall and Pigford
1954 Jaswon and Smith
1961 Gray
1966 Chernyshev
1969 Rolke and Wilheim

b. Numerical

		Type of Column
1962	Champagne	Pulsed
1965	Doninger	Packed
1966	Elkins	Spray and Packed

c. Experimental

1951	Huang	Spray
1956	Lavergne	Packed
1963	Clements	Packed
1963	Justice	Packed
1965	Doninger	Packed
1966	Elkins	Spray and Packed
1968	Doninger	Packed

TABLE 6

TIME-INVARIANT DYNAMIC MODEL NUMERICAL RESULTS

Characteristic Flow Condition	A-Matrix					B-Matrix		x_0-Initial State Variable Vector	ϕ-Matrix					Δ-Matrix		$\bar{x}$ (State Vector) at time = 30 min	Time Delay mins
A. Plug Flow	-0.82866	0.26772	0.0	0.0	0.0	0.56094	0.0	0.09869	0.47025	0.12286	0.01624	0.00144	0.00010	0.38911	0.00001	0.11837	Stage 1 = 0.0
	0.56094	-0.82866	0.26772	0.0	0.0	0.0	0.0	0.09595	0.25742	0.50428	0.12587	0.01644	0.00144	0.09443	0.00011	0.11500	2 = 0.0
	0.0	0.56094	-0.82866	0.26772	0.0	0.0	0.0	0.09019	0.07131	0.26373	0.50470	0.12587	0.01624	0.01635	0.00178	0.10801	3 = 1.00
	0.0	0.0	0.56094	-0.82866	0.26772	0.0	0.0	0.07814	0.01323	0.07219	0.26373	0.50428	0.12286	0.002190	0.02151	0.09349	4 = 1.5
	0.0	0.0	0.0	0.56094	-0.82856	0.0	0.26772	-0.05290	0.00187	0.01323	0.07131	0.25742	0.47025	0.00024	0.18571	0.06324	5 = 2.0
B. Constant Back-Mixing in Both Phases	-1.51105	0.60892	0.0	0.0	0.0	0.90214	0.0	0.09497	0.28710	0.16073	0.04685	0.00926	0.00136	0.49449	0.00021	0.11396	1 = 0.0
	0.90214	-1.51105	0.60892	0.0	0.0	0.0	0.0	0.08752	0.23813	0.35651	0.17444	0.04886	0.00926	0.17091	0.00189	0.10501	2 = 0.0
	0.0	0.90214	-1.51105	0.60892	0.0	0.0	0.0	0.07648	0.10283	0.25848	0.35949	0.17444	0.04685	0.04431	0.01363	0.09175	3 = 0.25
	0.0	0.0	0.90214	-1.51105	0.60892	0.0	0.0	0.06013	0.03010	0.10725	0.25845	0.35651	0.16073	0.00910	0.07766	0.07213	4 = 2.0
	0.0	0.0	0.0	0.90214	-1.51105	0.0	0.60892	0.03590	0.00655	0.03010	0.10283	0.23813	0.28710	0.00152	0.33377	0.04306	5 = 2.5
C. Constant Back-Mixing in Feed Phase Only	-0.92395	0.31781	0.0	0.0	0.0	0.61103	0.0	0.09814	0.43462	0.13387	0.02094	0.00220	0.00017	0.40819	0.00001	0.11772	1 = 0.0
	0.61103	-0.92895	0.31781	0.0	0.0	0.0	0.0	0.09455	0.25737	0.47488	0.13809	0.02127	0.00220	0.10593	0.00021	0.11336	2 = 0.0
	0.0	0.61103	-0.92885	0.31781	0.0	0.0	0.0	0.08766	0.07739	0.26549	0.47551	0.13809	0.02094	0.01979	0.00279	0.10503	3 = 0.5
	0.0	0.0	0.61103	-0.92885	0.31781	0.0	0.0	0.07442	0.01561	0.07862	0.26549	0.47488	0.13387	0.00287	0.02867	0.08910	4 = 1.5
	0.0	0.0	0.0	0.61103	-0.92885	0.0	0.31781	0.04896	0.00235	0.01561	0.07739	0.25737	0.43462	0.00034	0.21231	0.05859	5 = 3.0
D. Constant Back-Mixing in Solvent Phase Only	-1.41087	0.55982	0.0	0.0	0.0	0.85204	0.0	0.09546	0.30680	0.15928	0.04284	0.00780	0.00106	0.48208	0.00015	0.11454	1 = 0.0
	0.85204	-1.41087	0.55882	0.0	0.0	0.0	0.0	0.08854	0.24285	0.37212	0.17117	0.04445	0.00780	0.16017	0.00143	0.10623	2 = 0.0
	0.0	0.85204	-1.41087	0.55882	0.0	0.0	0.0	0.07800	0.09960	0.26098	0.37458	0.17117	0.04284	0.03965	0.01119	0.09356	3 = 0.25
	0.0	0.0	0.85204	-1.41087	0.55882	0.0	0.0	0.06191	0.02763	0.10334	0.26098	0.37212	0.15928	0.00123	0.31618	0.07425	4 = 0.5
	0.0	0.0	0.0	0.85204	-1.41087	0.0	0.55882	0.03739	0.00571	0.02763	0.09960	0.24285	0.30680	0.00123	0.31618	0.04484	5 = 1.0
E. Variable Back-Mixing in Both Phases	-0.98032	0.34355	0.0	0.0	0.0	0.63677	0.0	0.09605	0.42247	0.12768	0.02568	0.00443	0.00069	0.41869	0.00015	0.11526	1 = 0.0
	0.75052	-1.20782	0.45730	0.0	0.0	0.0	0.0	0.08874	0.27894	0.40395	0.14633	0.03644	0.00729	0.12485	0.00220	0.10647	2 = 0.1
	0.0	0.88322	-1.47322	0.59000	0.0	0.0	0.0	0.07673	0.10837	0.28262	0.35857	0.15642	0.04376	0.03069	0.01958	0.09205	3 = 0.2
	0.0	0.0	1.02540	-1.75759	0.73218	0.0	0.0	0.05875	0.03247	0.12231	0.27185	0.31558	0.14031	0.00569	0.11079	0.07048	4 = 0.5
	0.0	0.0	0.0	1.17232	-2.05143	0.0	0.8791	0.03357	0.00807	0.03920	0.12176	0.22466	0.19799	0.00132	0.40700	0.04028	5 = 1.25
F. Variable Back-Mixing in Feed Phase Only	-0.85093	0.27885	0.0	0.0	0.0	0.62564	0.0	0.09638	0.46268	0.12391	0.01776	0.00182	0.00015	0.39366	0.00001	0.11784	1 = 0.0
	0.58877	-0.88432	0.29555	0.0	0.0	0.0	0.0	0.08956	0.26162	0.48659	0.13082	0.01967	0.00210	0.09297	0.00023	0.11345	2 = 0.0
	0.0	0.60825	-0.92328	0.31503	0.0	0.0	0.0	0.07809	0.07719	0.26922	0.47583	0.13508	0.02118	0.01829	0.00320	0.10474	3 = 0.25
	0.0	0.0	0.62912	-0.96502	0.33590	0.0	0.0	0.06041	0.01576	0.03084	0.26976	0.46370	0.13426	0.00270	0.03297	0.08902	4 = 0.75
	0.0	0.0	0.0	0.65069	-1.00815	0.0	0.78936	0.03494	0.00248	0.01676	0.08193	0.26009	0.40679	0.00033	0.23162	0.05679	5 = 3.5
G. Variable Back-Mixing in Solvent Phase Only	-0.95806	0.33242	0.0	0.0	0.0	0.62564	0.0	0.09638	0.42896	0.12728	0.02443	0.00394	0.00057	0.41470	0.00011	0.11564	1 = 0.0
	0.72269	-1.15215	0.42947	0.0	0.0	0.0	0.0	0.08956	0.27671	0.41609	0.14488	0.03387	0.00631	0.12046	0.00167	0.10745	2 = 0.0
	0.0	0.83591	-1.37661	0.54269	0.0	0.0	0.0	0.07809	0.10339	0.29199	0.37408	0.15536	0.04083	0.02843	0.01591	0.09368	3 = 0.1
	0.0	0.0	0.95722	-1.62123	0.66400	0.0	0.0	0.06041	0.02943	0.11629	0.27403	0.33391	0.14324	0.00588	0.09723	0.07247	4 = 1.0
	0.0	0.0	0.0	1.09258	-1.87194	0.0	0.78936	0.03494	0.00691	0.03534	0.11743	0.23353	0.22095	0.00109	0.38473	0.04191	5 = 3.0

TABLE 7

COMPARISON BETWEEN WILBURN'S DIFFUSIONAL MODEL AND SEVEN DIFFERENT STAGEWISE MODELS

Type of Model and Conditions of Flow	Raffinate Conc. (x_{out})
Wilburn's Differential Model with Constant Back-mixing in Both Phases	0.0478947
Stagewise Model	
1. Plug-flow	0.05290
2. Constant back-mixing in both phases	0.0359
3. Constant back-mixing in solvent phase only	0.04896
4. Constant back-mixing in feed phase only	0.03739
5. Variable back-mixing in both phases	0.03359
6. Variable back-mixing in solvent phase only	0.04744
7. Variable back-mixing in feed phase only	0.03494

TABLE 8. EXPERIMENTAL VALIDATION OF THE DYNAMIC MODEL WITH SEVEN FLOW CONDITIONS

Inlet feed phase conc. (x_{in}) = 12.48 wt %
Inlet feed phase flowrate (G) = 52.967 gm/min
Inlet solvent phase conc. (y_{in}) = 0.0 wt %
Shaft speed (R_s) = 0.0 rpm

	Experimental			Raffinate Concentration x_{out} Calculated from the Dynamic Model													
				Case 1 NTU_p = 1.247							Case 2 NTU_M = 2.0						
	Solvent			Flow Condition Number							Flow Condition Number						
Time (mins.)	Conc. (Wt %)	Flowrate (gm/min)	Raffinate Conc. (x_{out})(Wt %)	1	2	3	4	5	6	7	1	2	3	4	5	6	7
16.605	10.63	119.175	3.98	4.526	5.293	4.54	5.286	5.874	4.532	5.873	1.823	2.388	1.833	2.382	2.997	1.828	2.996
17.37	10.56	110.719	4.44	4.574	5.344	4.587	5.332	5.906	4.579	5.904	1.852	2.424	1.862	2.419	3.019	1.857	3.018
18.225	10.67	93.373	4.85	4.702	5.48	4.716	5.473	5.992	4.708	5.991	1.932	2.524	1.942	2.518	3.081	1.937	3.079
19.26	10.61	98.291	4.91	4.784	5.536	4.798	5.552	6.039	4.79	6.037	1.99	2.587	1.999	2.581	3.116	1.994	3.114
20.25	10.63	91.935	4.55	4.888	5.66	4.902	5.653	6.101	4.894	6.100	2.061	2.668	2.071	2.662	3.162	2.066	3.161
21.465	10.68	92.843	4.69	4.973	5.736	4.986	5.729	6.145	4.978	6.144	2.123	2.731	2.133	2.725	3.196	2.128	3.195
22.38	10.63	92.313	4.59	5.048	5.80	5.061	5.794	6.182	5.053	6.130	2.179	2.786	2.19	2.780	3.225	2.185	3.224
23.31	10.63	91.027	4.64	5.12	5.861	5.133	5.854	6.216	5.125	6.215	2.224	2.837	2.245	2.832	3.252	2.24	3.25
24.255	10.63	92.843	4.75	5.171	5.898	5.185	5.892	6.235	5.177	6.233	2.276	2.871	2.286	2.865	3.266	2.261	3.265
25.35	10.68	90.043	5.51	5.232	5.946	5.245	5.94	6.262	5.237	6.261	2.324	2.912	2.334	2.907	3.288	2.329	3.286
26.415	10.69	91.632	5.16	5.275	5.975	5.288	5.969	6.276	5.281	6.275	2.359	2.938	2.369	2.933	3.293	2.364	3.297
27.36	10.61	93.524	5.26	5.302	5.988	5.314	5.982	6.278	5.307	6.277	2.382	2.95	2.392	2.945	3.300	2.368	3.299
28.425	10.55	91.027	5.09	5.34	6.013	5.35	6.007	6.291	5.344	6.290	2.413	2.972	2.423	2.967	3.311	2.418	3.310
29.25	9.47	89.211	7.65	5.382	6.045	5.395	6.039	6.31	5.387	6.310	2.447	3.000	2.457	2.994	3.326	2.452	3.324

TABLE 9. COMPARISON BETWEEN DIFFERENT FLOW CONDITIONS DYNAMIC RESPONSE ACCURACY

Number	Flow Condition	Root Mean Square Error (rms) Case 1'*	Case 2	Case 2'
1	Plug-Flow	0.003187	0.029206	0.026653
	Constant Axial Mixing			
2	a. in Both Phases	0.009686	0.023598	0.020816
3	b. in Feed Phase Only	0.00327	0.029109	0.026553
4	c. in Solvent Phase Only	0.009622	0.023650	0.02087
	Variable Axial Mixing			
5	a. in Both Phases	0.013685	0.019566	0.016384
6	b. in Feed Phase Only	0.00322	0.029156	0.026602
7	c. in Solvent Phase Only	0.013671	0.019577	0.016396

*in primed-number columns (1' and 2'), the last experimental point was excluded from the rms calculation.

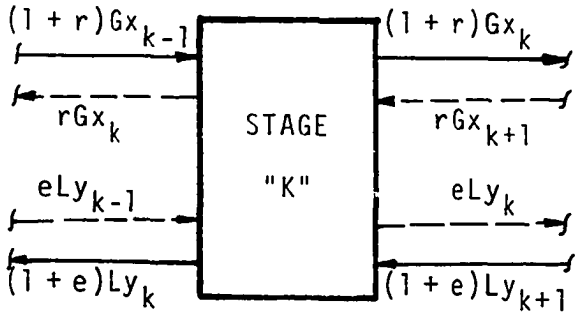

FIGURE 23. MIXED CELL DYNAMIC MODEL REPRESENTATION.

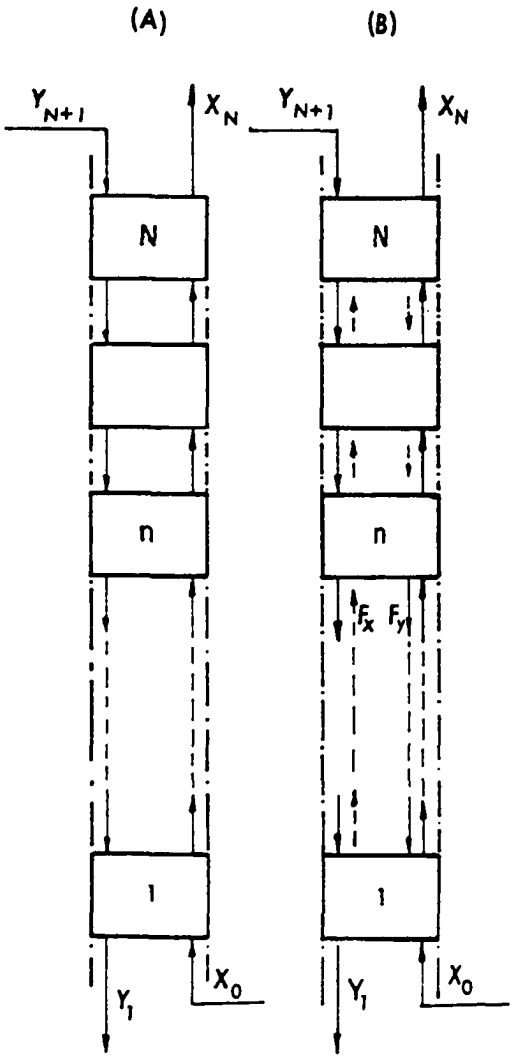

FIG. 24 STAGEWISE COUNTER-CURRENT EXTRACTION PROCESS.

A) Piston-Flow Model.

B) Constant or Variable Back-Mixing Model.

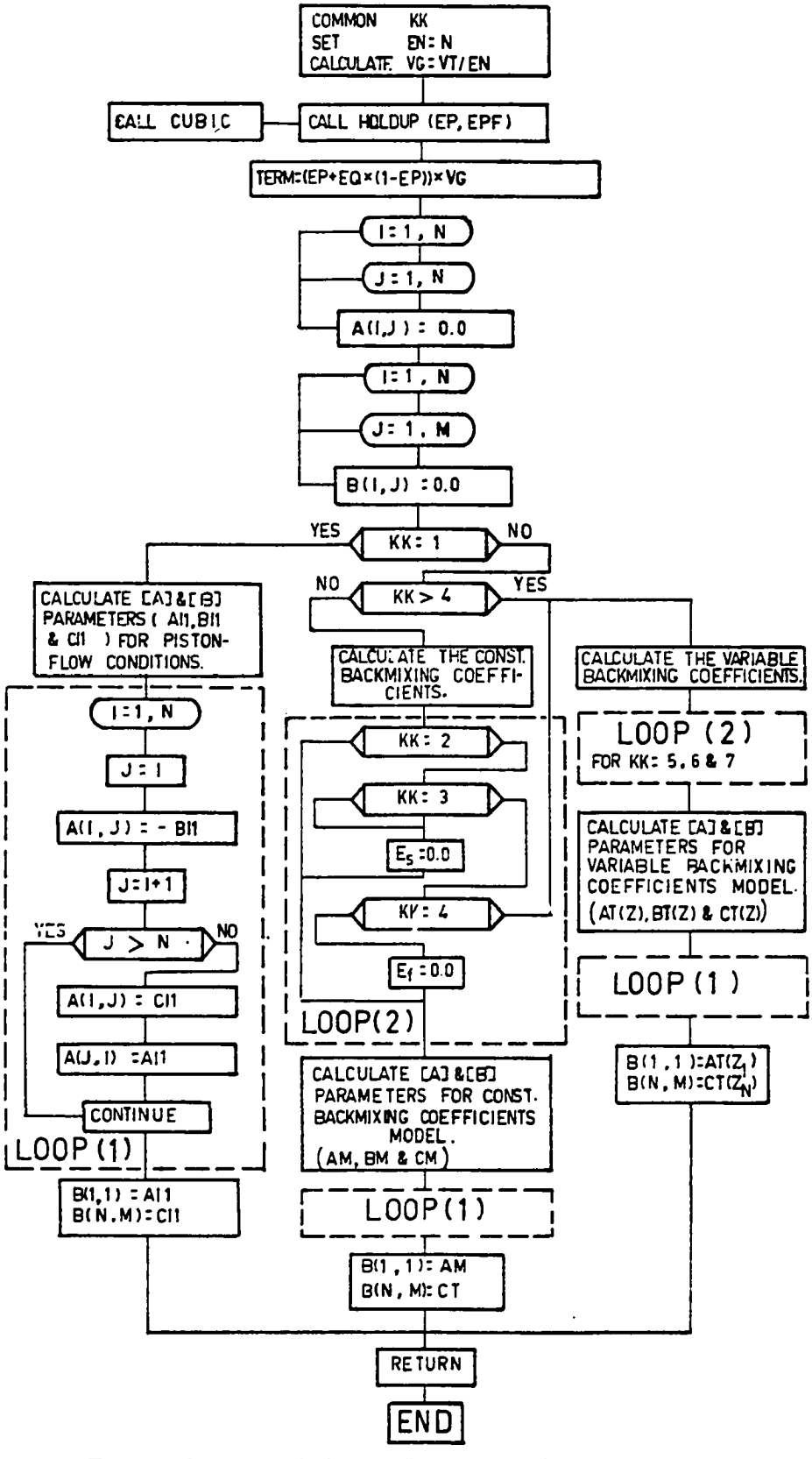

FIG 25 SUBROUTINE ABMAT FLOWDIAGRAM

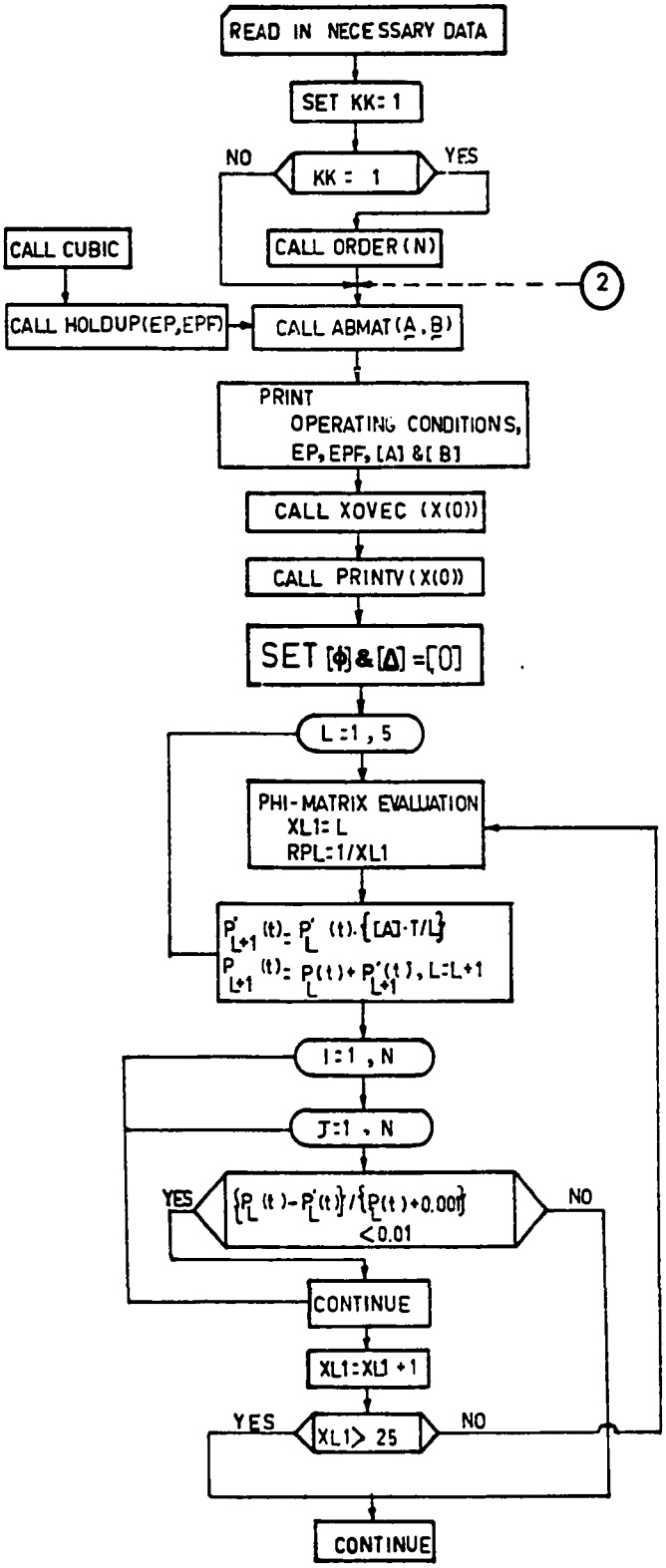
READ IN NECESSARY DATA
SET KK= 1
NO
KK = 1
YES
CALL CUBIC
CALL ORDER (N)
2
CALL HOLDUP(EP,EPF)
CALL ABMAT(A, B)
PRINT
OPERATING CONDITIONS,
EP, EPF, [A] & [B]
CALL XOVEC (X(0))
CALL PRINTV (X(0))
SET [Φ] & [Δ] =[0]
L =1 , 5
PHI-MATRIX EVALUATION
XL1= L
RPL=1/XL1
P'L+1 (t)= P'L (t).{[A]·T/L}
PL+1 (t)= PL(t) + P'L+1(t), L=L+1
I=1 , N
J=1 , N
YES
{PL (t)-P'L(t)}/{PL(t)+0.001}
<0.01
NO
CONTINUE
XL1=XL1 +1
YES
XL1> 25
NO
CONTINUE

(CONT'D) ...

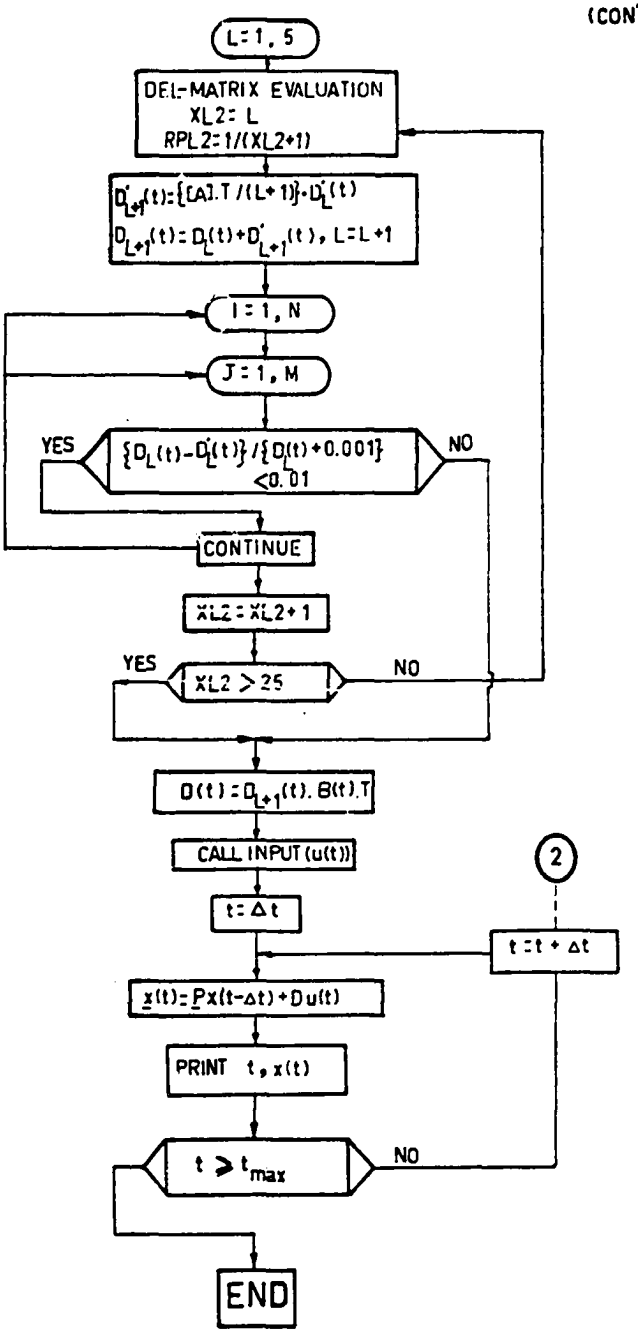

Fig. 26 Main Program Details.

CALCULATING SYSTEM RESPONSE FOR:
1) TIME-INVARIANT MODEL.
2) TIME-VARYING MODEL.

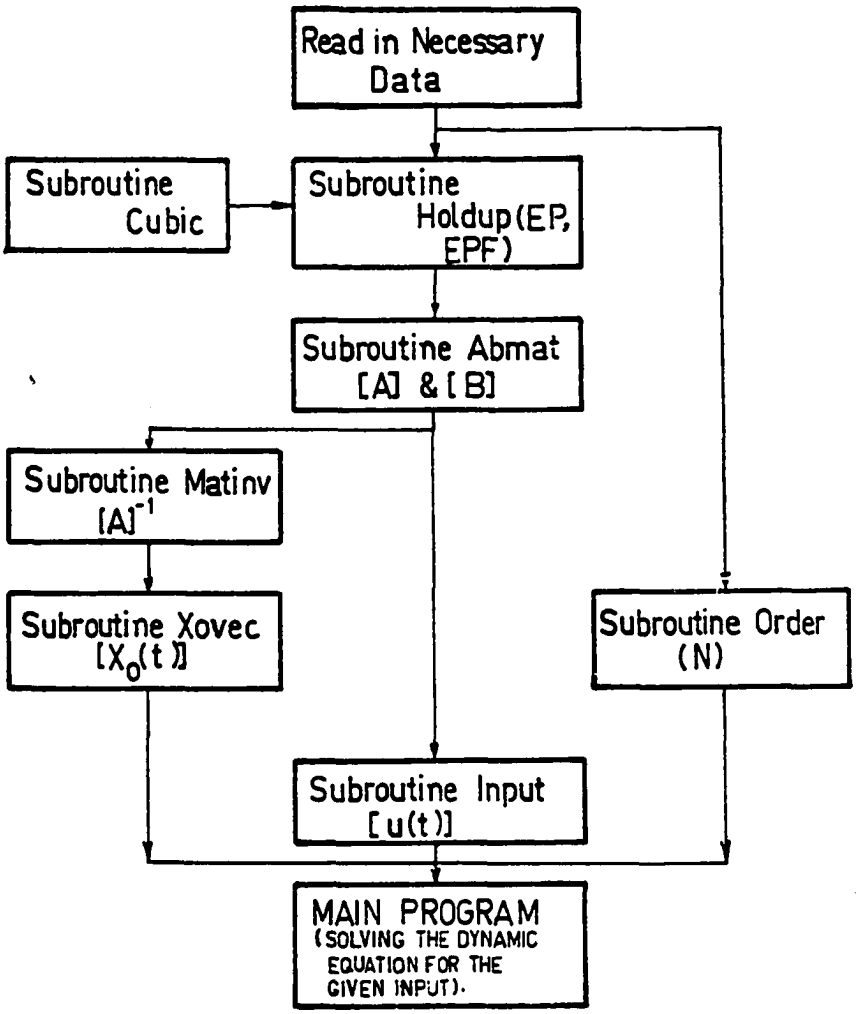

Fig. 27 Outlines For The Dynamic Model Algorithm.

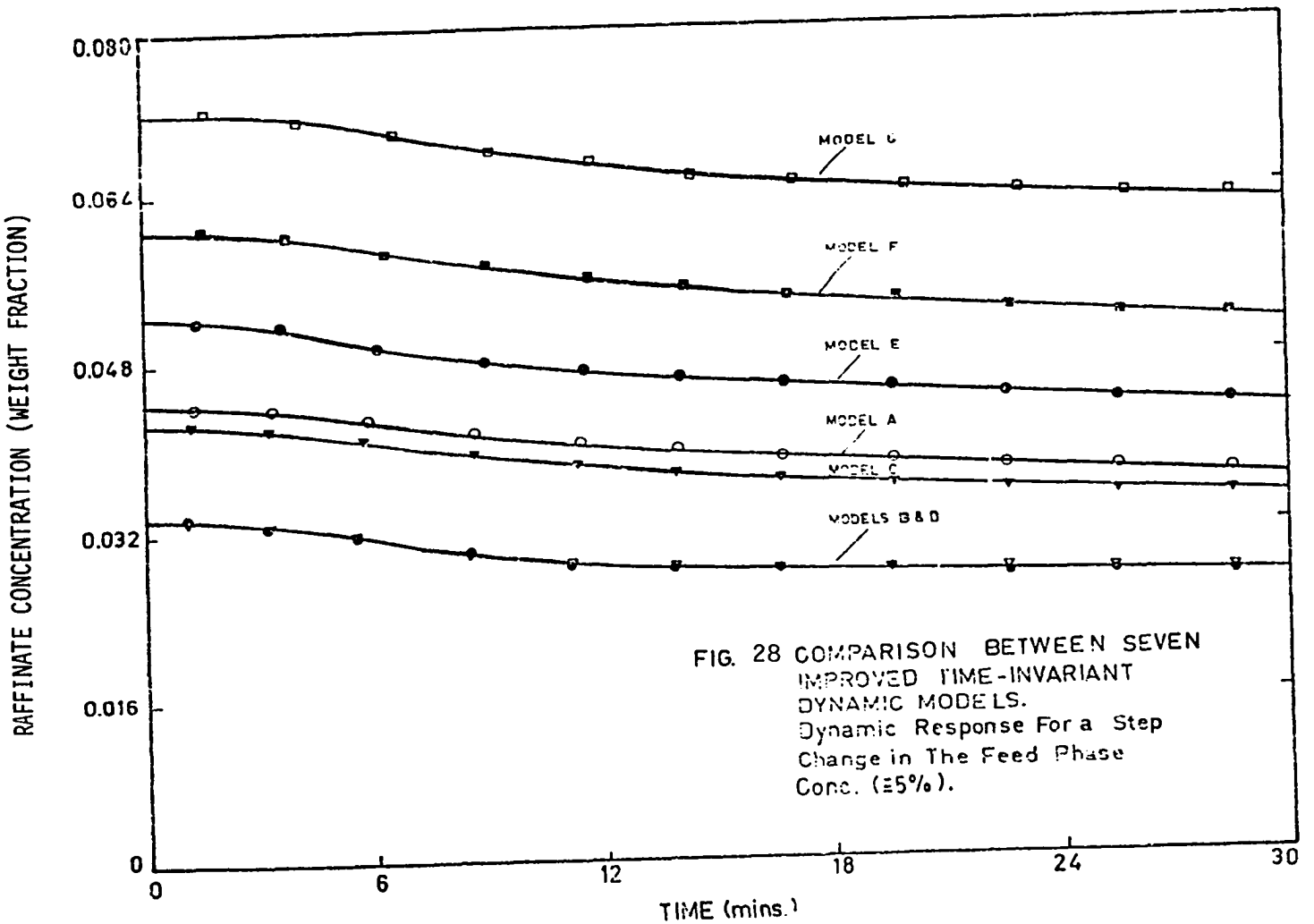

FIG. 28 COMPARISON BETWEEN SEVEN IMPROVED TIME-INVARIANT DYNAMIC MODELS. Dynamic Response For a Step Change in The Feed Phase Conc. (±5%).

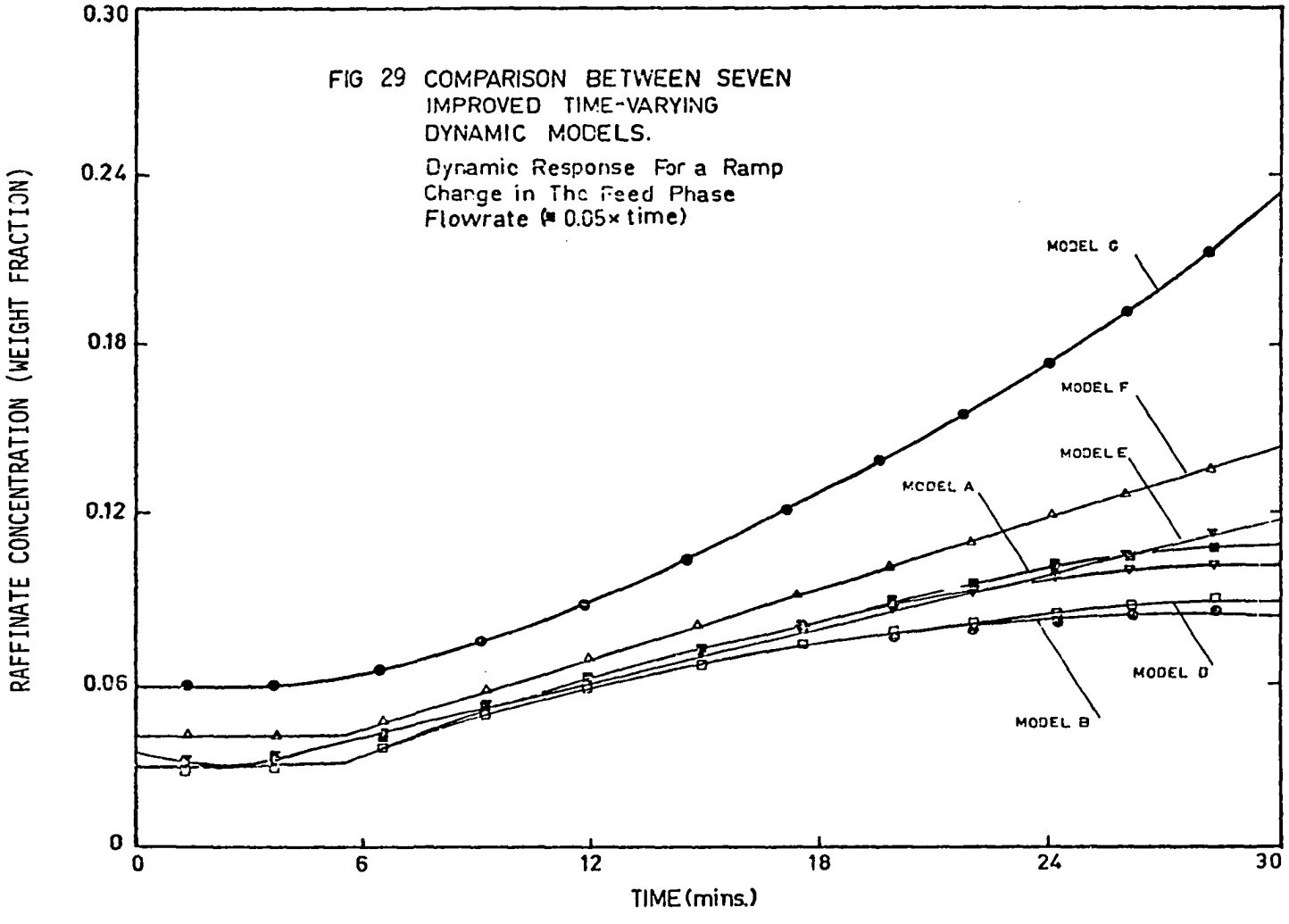
FIG 29 COMPARISON BETWEEN SEVEN IMPROVED TIME-VARYING DYNAMIC MODELS.
Dynamic Response For a Ramp Change in The Feed Phase Flowrate (≈ 0.05× time)
RAFFINATE CONCENTRATION (WEIGHT FRACTION)
TIME (mins.)
0.30
0.24
0.18
0.12
0.06
0
0
6
12
18
24
30
MODEL G
MODEL F
MODEL E
MODEL A
MODEL D
MODEL B

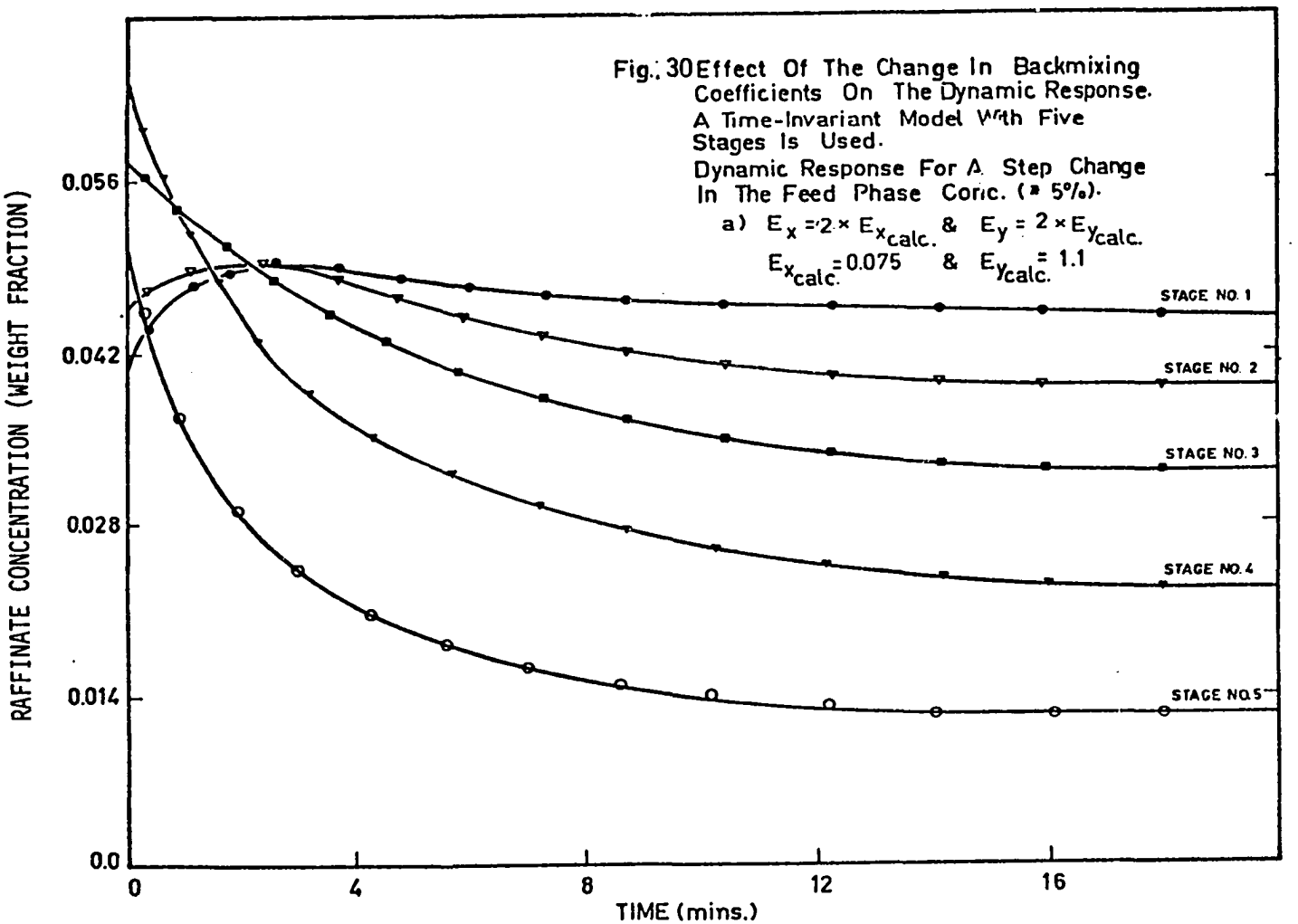

Fig. 30 Effect Of The Change In Backmixing Coefficients On The Dynamic Response. A Time-Invariant Model With Five Stages Is Used. Dynamic Response For A Step Change In The Feed Phase Conc. (± 5%).

a) $E_x = 2 \times E_{x_{calc.}}$ & $E_y = 2 \times E_{y_{calc.}}$

$E_{x_{calc.}} = 0.075$ & $E_{y_{calc.}} = 1.1$

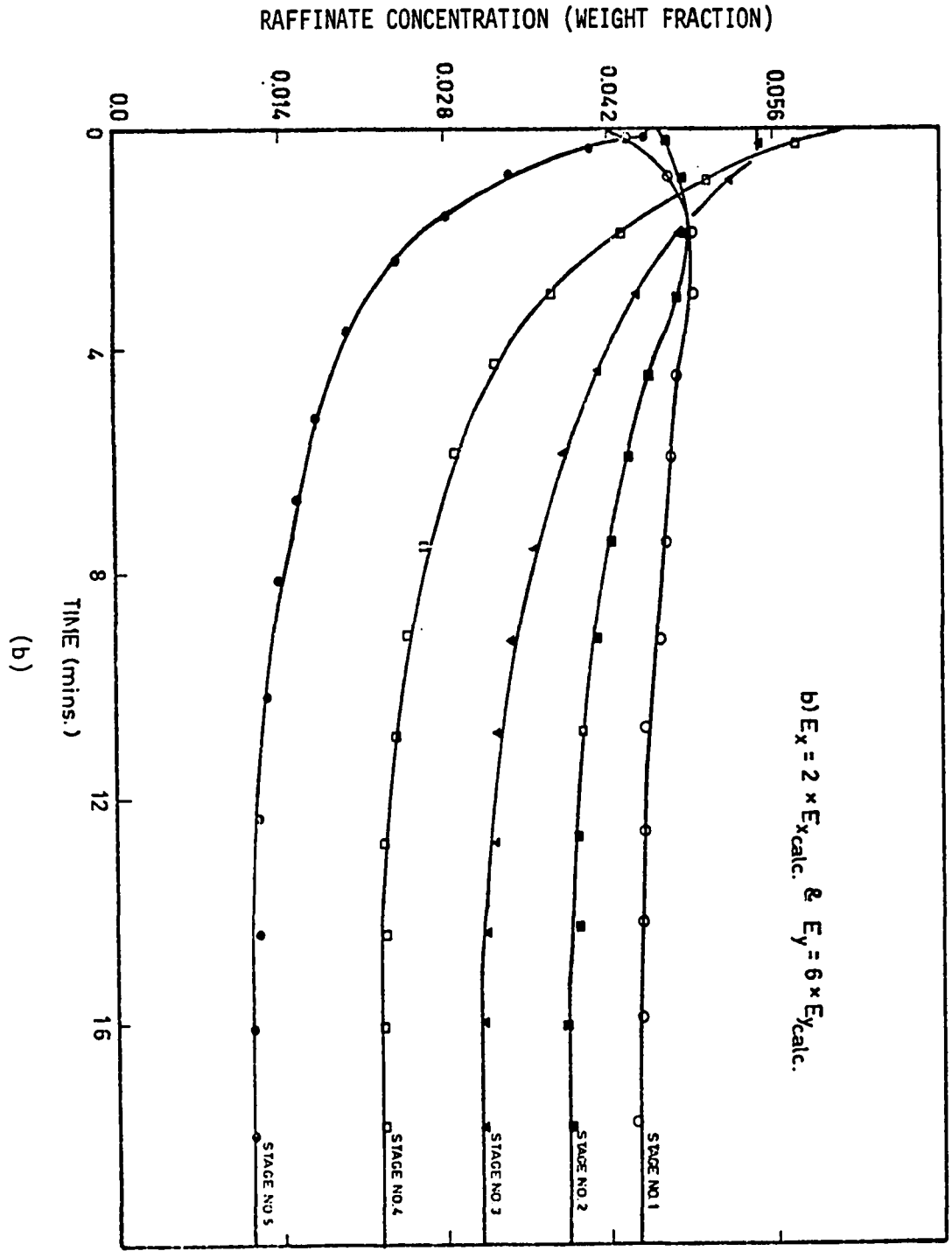
RAFFINATE CONCENTRATION (WEIGHT FRACTION)
0.0
0.014
0.028
0.042
0.056
0
4
8
12
16
TIME (mins.)
b) $E_x = 2 \times E_{x_{calc.}}$ & $E_y = 6 \times E_{y_{calc.}}$
STAGE NO 1
STAGE NO 2
STAGE NO 3
STAGE NO 4
STAGE NO 5

(b)

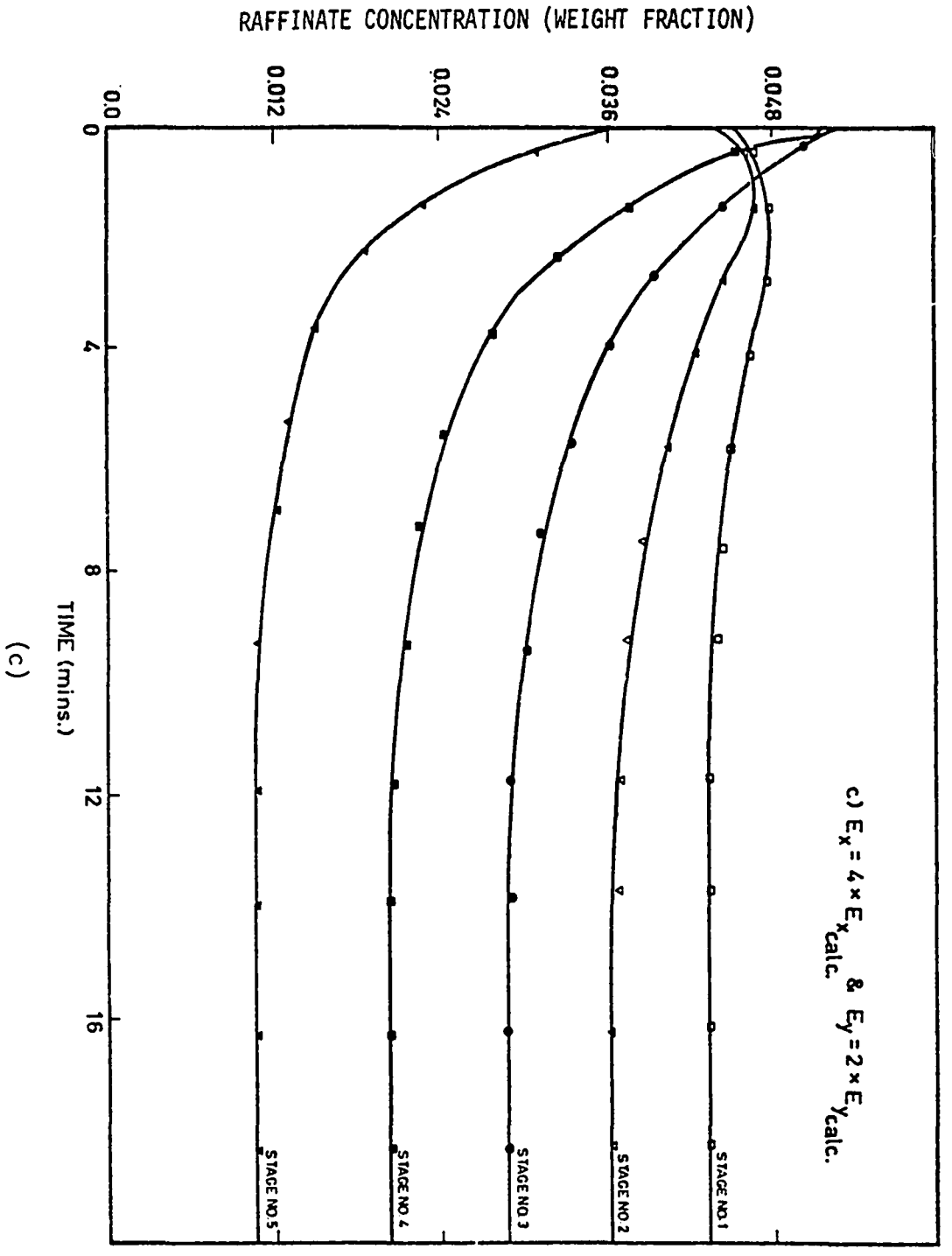
RAFFINATE CONCENTRATION (WEIGHT FRACTION)
0.0
0.012
0.024
0.036
0.048
0
4
8
12
16
TIME (mins.)
c) $E_x = 4 \times E_{x_{calc.}}$ & $E_y = 2 \times E_{y_{calc.}}$
STAGE NO. 1
STAGE NO. 2
STAGE NO. 3
STAGE NO. 4
STAGE NO. 5

(c)

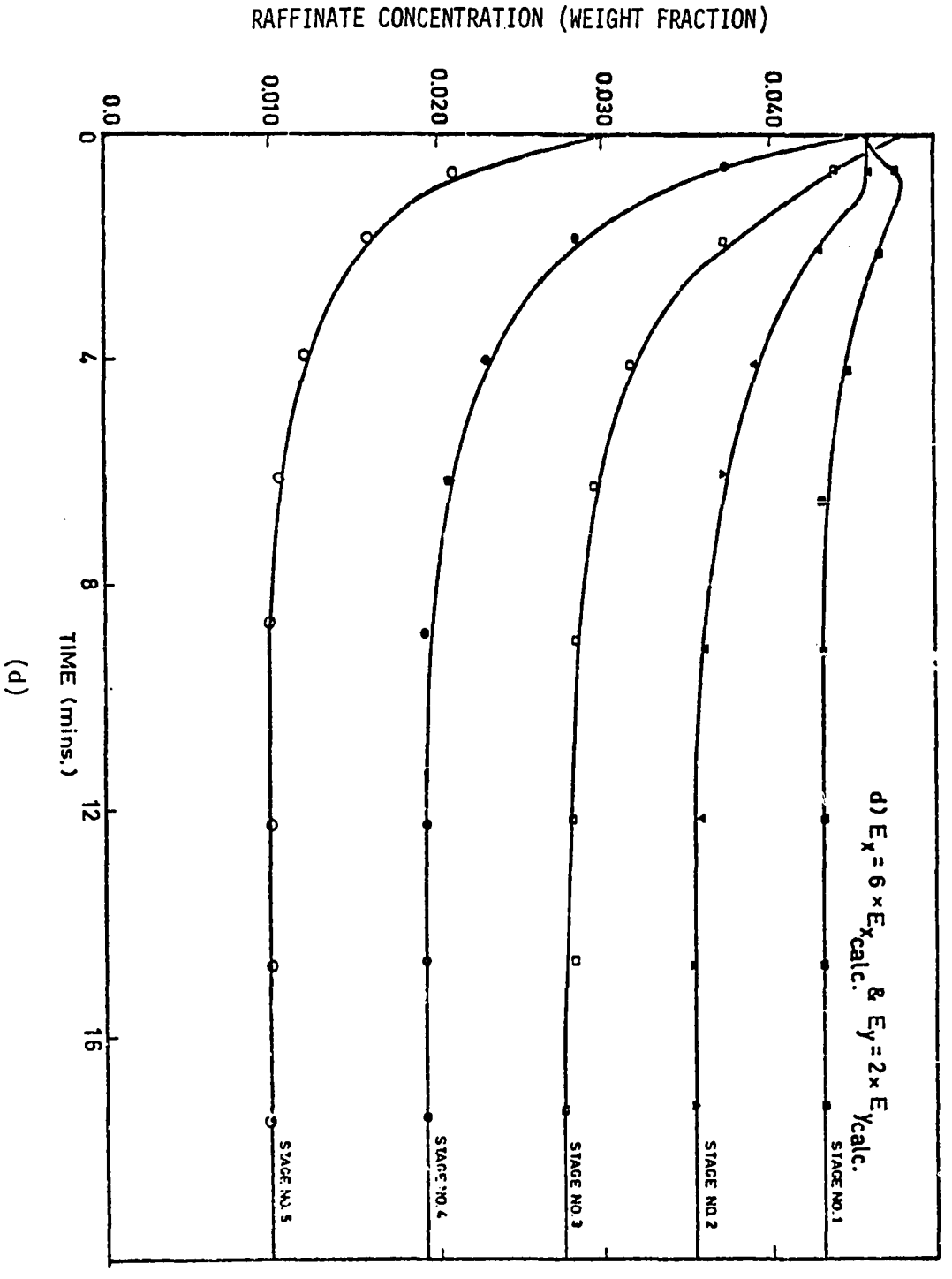
RAFFINATE CONCENTRATION (WEIGHT FRACTION)
0.0
0.010
0.020
0.030
0.040
0
4
8
12
16
TIME (mins.)
d) $E_x = 6 \times E_{xcalc.}$ & $E_y = 2 \times E_{ycalc.}$
STAGE NO.1
STAGE NO.2
STAGE NO.3
STAGE NO.4
STAGE NO.5

(d)

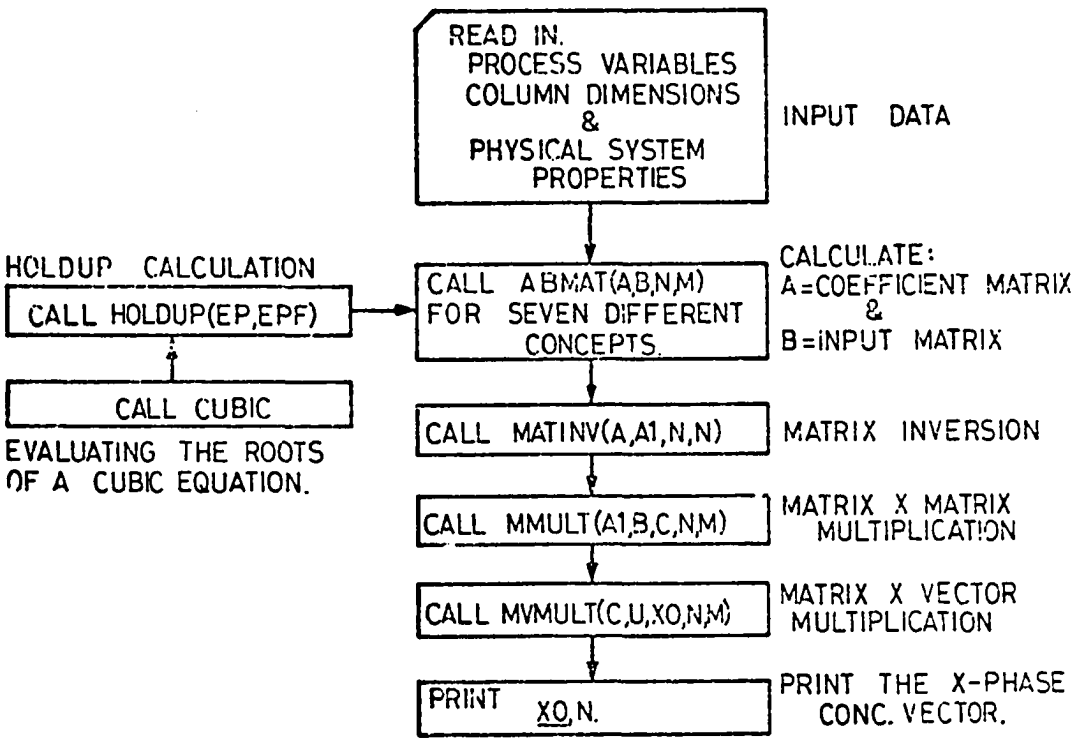

FIG. 31

GENERAL OUTLINES FOR A UNIQUE STEADY-STATE STAGEWISE MODEL FOR SEVEN CONCEPTS OF FLOW.

CHAPTER VI

IMPLICATIONS OF THE STUDY FOR DESIGN AND CONTROL

In the previous chapters of this dissertation a systematic development of the major parts of the study were developed. Kept in mind during the various stages of the work was the fact that it is impossible to account for all the characteristics of the process in a reasonable a priori analytical form, and it is of little value to rely fully on an experimental approach without having a concrete theoretical understanding of the process. On all various levels of the study experimental validation of the theoretical models proved fruitful.

In this chapter, use of the study is demonstrated by putting the guidelines for design and control of a liquid-liquid rotating disc extraction column.

Design Procedure

Data Given:

Liquid System Properties

Equilibrium Relationship

Capacity or Throughput Desired

Required:

Calculate column diameter and height assuming that geometrical configuration of the column is known, i.e. $\frac{H_c}{D_r}$, $\frac{D_r}{D_s}$ and $\frac{D_s}{D_c}$. The latter ratios can be established from pilot scale experimental data after allowing for scaling up.

1. Column diameter

Step 1: Calculate "slip or characteristic velocity" using Equation (II-2).

Step 2: Use holdup algorithm to calculate, using Equations (II-3) and (II-6), the permissible superficial velocity ratio R ($\equiv V_d/V_c$), after assuming operating rates at safe values below flooding.

Step 3: Use the calculated superficial velocity ratio R and the desired column throughput (G + L) to calculate the individual superficial velocities and column diameter.

2. Column height

Step 1: Calculate Peclet numbers or axial mixing coefficients from valid correlations [e.g., for rotating disc contactor, (II-18) and (II-20)].

Step 2: Calculate plug-flow number of transfer units (NTU_p) to achieve a desirable recovery of solute, given the inlet feed concentration, using Equation (III-18).

Step 3: Estimate the possible operating range for the extraction factor Δ ($\equiv mG/L$).

Step 4: Use steady-state model with axial mixing and ends effect algorithm (STSM #4) to calculate the

concentration profile and measured number of transfer units (NTU_M).

Step 5: From assumed stage efficiency, based on pilot scale experiments, the actual number of stages, and hence, the total height of the column is calculated.

Steady State Optimum Operation

Data Given:

Column configuration

Liquid system physical properties

Equilibrium relationship

Peclet numbers

Plug-flow number of transfer units

Process constraints, Equations (IV-3) to (IV-7)

Process limits, Equations (IV-8) to (IV-9)

Required:

Optimum combination of input variables to give a minimum height of transfer unit (HTU_M), a minimum power input, and a maximum throughput, Equations (IV-19) and (IV-20).

Procedure:

Step 1: Use steady-state optimization algorithm with optimum gradient search technique developed in Chapter IV, to optimize the process performance with respect to a valid steady-state model.

Step 2: Include process constraints with the objective function to obtain unconstrained one in a form similar to the one described in Chapter IV.

Step 3: Read in given data and more than one initial starting guess. This is necessary to ensure that the evaluated optimum is a global rather than local in the feasible range.

Optimal Control and Stability Studies

The dynamic model developed and validated experimentally in Chapter V is put in the state-space form and solved in time-domain. This is very suitable for optimal control and stability studies in real-time systems. Also, the dynamic response studies carried out in Chapter V proved that the problem at hand, for either time-invariant or time-varying, is linear with variable time-delay and variable order. This facilitates the process of designing a suitable optimal control technique to be used.

Usually in optimal control, it is desired to find the sequence of inputs $U(K)$, $K = 0, 1, \cdots$, for the dynamic system of equations (V-23), such that the system is driven towards a desired level of operation in an optimum fashion. It can be practically proposed that a fast response with a minimum overshoot is satisfactory. The overshoot requirements lead to stability considerations. Therefore, it is recommended to satisfy necessary conditions for stable response when designing a control strategy. Further work is required in this aspect employing for example Lyapunov's direct method.

Computer Control

The ultimate goal of this study is to be able to apply it for on-line computer control purposes. In real-time systems computer space and CPU time are important parameters. Therefore, the most likely control strategy to be used would rely mainly on performing the most infrequent calculations off-line, such as the steady-state optimization, while supervisory and optimal control policy should be carried out on-line. Figure 32 shows a schematic of the interfacing, supervisory control and optimization and optimal control heirarchy.

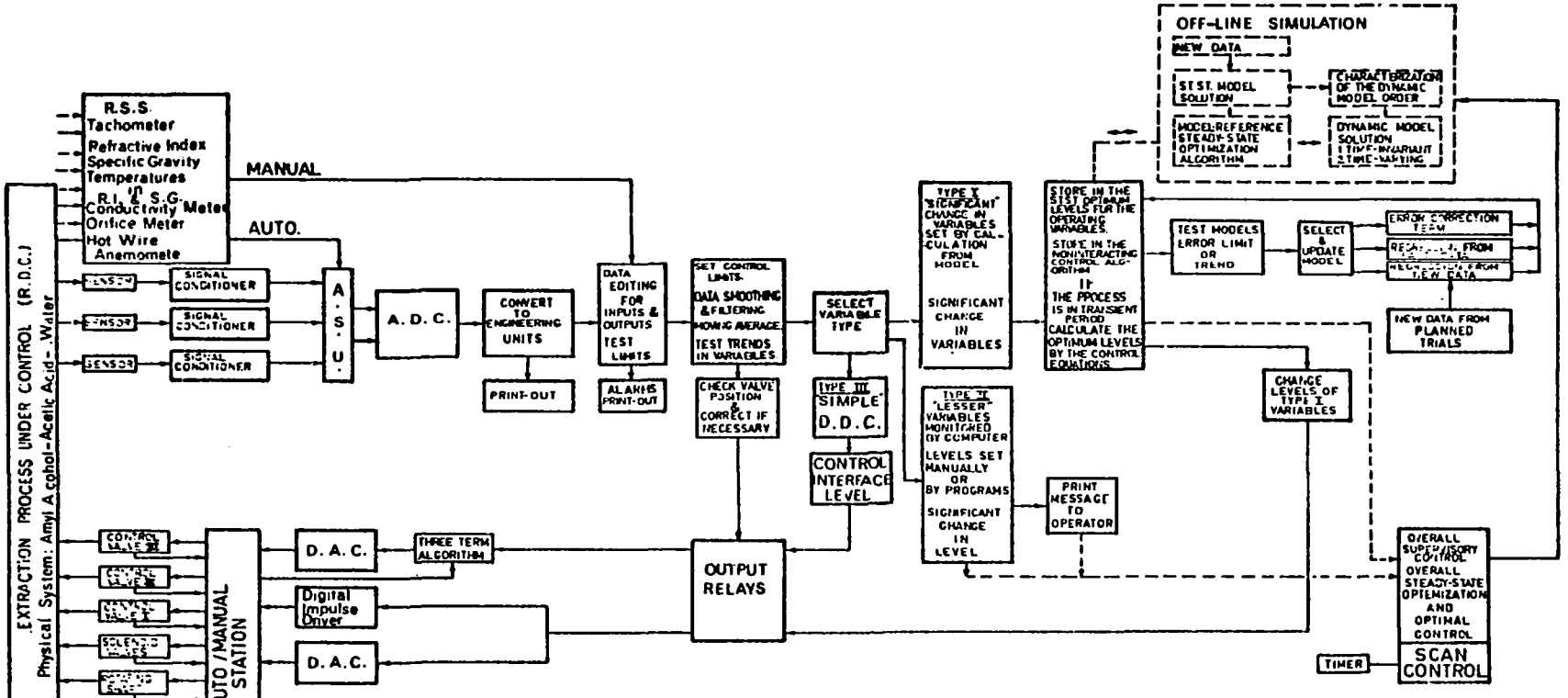

FIG. 32
SCHEMATIC OF AN ON-LINE COMPUTER CONTROL SYSTEM FOR A MECHANICALLY AGITATED LIQUID-LIQUID EXTRACTION PROCESS.

NOMENCLATURE

A	amplitude of the sinusoidal wave, or cross sectional area of contactor
a	interfacial area per unit volume
C_R	constriction area ratio
D	diffusion coefficient, or eddy diffusivity
D_i	diameter (i = c for column, i = r for rotor, and i = s for stator)
D_m	function of column configuration
d	drop diameter
E_i	backmixing coefficient of i-th phase (i = x for feed phase and i = y for solvent phase)
e_i	superficial eddy diffusivity ($= \varepsilon_i E_i$)
f	backmixing coefficient x-phase (stagewise models)
f_i	mean actual rate of interstage mixing
G	feed phase mass flow rate
g	acceleration of gravity
H	compartment height
h	variable height measured from feed phase entrance point
HTU	height of transfer unit
K_i	Weighting factors

K_x overall mass transfer coefficient with respect to x-phase

L solvent phase mass flowrate

m distribution coefficient (for linear equilibrium relationship)

m_c = x_c/x_d, the concentration in feed phase if it is continuous to it when it is dispersed

N rotating disc angular speed (rpm), or total number of stages

n number of compartments

NTU number of transfer units

P_{con} power consumption by the rotating shaft

Pe_i Peclet number for the i-th phase

q volume of tracer of unit concentration which would correspond to the actual amount of tracer introduced into the fluid

R velocity ratio or (G/mL), Table 2

R_d = $G_c m_c/G_d$, Table 2

R_N rotating shaft speed

R_e ratio of the effective and molecular diffusion coefficients

s backmixing coefficient y-phase (stagewise models)

T column throughput (G + L)

T_i i-th constraint

T_x $(K_x az)/G$

T_y $(K_x az)/L$

t	time
U	average flow velocity
V	column total volume
$\bar{V}$	characteristic velocity
V_i	superficial velocity of the i-th phase
x	feed phase concentration, or state variable (Chapters IV, V)
x_i	concentration of the tracer at i-th sampling interval
x^*	equilibrium feed concentration (for linear equilibrium $x^* = my$)
X	dimensionless feed phase concentration
y	solvent phase concentration
Y	dimensionless solvent phase concentration
W_i	weighting factor (weighting constraints among each other)
z	column height
Z	column height in dimensionless form

Greek Symbols

α	velocity coefficient
γ	interfacial tension
Γ_z	dimensionless concentration of x-phase, defined in the text
δ	dimensionless height of the column bottom end
Δ	extraction factor (= mG/L), or dimensionless height of the column top end
ε	holdup volume fraction

ξ phase angle

μ viscosity

ϕ the dissipation of energy per unit volume

ρ density

σ^2 the variance of the x-phase

θ_i ($= \tau_i$) time of taking the i-th sample

$\chi(u)$ functional of velocity

$\chi(d)$ functional of drop diameter

ψ_z dimensionless concentration of x-phase, defined in the text

ω angular frequency

Subscripts

a pertaining to before injection point

a_x axial

b pertaining to after injection point

c continuous

d dispersed

e extract

f feed, or flooding

l longitudinal

M measured

n non-quadratic

o the value at point of injection

P plug-flow

q quadratic

r reverse, rotor, or raffinate

s solvent phase, or stator

T true

Superscripts

1 at dimensionless height Z = 1, and just outside the column

0 at dimensionless height Z = 0, and just before entering the column

REFERENCES

1. Eykhoff, P., IRE-Trans. Aut. Control, 8, 347 (1963).
2. Tapley, B. D., and Lewallen, J. M., "Comparison of Several Numerical Optimization Methods," JOTA, 1, No. 1, 2-32 (1967).
3. Mumford, C. J., "Advance in equipment for liquid-liquid extractors," Brit. Chem. Eng., 13, No. 7, 981-986 (1968).
4. Reman, G. H., and Van Der Vusse, J. G., Petroleum Refiner, 34, 44 (1955).
5. Reman, G. H., "Influence of design variables on capacity and efficiency of RDC," JOINT Symposium of Scaling up (1957; Instn. Chem. Engrs.), 535-540.
6. Misek, T., "Operating conditions in mechanical liquid extractors," Int. Chem. Eng., 8, No. 3, 439-442 (1968).
7. Reman, G. H., Proc. Third World Petroleum Congress, Hague, Section III, 121 (1968).
8. Kagan, S. Z.; Trukhanov, V. G.; and Kavalev, Yu. N., "Liquid Extraction," (A review of work during 1965-1966). Theor. Found. of Chem. Eng., 2, No. 1, 17-27 (1968).
9. Misek, T., and Rozkos, B., "Dephenolization of waste waters in rotating disc extractors," Int. Chem. Eng., 6, No. 1, 130-137 (1966).

10. Watson, J. S., McNeese, L. E., Day. J., and Corroad, P. A., "Flooding Rates and Holdup in Packed Liquid-Liquid Extraction Column," AIChE J., 21, No. 6, 1080-1086 (1975).

11. Miyanami, K., Tojo, K., Yano, T., Miyaji, K. and Minami, I., "Drop Size Distributions and Holdups in a Multi-stage Vibrating Disk Column," C.E.S., 30, 1415-1420 (1975).

12. Laddha, G. S., Krishnan, T. R., Viswanathan, S., Vedaiyan, S., Degaleesan, T. E., and Hoelscher, H. E., "Some Performance Characteristics of Liquid Phase Spray Columns," AIChE J., 22, No. 3, 456-462 (1976).

13. Weinstein, B., and Treybal, R. E., "Liquid-Liquid Contacting in Unbaffled Agitated Vessels," AIChE J., 19, No. 2, 304-312 (1973).

14. Delichatsios, M. A., and Probstein, R. F., "The Effect of Coalescence on the Average Drop Size in Liquid-Liquid Dispersions," I & EC--Fund., 15, No. 2, 134-138 (1976).

15. Park, J. Y., and Blair, L. M., "The Effect of Coalescence on Drop Size Distribution in an Agitated Liquid-Liquid Dispersion," C.E.S., 30, 1057-1064 (1975).

16. Standart, G. L., Cullinan, H. T., Pabarah, A., and Louizos, N., "Ternary Mass Transfer in Liquid-Liquid Extraction," AIChE J., 21, No. 3, 554-559 (1975).

17. Sethy, A., and Cullinan, H. T., "Transport of Mass in Ternary Liquid-Liquid System," AIChE J., 21, No. 3, 571-582 (1975).

18. Westerterp, K. R., and Landsman, P., "Axial mixing in a RDC--Part I: Apparent Longitudinal Diffusion," C.E.S., 17, 363-372 (1962).

19. Westerterp, K. R., and Landsman, P., "Axial mixing in a RDC--Part II: Backmixing," C.E.S., 17, 373-377 (1962).

20. Reman, G. H., C.E.P., 62, No. 9, 56 (1966).

21. Kung, E. Y., and Beckman, P. B., "Dispersed-phase holdup in a RDC," A.I.Ch.E. Jr., 7, No. 2, 319-324 (1961).

22. Strand, C. P.; Olney, R. B., and Beckman, G. H., A.I.Ch.E. Jr., 8, No. 2, 252 (1962).

23. Vermijs, H. J. A., and Kramers, H., "Liquid-liquid extraction in a RDC," C.E.S., 3, 55-64 (1954).

24. Logsdail, D. H.; Thornton, J. D., and Pratt, H. R. C., "Liquid-liquid extraction Part XIV: Flooding rates and performance data for a RDC," Trans. Instn. Chem. Engrs., 35, 301-315 (1957).

25. Thornton, J. D., Industrial Chemist, 39, 298 (1963).

26. Levenspiel, O., and Smith, W. K., "Notes on the diffusion type model for the longitudinal mixing of fluids in flow," C.E.S., 6, 224-233 (1957).

27. Miyauchi, T., and Vermeulen, T., "Longitudinal dispersion in two-phase continuous-flow operation," I & EC (Fund.), 2, No. 2, 113-126 (1963).

28. Miyauchi, T.; Mitsutak, H.; and Havase, I., "Longitudinal dispersion in rotating impeller types of contactors," A.I.Ch.E. Jr., 12, No. 3, 508-513 (1966).

29. Taylor, G., "The dispersion of matter in turbulent flow through a pipe," Proc. Roy. Soc. Series A, 220, 446-468 (1954).

30. Taylor, G., "Conditions under which dispersion of a solute in a stream of solvent can be used to measure molecular diffusion," Proc. Roy. Soc. Series A, 219, 473-477 (1953).

31. Miyauchi, T., and Vermeulen, T., "Diffusion and back flow models for two-phase axial dispersion," I & EC (Func.), 2, No. 4, 304-310 (1963)

32. Rod, V., "Calculation of extraction columns with longitudinal mixing," Brit. Chem. Eng., 9, No. 5, 300-304 (1964).

33. Danckwerts, P. V., C.E.S., 2, 1 (1953).

34. Danckwerts, P. V., Trans. Faraday Soc., 46, 300 and 701 (1951).

35. Van Der Laan, E. Th., "Notes on the diffusion-type model for the longitudinal mixing in flow," C.E.S.-Letters, 7, 187-191 (1957).

36. Hazlebeck, D. E. and Geankoplis, C. J., "Axial dispersion in a spray-type extraction tower," I & EC (Fund.), 2, No. 4, 310-315 (1963).

37. Ebach, E. A., and White, R. R., "Mixing of fluids through beds of packed solids," A.I.Ch.E. Jr., 4, No. 2, 161-169 (1958).

38. Kerkhof, P. M., and Thijssen, H. C., C.E.S., 29, 1427-1434 (1974).

39. Liles, A. W., and Geankoplis, C. J., "Axial diffusion of liquids in packed beds and end effects," A.I.Ch.E. Jr., 6, No. 4, 591-595 (1960).

40. Gel'perin, N. I.; Pebalk, V. L.; Shashkova, M. N., and Kuznetsova, M. I., "Longitudinal mixing in extraction column with mechanical stirring of phases," Theor. Found. of Chem. Eng., 1, No. 5, 552-559 (1967).

41. Gel'perin, N. I., and Pebalk, V. L., "Liquid Extraction (A survey)," Theor. Found. of Chem. Eng., 1, No. 5, 497-517 (1967).

42. Hinze, J. O., A.I.Ch.E. Jr., 1, No. 3, 289 (1955).

43. Vermeulen, T.; Williams, G. M., and Langlais, G. E., C.E.P., 51, No. 2, 85 (1955).

44. Miyauchi, T., and Oya, H., "Longitudinal dispersion in pulsed perforated-plate columns," A.I.Ch.E. Jr., 11, No. 3, 395-402 (1965).

45. Olney, R. B., "Droplet characteristics in a countercurrent contactor," A.I.Ch.E. Jr., 10, No. 6, 827-835 (1964).

46. Calderbank, P., and Korchinski, J., C.E.S., 6, 65 (1956).

47. Handlos, R., and Baron, T., A.I.Ch.E. Jr., 3, 127 (1957).

48. Skelland, A. H. P., and Wellek, P. M., A.I.Ch.E. Jr., 10, No. 4, 491 (1964).

49. Skelland, A. H. P., and Copnich, A. R. H., Canad. Jr. Chem. Enging., 43, No. 4, 491 (1964).

50. Wellek, R. M. and Skelland, A. H. P., A.I.Ch.E. Jr., 11, No. 3, 557 (1965).

51. Higbie, R., Trans. Amer. Instn. Chem. Engrs., 31, 365 (1935).

52. Levich, V. G., "Physco-Chemical Hydrodynamics," Prentice-Hall, (1963).

53. Kafarov, V. V.; Vygon, V. G., and Gordeev, L. S., "Hydrodynamic models with stagnant zones for packed extraction zones," Int. Chem. Eng., 8, No. 3, 415-419 (1968).

54. Sleicher, C. A., Jr., "Axial mixing and extraction efficiency," A.I.Ch.E. Jr., 5, No. 2, 145-149 (1959).

55. Sleicher, C. A., Jr., "Entrainment and extraction efficiency of mixer-settlers," A.I.Ch.E. Jr., 6, No. 3, 529-531 (1960).

56. Hartland, S., and Mecklenburgh, J. C., "A comparison of differential and stagewise counter current extraction with backmixing," Chem. Eng. Sci., 21, 1209-1221 (1966).

57. Hartland, S., and Mecklenburgh, J. C., "Design of Differential counter-current extraction with backmixing I. Exact methods," Instn. Chem. Engrs. Sym. Ser., 26, 115 (1967)

58. Wilburn, N. P., "Mathematical determination of concentration profiles in a two-phase continuous counter-current extractor," I & EC (Func.), 3, No. 3, 189-195 (1963).

59. Treybal, R. E., "Mass-Transfer Operations," McGraw-Hill Co., (1968).

60. Spang III, H. A., "A review of minimization techniques for nonlinear functions," SIAM-Review, 4, No. 4, 343-365 (1962).

61. Carroll, C. W., "The Created Response Surface Technique for optimizing restrained systems," Oper. Res., 9, 169-185 (1961).

62. Fiacco, A. V., and McCormick, G. P., "The sequential unconstrained minimization for nonlinear programming, A Primal-Dual Method," Mang. Sci., 10, No. 1, 360-366 (1964).

63. Fiacco, A. V., and McCormick, G. P., "Extensions of SUMT for Nonlinear Programming: Equality constraints and extrapolation," Mag. Sci., 12, No. 11, 816-828 (1966).

64. Hestenes, M. R., and Stiefel, E., "Methods of Conjugate Gradients for solving Linear Systems," Jr. Res. N.B.S., 49, 409-436 (19).

65. Davidon, W. C., "Variance Algorithm for Minimization," Computer Jr., 10, No. 4, 406-410 (1968).

66. Goldfarb, D., "Extension of Davidon's Variable Metric Method to minimization under linear inequality and equality constraints," SIAM Jr. Appl. Math., 17, No. 4, 739-764 (1969).

67. Bard, Y., "Comparison of gradient methods for the solution of nonlinear parameter estimation problems,"

SIAM Jr. Num. Analy. 7, 157-186 (1970).

68. Myers, G. E., "Properties of the Conjugate-Gradient and Davidon Methods," JOTA, 2, No. 4, 209-219 (1968).

69. Beckey, G. A., and McGhee, R. B., "Gradient Methods for the Optimization of dynamic system parameters by Hybrid Computation," Balakrishnam, A. V., and Neustadt, L. W. (Editors), "Computing Methods in Optimization Problems," Proc. of a conference held at University of California, Los Angeles (1964), pp. 305-327.

70. Fletcher, J. R., and Reeves, C. M., "Function Minimiaztion by Conjugate Gradients," Computer Jr., 7, No. 2, 149-154 (1969).

71. Fletcher, J. R. and Powell, M. J. D., "A Rapidly Convergent Descent Method for Minimization," Computer Jr., 6, 163-168 (1963).

72. Tapley, B. D., and Lewallen, J. M., "Comparison of Several Numerical Optimization Methods," JOTA, 1, No. 1, 1-32 (1967).

73. Moorhead, D. H., and Himmelbou, D. M., "Optimization of Operating Conditions in a Packed Liquid-liquid Extraction Column," I & EC (Fund.), 1, No. 1, 68-72 (1962).

74. Goldfarb, D., and Lapidus, L., "Conjugate Gradient for nonlinear programming problems with linear constraints," I & EC (Fund.), 7 No. 1, 142-151 (1968).

75. Stewart III, G. W., "A modification of Davidon's minimization method to accept difference approximation of

derivatives," Jr. of The Association for Computer Machinery, 14, No. 1, 72-83 (1967).

76. Pang, K. H., and Johnson, A. I., "The Determination of Theoretical Frequency Response of Stagewise Processes," Can. J. Chem. Eng., 47, 477-482 (1969).

77. Marshall, W. R., Jr. and Pigford, R. L., "The Application of Differential Equations to Chemical Engineering Problems," Univ. of Delaware (1947).

78. Lapidus, L. and Amundson, N. R., "Stagewise Absorption and Extraction Equipment: Transient and Unsteady State Operation," I & EC, 42, 1071-1078 (1950).

79. Gray, R. I., and Prados, J. W., "The Dynamics of a Packed Gas Absorber by Frequency Response Analysis," A.I.Ch.E. J., 9, 211-216 (1963).

80. Gray, R. I., "The Dynamics of a Packed Gas Absorber by Frequency Response Analysis," Ph.D. dissertation, The Univ. of Tennesee, Knoxville, Tennessee (1961)

81. Wilde, D. J., "The Operating Behavior of Multistage Systems--I: The Steady-State and II: The Impulse Response," Chem. Eng. Sci., 16, 352-363 (1961) and 17, 447-456 (1962).

82. Biery, J. C., and Royland, D. R., "Dynamic Simulation of a Liquid-Liquid Extraction Column," I & EC-Fund., 2 44-50 (1963)

83. Hartland, S. and Mechlenburgh, J. C., "A Comparison of Differential and Stagewise Countercurrent Extraction

with Backmixing," Chem. Eng. Sci., 21, 1209-1221 (1966).

84. Kafarov, V. V.; Vygon, V. G., and Gordeev, L. S., "Mathematical Analysis of Cell Model with Backmixing Between Cells," Theor. Found. Chem. Eng., 2, 59-64 (1968).

85. Lees, F. P. "The Frequency Response of a Packed Gas Absorption Column," Chem. Eng. Sci., 23, 97-107 (1968).

86. Pollock, G. G. and Johnson, A. I., "The Dynamics of Extraction Processes: Part I: Introduction and Critical Review of Previous Work; Part II: Comparison of Dynamic Testing Methods and Their Application to Extraction Process; Part III: The Determination of Steady State and Transient Concentration Profiles," Can. J. Chem. Eng., 47, 469-476 and 565-575 (1969), and 48, 64-72 (1970).

87. DiLiddo, B. A., and Walsh, T. J., I & EC, 53, 801 (1961)

88. Watjen, J. W., and Hubbard, P. M., "The Dynamic Behavior of a Pulsed-Plate Extraction Column," A.I.Ch.E. J., 9, 614-616 (1963).

89. Chiu, L. L., "Dynamic Response of a Liquid-Liquid Extraction Column to Step Changes in Feed Composition," M.Eng. Thesis, Univ. of Florida (1963).

90. Foster, H. R., Jr., "Transient Solution to the Equations Describing a Stagewise Countercurrent Extraction Process," M.S. Thesis, Univ. of Washington (1964).

91. Staffin, H. K. and Chu, J. C., AIChE J., 10, 98 (1964).

92. Evans, D. R., Ph.D. dissertation, Iowa State Univ. of Science and Technology, Ames, Iowa (1965).

93. Burns, P. E. and Hanson, C., Brit. Chem. Eng., 12, No. 1, 75 (1967).

94. Jaswon, M. A., and Smith, W., "Countercurrent Transfer Processes in the Nonsteady State," Proc. Royal Soc. (London), A225, 226-244 (1954).

95. Chernyshev, V. N., "The Dynamics of Mass Transfer in Countercurrent Extraction Equipment," Intern. J. Chem. Eng., 6, No. 4, 608-618 (1966).

96. Champagne, F., "Transient Solution to the Equations Describing a Differential Countercurrent Extraction Process," M.Sc. Thesis, Univ. of Washington (1962).

97. Doninger, J. E., and Stevens, W. F., "The Dynamic Behavior of a Packed Liquid Extraction Column," AIChE J., 14, 591-599 (1968)

98. Elkins, L. G., "Steady-State and Dynamic Analyses of Continuous Countercurrent Liquid-Liquid Extraction Columns," Ph.D. dissertation, Vanderbilt Univ. (1966).

99. Clements, W. C. and Schnell, K. B., Jr., I & EC--Process Des. Develop, 2, 94 (1963).

100. Justice, R. G., and Schnelle, K. B., Jr., Paper 46B presented at the AIChE Philadelphia Meeting, Dec. 1965.

101. Doninger, J. E., "The Dynamic Behaviour of a Packed Liquid Extraction Column," Ph.D. dissertation, Northwestern Univ., Evanston, Illinois (1965).

102. Lapidus, L., and Luus, R., Computational Problems in Process Control, Blaisdell Pub. Co., N.Y., 1967.

103. Friedly, J. C., "Dynamic Behavior of Processes," Prentice-Hall, Inc., 1972.

104. Hanson, C., Editor, "Recent Advances in Liquid-Liquid Extraction," Pergamon Press (1971).

105. Skelland, A. H. P., "Diffusional Mass Transfer," John Wiley Interscience, 1974.

106. Sherwood, T. K., Pigford, R. L., and Wilke, C. R., "Mass Transfer," McGraw-Hill Book Co., 1975.

107. Jenson, V. G., and Jeffreys, G. V., "Mathematical Methods in Chemical Engineers," Academic Press, 1963.

108. Huag, H. F., "Backmixing in Multistage Agitated Contactors--a Correlation," AIChE Jr., 17, No. 3, 585-589 (1971).

109. Strainthorp, F. P., and Sudall, N., "Back-Mixing in an RDC," Trans. Instr. Chem. Engrs., 42, T198-T208 (1964).

110. Pratt, H. R. C., "A Simplified Analytical Design Method for Differential Extractors With Backmixing," I&EC Process Des. Dev., 15, No. 1, 34-41 (1976).

APPENDIX A

UNIQUENESS OF THE STEADY-STATE SOLUTION FOR THE THREE-SECTION COLUMN MODEL

The solution of Equation (III-12) which satisfies the boundary condition (III-13) to (III-16) for a three-section column model with axial mixing was solved analytically by Wilburn[1,2] as an extension of one-section column model primarily solved by Miyauchi, et al. The equations for the eignevalues are similar for the three sections and given by Wilburn as follows.

Eigenvalue Determination

Extraction factor (mG/L) $\neq$ 1.

$$\psi_j = \sum_{i=1}^{4} A_{ij} e^{\lambda_{ij} z_j}$$

$$\Gamma_j = \sum_{i=1}^{4} a_{ij} A_{ij} e^{\lambda_{ij} z_j} \qquad \text{(A-1)}$$

The eigenvalues are

$$\lambda_{1j} = 0$$

$$\lambda_{2j} = \frac{\alpha_j}{3} + 2\sqrt{p_j} \cos \frac{u_j}{3}$$

$$\lambda_{3j} = \frac{\alpha_j}{3} + 2\sqrt{p_j} \cos\left(\frac{u_j}{3} + \frac{2\pi}{3}\right) \qquad \text{(A-2)}$$

$$\lambda_{4j} = \frac{\alpha_j}{3} + 2\sqrt{p_j} \cos\left(\frac{u_j}{3} + \frac{4\pi}{3}\right)$$

where u_j is determined as an angle between 0 and π such that

$$\cos u_j = q_j/(p_j)^{3/2} \tag{A-3}$$

and

$$p_j = \left(\frac{\alpha_j}{3}\right)^2 + \frac{\beta_j}{3}$$

$$q_j = \left(\frac{\alpha_j}{3}\right)^2 + \frac{\alpha_j\beta_j}{6} + \frac{\gamma_j}{2} \tag{A-4}$$

with

$$\alpha_1 = -Pe_y$$

$$\alpha_2 = Pe_x - Pe_y$$

$$\alpha_3 = Pe_x$$

$$\beta_3 = \beta_1 = N_{o_x} Pe_x + N_{o_x} Pe_y \Delta$$

$$\beta_2 = N_{o_x} Pe_x + Pe_x Pe_y + N_{o_x} Pe_y \Delta$$

$$\gamma_1 = N_{o_x} Pe_x Pe_y$$

$$\gamma_2 = N_{o_x} Pe_x Pe_y (1 - \Delta)$$

$$\gamma_3 = -N_{o_x} Pe_x Pe_y \Delta$$

The necessary condition for mass transfer is,

$$q^2 - p^3 < 0 \tag{A-5}$$

The left hand side of this inequality goes to zero only when perfect mixing is reached in each phase.

The solution of this model is obtained analytically in a closed form for linear equilibrium relationship with average values for holdup and axial mixing (i.e. constant with respect to the height). Therefore,

the four eigenvalues, corresponding to each section of the column (j), obtained from equation (A-2) are exact and related only to P_{e_x}, P_{e_y}, N_{o_x}, and Δ.

Uniqueness Criteria

The sufficient conditions for the existence of a unique solution for the steady-state differential equations are obtained from an eigenvalue problem. If there are two linearly independent eigenfunctions with the same eigenvalue, one would expect that this eigenvalue will have multiple solutions.[5,6]

Applying this principle to Equation (A-2), for the eigenvalues, one would find that the conditions under which this would occur are:

1. For $\lambda_{2j} = \lambda_{3j}$ the following conditions must be satisfied.

$$\cos\frac{u_j}{3} = \cos\left(\frac{u_j}{3} + \frac{2\pi}{3}\right)$$

$$= \cos\frac{u_j}{3}\cos\frac{2\pi}{3} - \sin\frac{u_j}{3}\sin\frac{2\pi}{3}$$

$$\tan\frac{u_j}{3} = -1.732051$$

$$\frac{u_j}{3} = \tan^{-1}(-1.732051)$$

$$= 120° \text{ or } 300°$$

Therefore, $u_j = 2\pi$ or 5π, both outside the range $0 \leq u_j \leq \pi$. (A-6)

2. For $\lambda_{3j} = \lambda_{4j}$, the following conditions must be satisfied:

$$\cos\left(\frac{u_j}{3} + \frac{2\pi}{3}\right) = \cos\left(\frac{u_j}{3} + \frac{4\pi}{3}\right)$$

$$\cos\frac{u_j}{3}\cos\frac{2\pi}{3} - \sin\frac{u_j}{3}\sin\frac{2\pi}{3} = \cos\frac{u_j}{3}\cos\frac{4\pi}{3} - \sin\frac{u_j}{3}\sin\frac{4\pi}{3}$$

Therefore, $$\sin\frac{u_j}{3} = 0$$

$$u_j = 0 \text{ or } u_j = 3\pi \text{ (outside the feasible range)} \qquad \text{(A-7)}$$

3. For $\lambda_{2j} = \lambda_{4j}$, the following conditions must be satisfied:

$$\cos \frac{u_j}{3} = \cos\left(\frac{u_j}{3} + \frac{4\pi}{3}\right)$$

$$= \cos \frac{u_j}{3} \cos \frac{4\pi}{3} - \sin \frac{u_j}{3} \sin \frac{4\pi}{3}$$

$$\frac{u_j}{3} = \tan^{-1}(1.732051)$$

$$= 60°$$

Therefore,

$$u_j = \pi \qquad \text{(A-8)}$$

4. For $\lambda_{1j} = \lambda_{2j} = \lambda_{3j} = \lambda_{4j}$, the following condition must be satisfied:

$$Pe_x = Pe_y = 0 \qquad \text{(A-9)}$$

From Equations (A-6) to (A-8), u_j must be equal to either zero or π to have repeated eigenvalues. Equation (A-3) becomes

$$q_j^2 - p_j^3 = 0 \qquad \text{(A-10)}$$

This would happen only if both Pe_x and Pe_y are equal to zero, which is the same as condition (A-9). Under this condition complete mixing is taking place and inequality (A-5) is violated.

<u>Analogy Between Steady-State Models for Liquid-Liquid Extraction with Axial Mixing and Tubular Reactor with Axial Mixing (TRAM)</u>

The phenomenon of multiplicity of the steady-state in chemical reactors has been investigated both theoretically and experimentally by many workers.[5,7] The problem lends itself to either studying the characteristics or solving the set of nonlinear differential

equations.representing the process. Many successful techniques appear in the literature to find the number of multiple steady-state solutions with or without solving the equivalent equations. Among these techniques are the abstract spaces method,[3] orthogonal collocation,[4] or certain topological theorems.[6]

The extraction problem would need a similar analysis to that carried out for the TRAM problem if the analytical solution is not possible. This would occur if the mass-transfer rate or the equilibrium relationship is nonlinear and the study would correspond to that for the TRAM problem with a first-order irreversible chemical reaction in a non-adiabatic reactor.

If the extraction problem considered has variable holdup and/or variable axial mixing along the column axis besides nonlinear equilibrium relationship, then an approximation technique based on the idea of orthogonal collocation would be recommended for the purpose.

References

1. Wilburn, N. P., "Mathematical Determination of Concentration Profiles in Two-Phase Continuous Countercurrent Extractors," I & EC Fund., 3, No. 3, 189-195 (1964).
2. Wilburn, N. P., and Nicholson, W. L., "Non-linear Model Determination of Concentration Profiles in Two-Phase Countercurrent Extractors," A.I.Ch.E.--I. Chem. E. Symposium Series No. 1, 1965, 105-111 (London: Instrn. Chem. Engrs.).
3. Han, C. D., and Agramal, S., "Function Space Methods for Analysis of Nonadiabatic Tubular Reactors with Axial Mixing--I--Uniqueness criteria of the steady-state and computation of the steady state profiles," C.E.S., 28, 1617-1627 (1973).
4. Van Den Bosch, B., and Padmanabhan, L., "Use of Orthogonal Collocation Methods for the Modelling of Catalyst Particles--I--Analysis of the Multiplicity of the Solutions," C.E.S., 29, 1217-1225 (1974).
5. Hlavacek, H., and Hofmann, H., "Modelling of Chemical Reactors--XVI--Steady-State Axial Heat and Mass Transfer in Tubular Reactors--An analysis of the uniqueness of solutions," C.E.S., 25, 173-185 (1970).
6. Luss, D., and Amundson, N. R., "Uniqueness of the Steady State Solutions for Chemical Reaction Occurring in a Catalyst Particle or in a Tubular Reactor with Axial Diffusion," C.E.S., 22, 253-266 (1967).
7. Schneider, D. R., Aris, R., and Amundson, N. R., "An Analysis of Chemical Reactor Stability and Sensitivity--XIV--The Effect of the Steady-State Hypothesis," C.E.S., 28, 885-896 (1973).

APPENDIX B

GRADIENT OPTIMIZATION ALGORITHMS

1. Conjugate Gradient Method[1,2,4]
2. Fletcher-Powell Method[1,3,4]
3. Variable Metric Method[5]
4. Optimum-Gradient Method[6]

References

1. Kuester, J. L., and Mize, J. H., "Optimization Techniques with Fortran," McGraw-Hill Pub. Co., 1973.
2. Fletcher, J. R., and Reeves, C. M., "Function Minimization by Conjugate Gradients," Computer Jr., 7, No. 2, 149-154 (1969).
3. Fletcher, J. R., and Powell, M. J. D., "A Rapidly Convergent Descent Method for Minimization," Computer Jr., 6, 163-168 (1963).
4. IBM-System/360 Scientific Subroutine Package, H20-0205-3, 221-229 (1968).
5. Davidon, W. C., "Variance Algorithm for Minimization," Computer Jr., 10, No. 4, 406-410 (1968).
6. Beckey, G. A., and McGhee, R. B., "Gradient Methods for the Optimization of Dynamic System Parameters By Hybrid Computation," Balakishnan, A. V., and Neustadt, L. W. (Editors), Computing Methods in Optimization Problems, Proc. of a conference held at University of California, Los Angeles (1964), 305-327.

Start iteration cycle for every N + 1 iterations

Calculate square of the gradient and terminate if zero

Calculate directional vector and derivative

Calculate scale factor used in linear search

Calculate function value and gradient at the new point

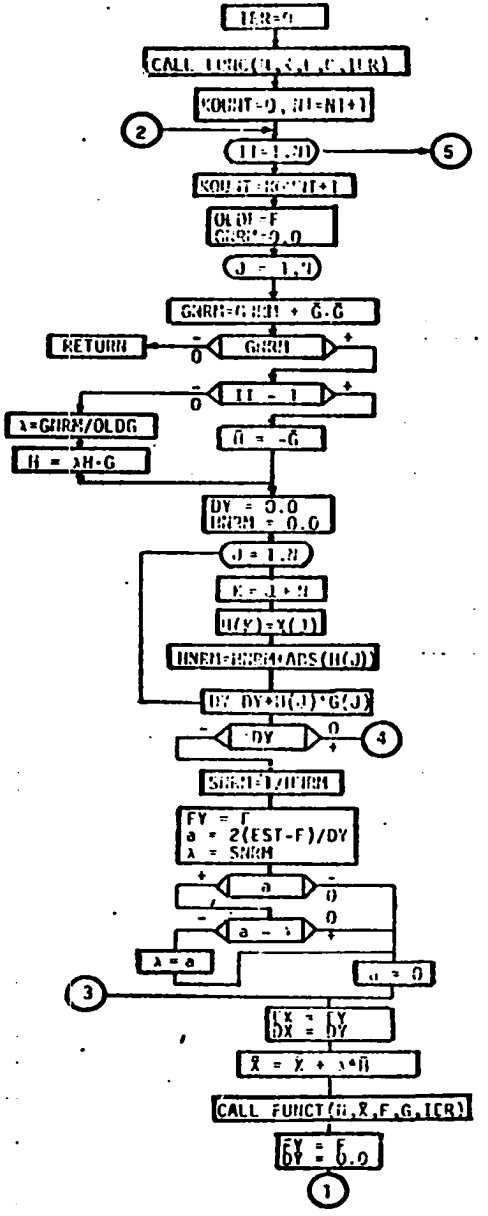

First step is taken in the negative direction of the gradient (steepest descent)

Search for minimum along direction H.

Use estimate for step size only if it is positive and less than SNRM

Save function and derivative for old argument

Step along H

Terminate search if the function value indicates that a minimum has been passed.

Repeat search and double step size for further searches

Linear search indicates that no minimum exists.

Calculate directional derivative

Repeat cubical interpolation

Calculate difference of new and old argument vector

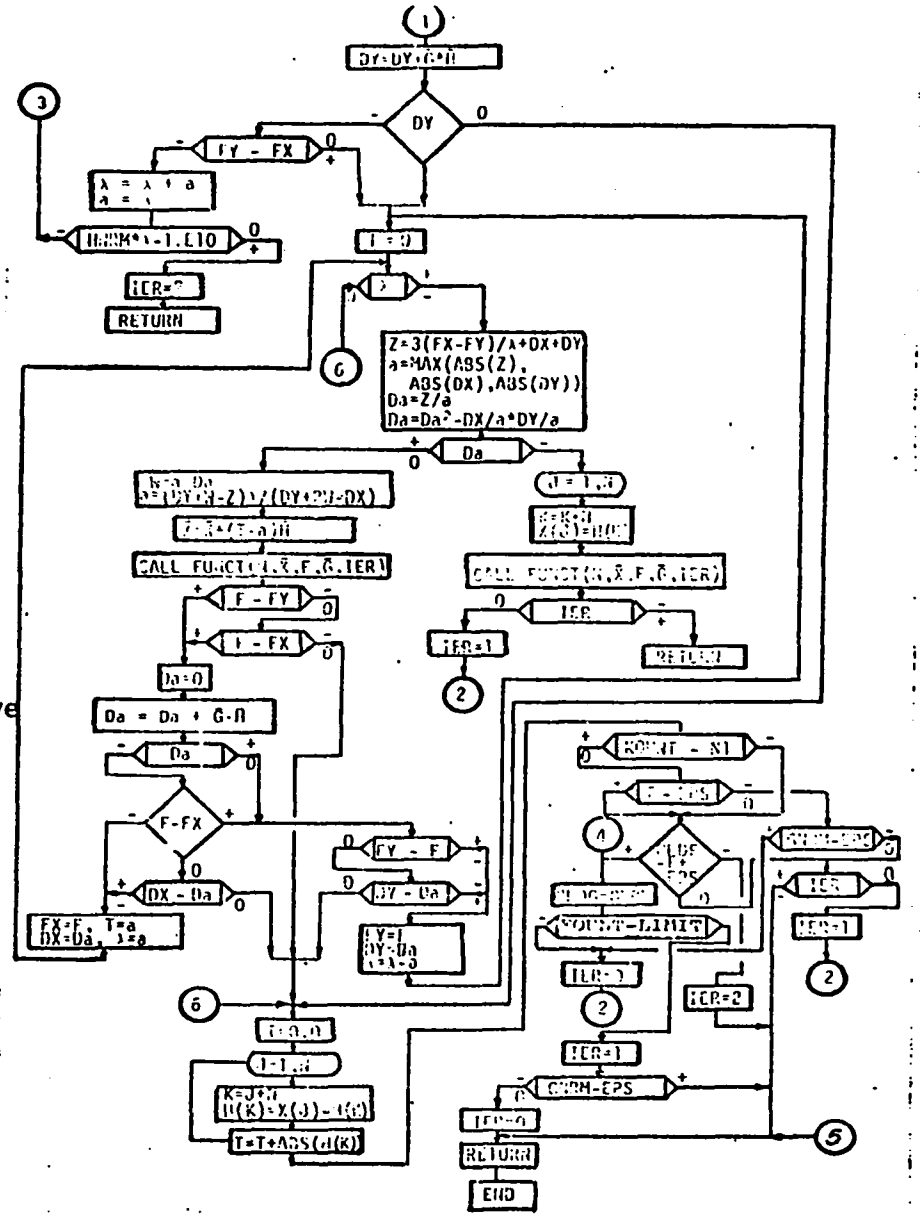

Calculate directional derivative DY for new argument. Terminate search if DY is positive. If DY = 0, the minimum is found.

Interpolate cubically in the interval defined by the search above and calculate x for which the function value is minimum.

Terminate the search

C-G-M
2/2

FIGURE B-1. Conjugate Gradient Method

Reset iteration counter

Save function value, argument vector and gradient vector

Check whether function will decrease stepping along H

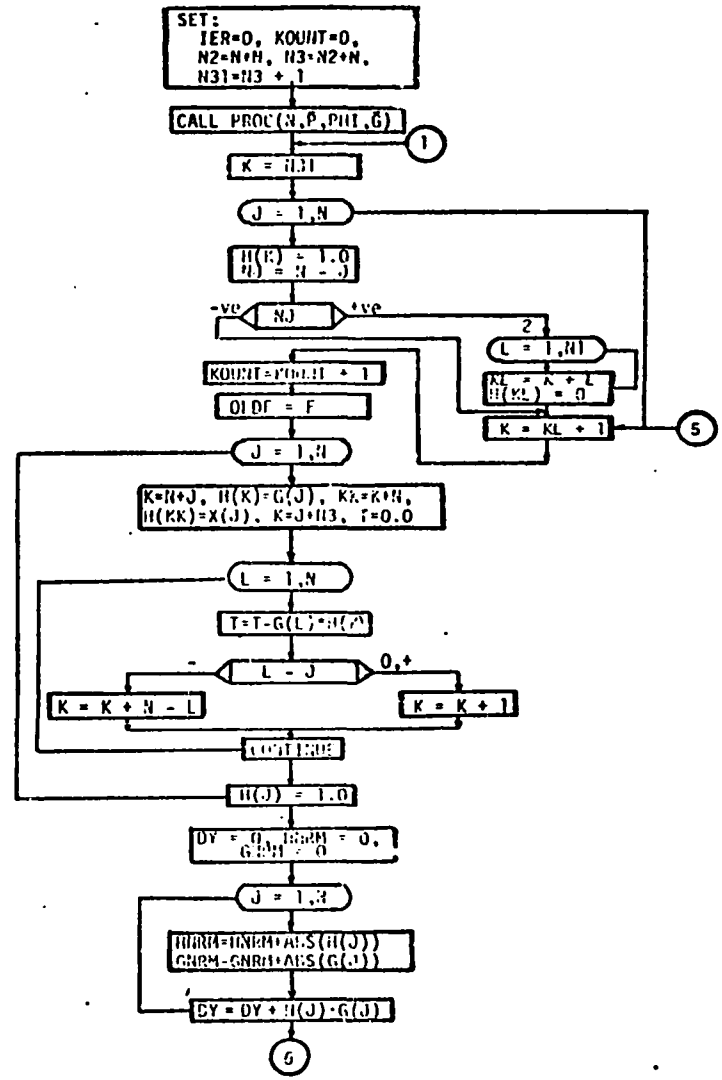

Set metric matrix (in vector form) equal to unity.

Determine direction vector H.

Calculate directional derivative and test values for direction vector H and gradient vector G

Save function and gradient of old argument

Step argument along direction H

Terminate search if DY is +ve, and if DY is zero the minimum is found

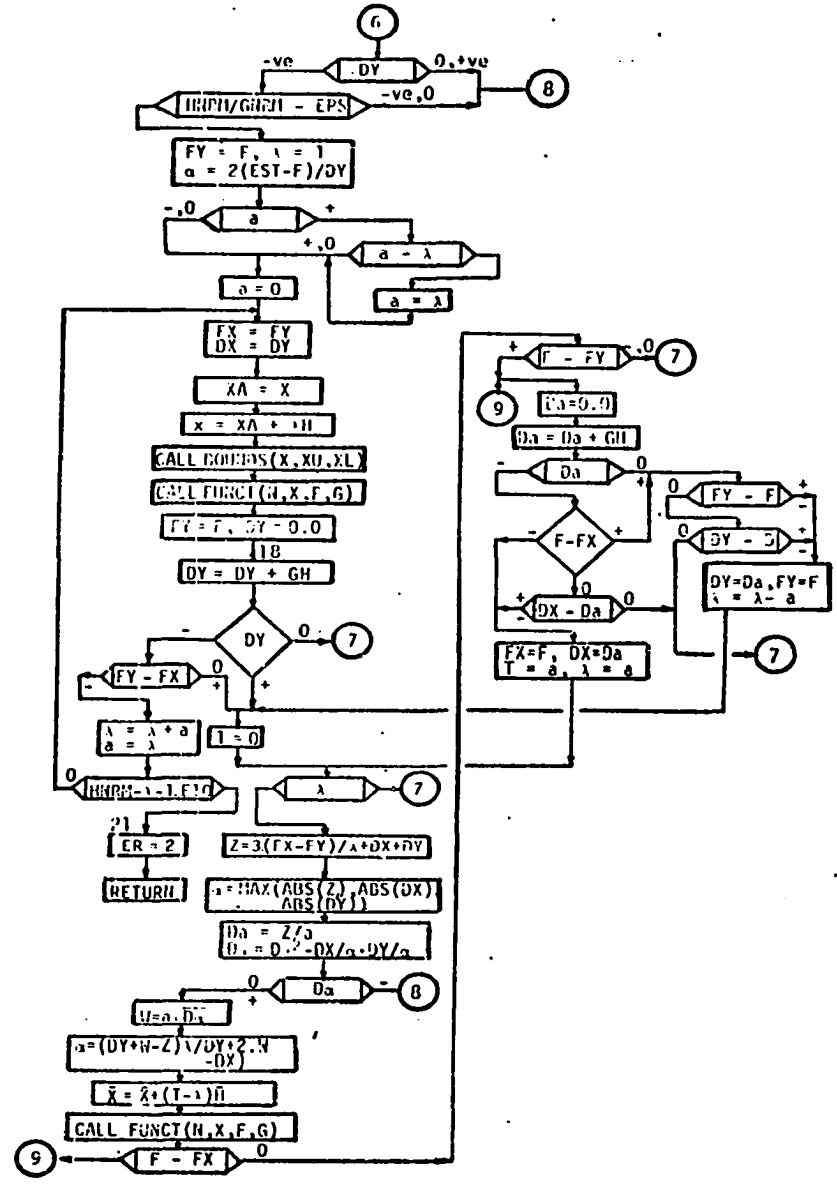

Repeat search in direction of steepest descent if directional derivative appears to be positive or zero

Interpolate cubically in the interval defined by the search

Calculate difference vectors for argument and gradient from the consecutive iterations

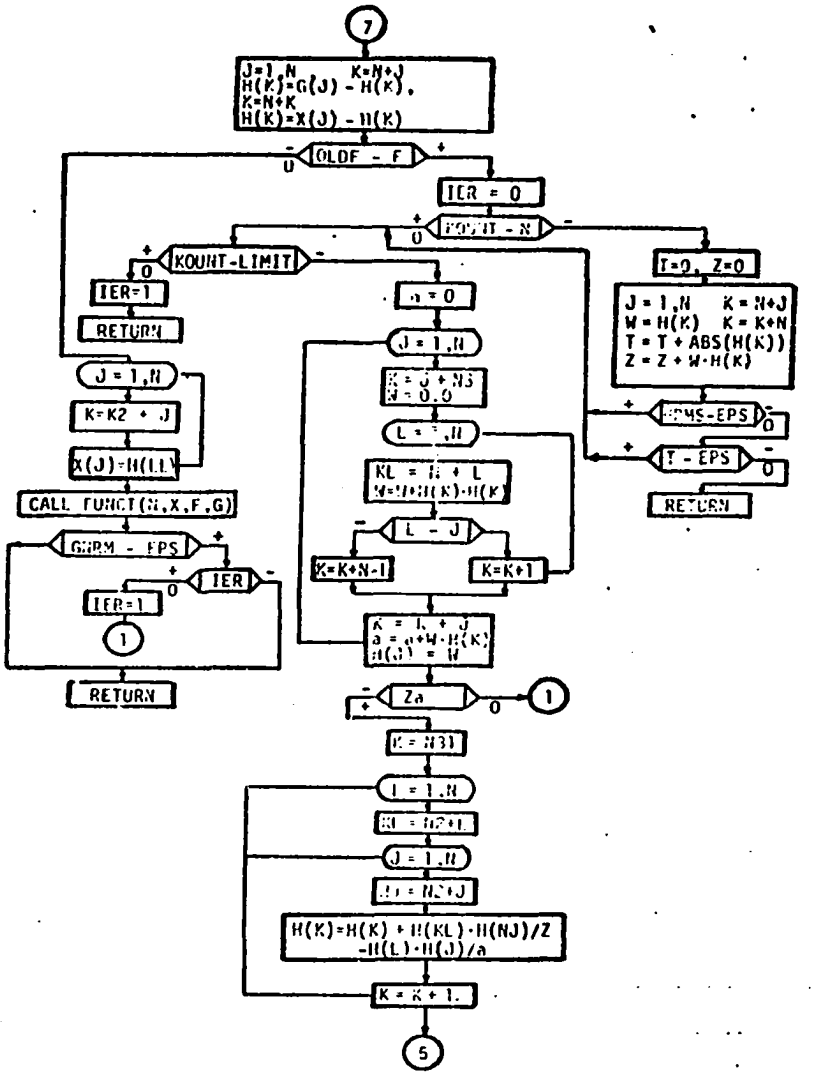

Repeat the search in the steepest descent if results are not satisfactory

Update the metric matrix H

F-P-M
3/3

FIGURE B-2. Fletcher-Powell Method

Calculate the direction of the step S and the component of the gradient in the direction of the step (GS)

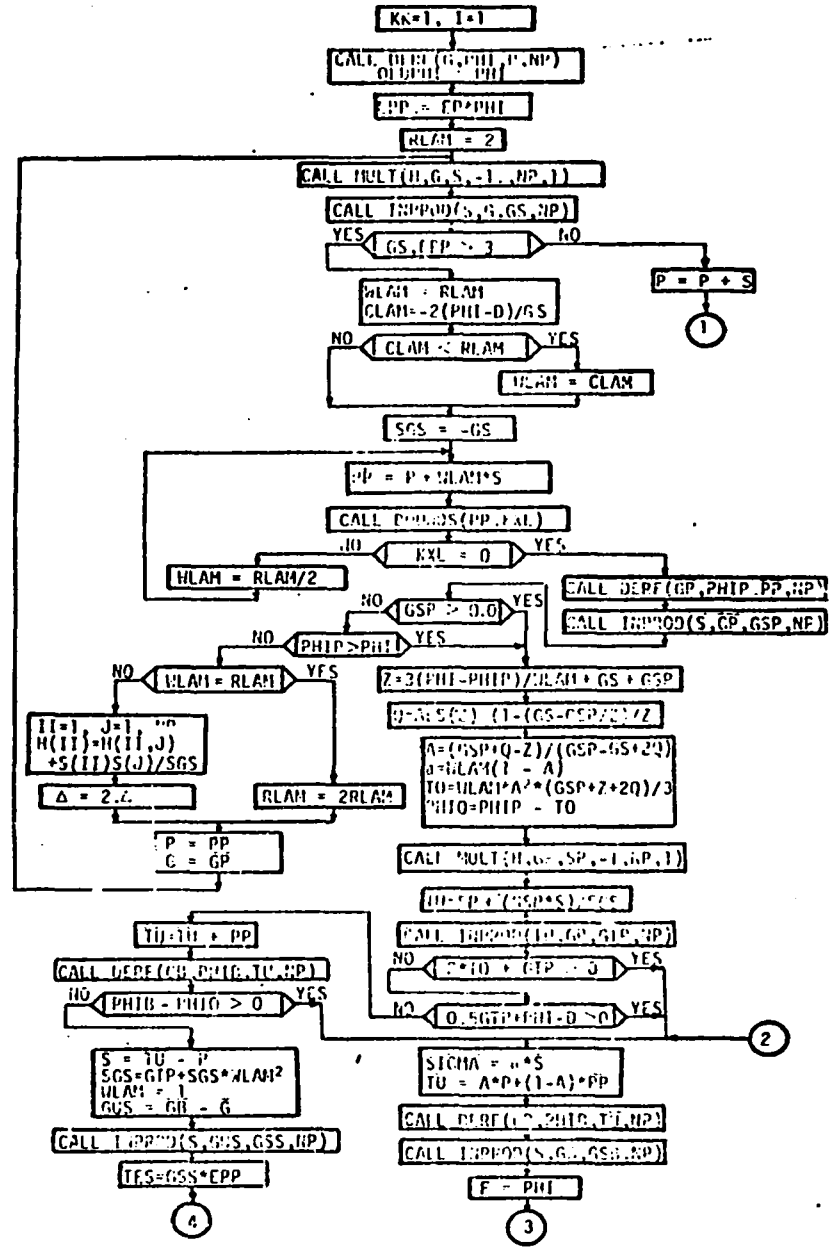

Step in ⊥ler direction

Evaluate function and gradient at the new point

Interpolate cubically

Check step ⊥ler to predicted minimum.

Calculate the function at the interpolated point and determine if a local minimum has been reached

Modifying the metric matrix H on the basis of information obtained about the function along the direction s

Setting the metric matrix equal to identity after N + 1 iterations.

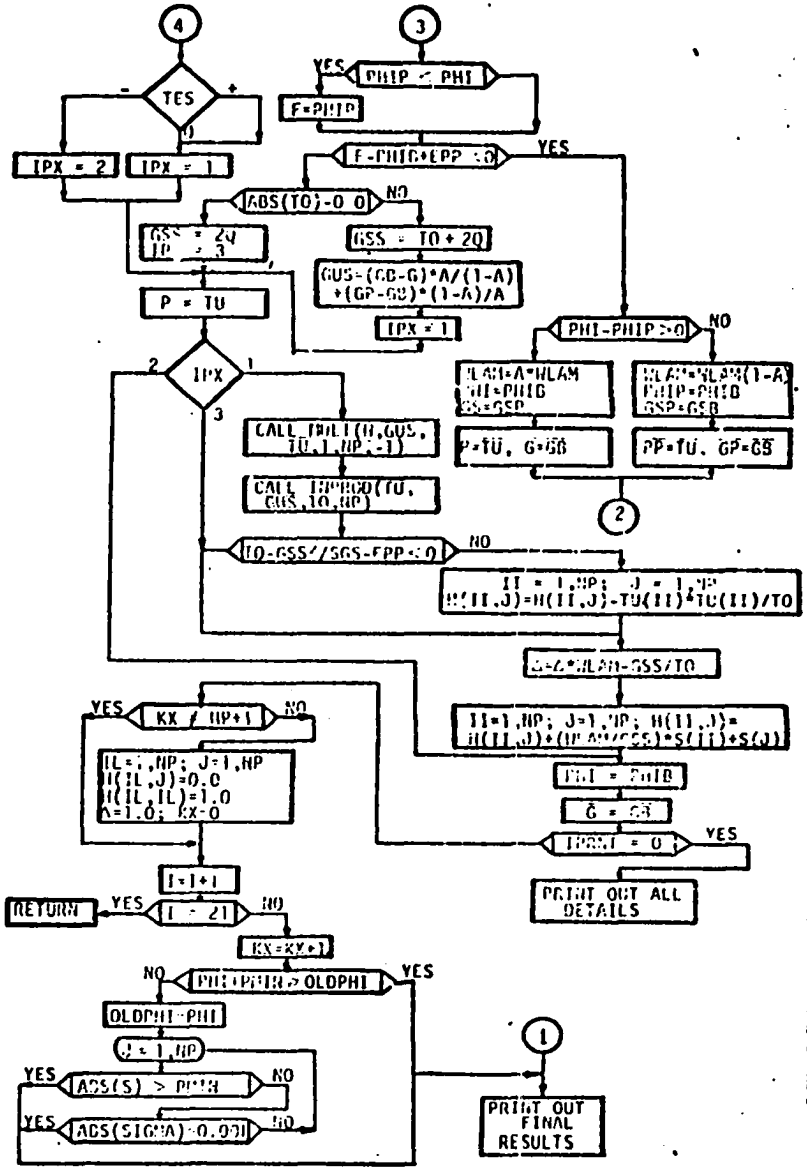

FIGURE B-3. Variable Metric Method

Read in constants

Calculate gradient vector and square of gradient magnitude $|\nabla\phi|^2$

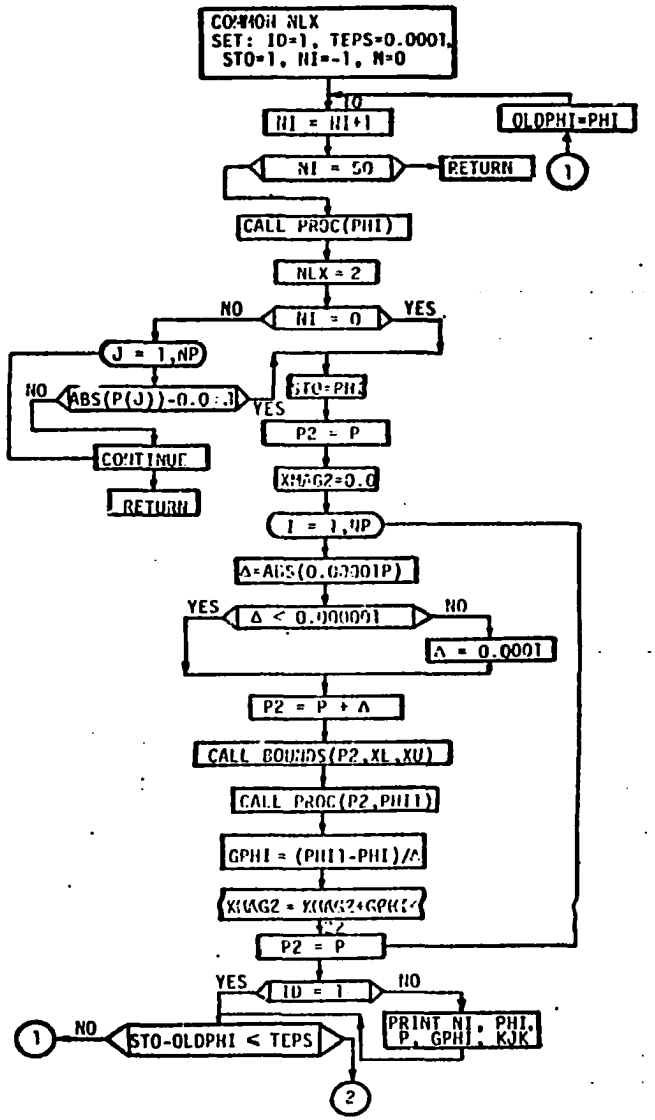

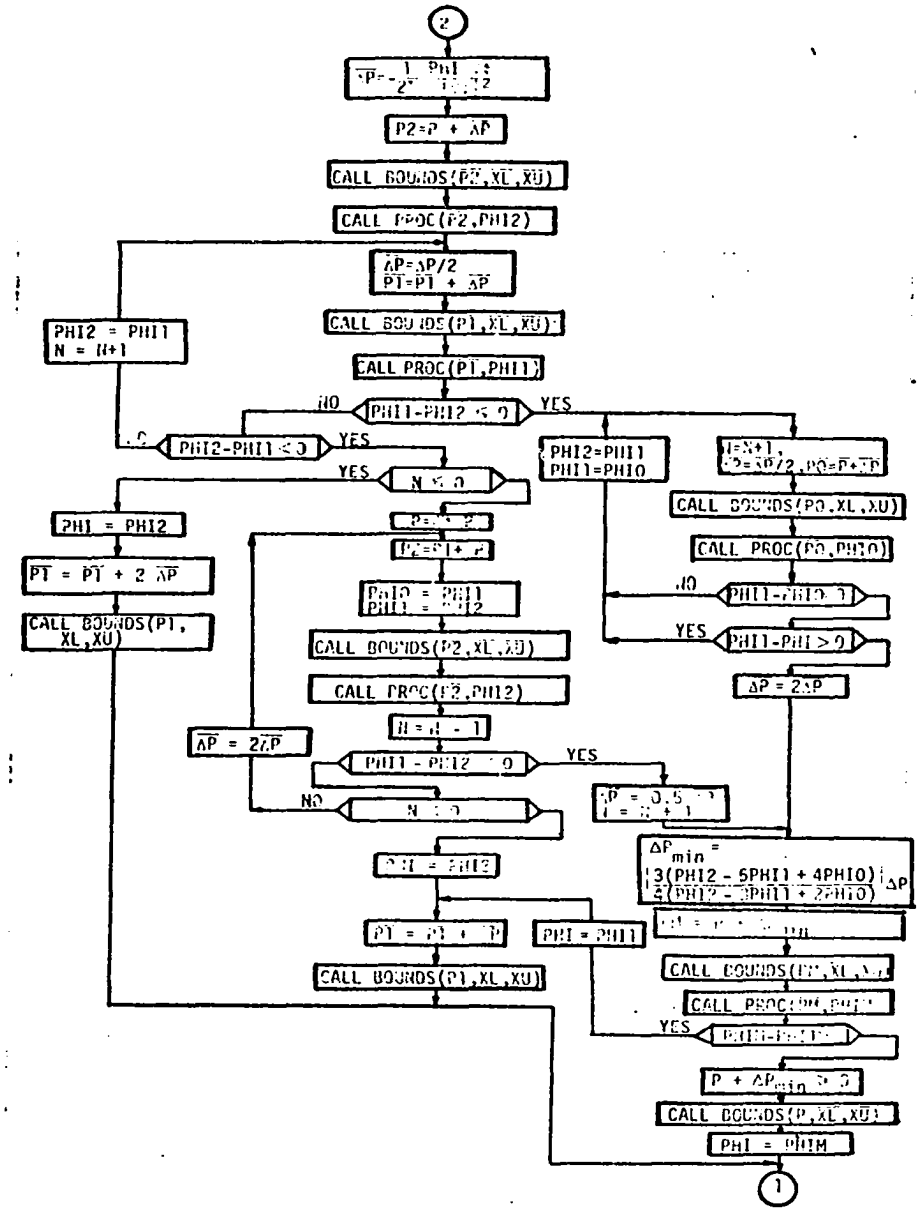

FIGURE B-4. Optimum Gradient Method